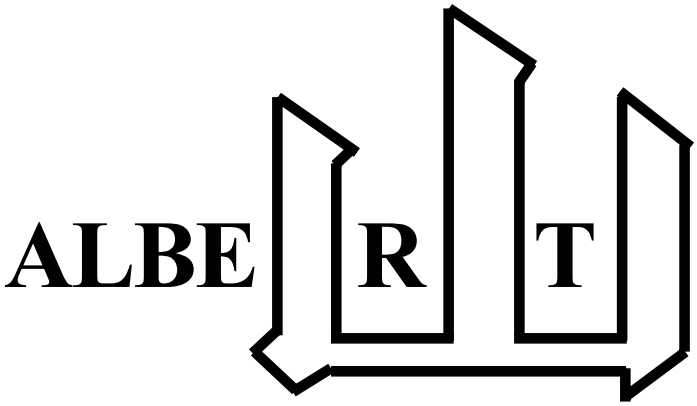

Part II: Excursion guide

33

May 2005
ISSN 0619-4324

Contents

The primary aim of ALBERTIANA is to promote the interdisciplinary collaboration and understanding among members of the I.U.G.S. Subcommission on Triassic stratigraphy. Within this scope ALBERTIANA serves as the newsletter for the announcement of general information and as a platform for discussion of developments in the field of Triassic stratigraphy. ALBERTIANA thus encourages the publication of anouncements, literature reviews, progress reports, preliminary notes etc. - i. e. those contributions in which information is presented relevant to current interdisciplinary Triassic research. An electronic version of ALBERTIANA is also available in PDF format at the

ALBERTIANA website

at http://www.bio.uu.nl/~palaeo/Albertiana/Albertiana01.htm.

Permian-Triassic Sequences in Meishan and Hushan, Lower Yangtze
Guide to the Pre-Symposium Field Excursion of the International Symposium on the Triassic Chronostratigraphy and Biotic Recovery (23-25 May 2005, Chaohu, China)

Zhao Laishi

State Key Laboratory of Geo-Processes and Mineral Resources, China University of Geosciences, Wuhan 430074, China; lszhao@cug.edu.cn

Introduction

This field excursion is designed to provide participants an opportunity to visit some different Permian- Triassic sequences on the Lower Yangtze block, southeast China. Two localities, Meishan in Changxing and Hushan in Nanjing, will be closely examined during this excursion (Fig. 1).

During the Permian-Triassic transition the Lower Yangtze sea had a clear paleogeographical differentiation and it became deeper from south to north. The Permian-Triassic sequence from the Changhsingian to the Lower Triassic at Meishan was formed on a relatively shallow carbonate platform while the strata at Hushan show an environment of shallow basin or deeper shelf. Chaohu is also on the Lower Yangtze block, but it was even in a deeper part than Hushan during the Permian-Triassic transition and the sequence will be visited during the mid-Symposium field excursion. Therefore, the pre-Symposium and mid-Symposium field excursions cover all the Permian-Triassic sequences of various facies in the Lower Yangtze region.

During the excursion we will have a stop at the Nanjing Institute of Geology and Paleontology in Nanjing to visit the paleontological museum and colleagues at the institute.

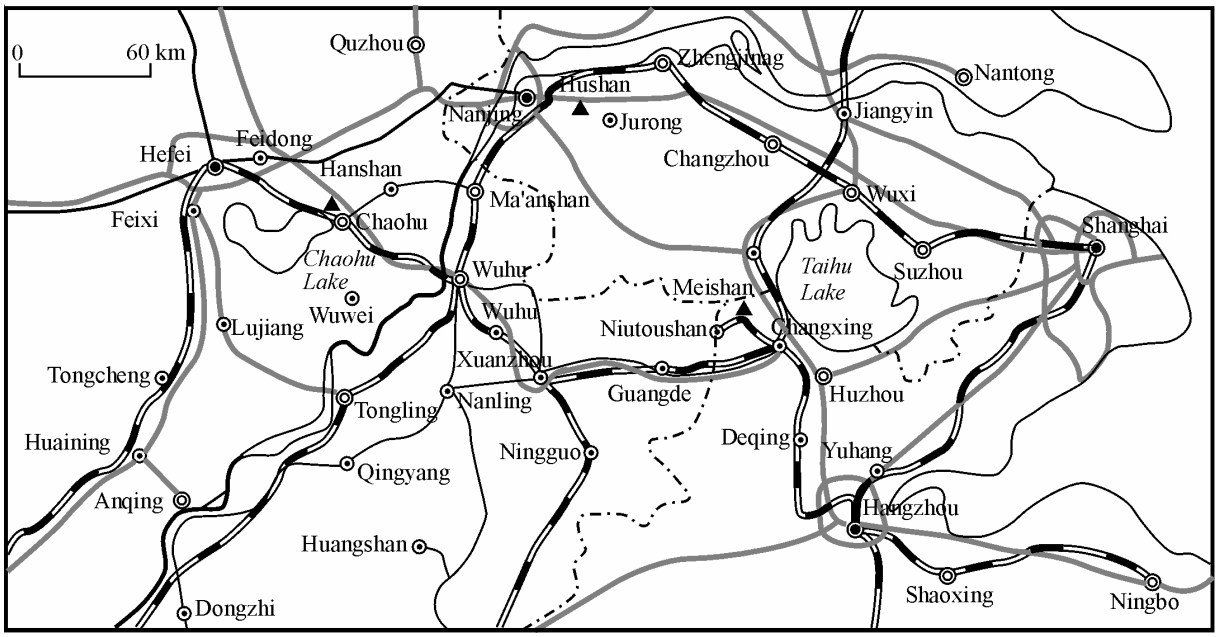

Figure 1. Location map of the field excursion

Meishan in Changxing County, Zhejiang Province

Meishan is situated in the Changxing County, Zhejiang Province, about 20 km to the county town. Changxing is in the northwestern Zhejiang Province, bordered with the Jiangsu and Anhui provinces. The exact location of Meishan Section D is 31°4¢55²N and 119°42'¢22.9²E. This section is well protected and freely accessible to scientific researchers by railway from Hangzhou or by expressway from Shanghai, Nanjing and Hangzhou (within 2-3 hours' drive). A branch railway and highway connect Changxing with Meishan and Xinhuai, the nearest village to Meishan Section D. The stratigraphical succession is well exposed and not very structurally disturbed. The Meishan quarries were excavated to use the limestone of the Changxing Formation for construction, thus providing several PTB sections named from A to E and Z from west to east, and Section D is in the middle of the quarried outcrops.

At Meishan, the following spots will be visited: (1) GSSP for the base of the Changhsingian; (2) standard sequence of the Changhsingian Stage; (3) GSSP of the Permian-Triassic boundary; and (4) Lower Triassic sequence.

Spot 1: GSSP candidate for the base of the Changhsingian

The GSSP for the base of the Changhsingian Stage has been proposed at Meishan Section D and the proposal has been voted through the boundary working group, SPS and ICS and is waiting for the final ratification of the IUGS (Jin et al., 2005). The proposed boundary is at the FAD of conodont *Clarkina wangi* (defined by the high fused wall-like carina) within the lineage from *Clarkina longicuspidata* to *Clarkina wangi*, at a point of 88 cm above the base of the Changxing Limestone in the lower part of Bed 4 (base of 4a-2) at Meishan Section D (Fig. 2), just above the flooding surface of the second parasequence in the Changxing Limestone. Secondary markers for correlation include a magnetic reversal from normal to reverse within the *C. wangi* Zone as well as changes in fusulinid and ammonoid faunas. There are no major stable isotopic excursions coinciding with the boundary, but the Lower Changhsingian is generally enriched with respect to $\delta^{13}C$ values compared with the Upper Wuchiapingian (Fig. 3).

Description of the Wuchiapingian-Changhsingian boundary succession at Meishan Section D:

Changxing Formation (Limestone)

Bed 5 (depth, 211-370 cm). Dark grey thin- to medium-bedded bioclastic micritic limestone with siliceous bandings, with normal graded beddings and small sandy wavy beddings. Non-fusulinid foraminifers (330-370 cm): *Glomospira* sp.; (290-330 cm): *Frondicularia ovata,*

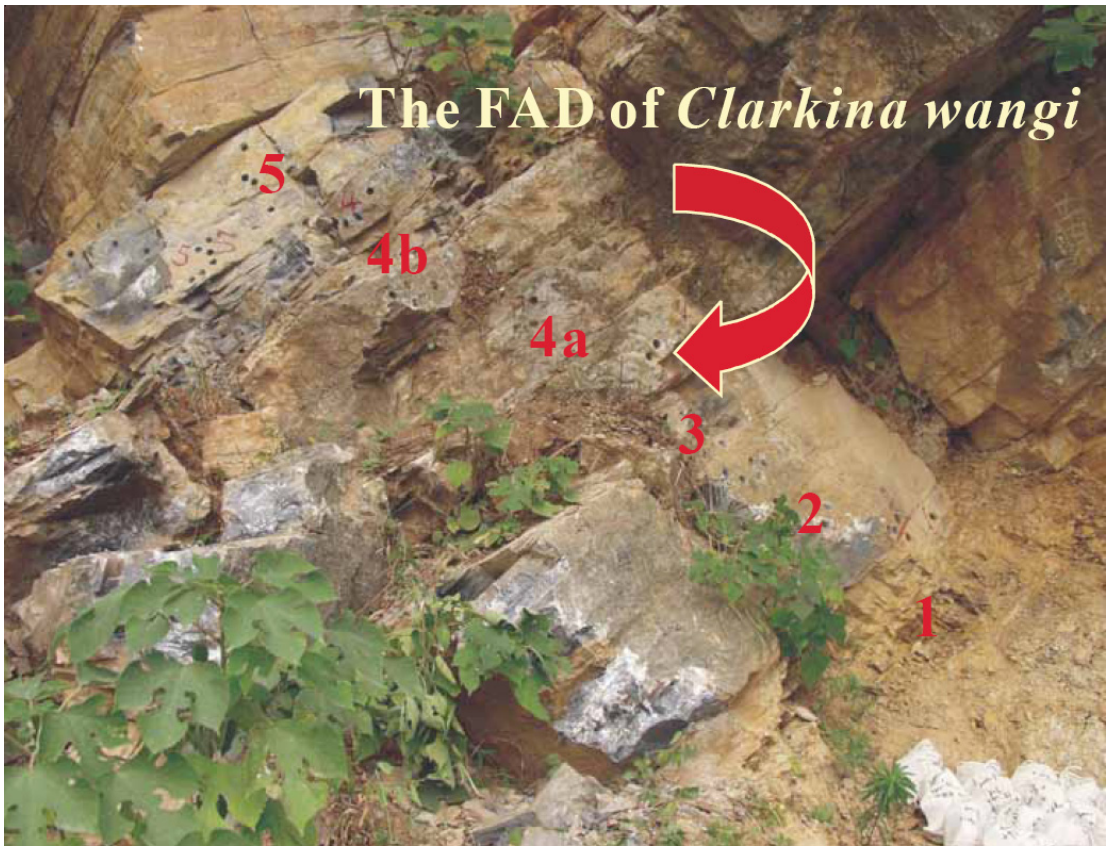

Figure 2. Proposed GSSP for the base of the Changhsingian at Meishan Section D

Damgarita sp., *Nodosaria krotovi* (250-290 cm): *Geinitzina uralica, Globivalvulina distensa*, *Nodosaria longissima*, *Damgarita* sp., *Pseudonodosarlina* sp.; (210-250 cm): *Damgarita* sp., *Frondicularia* sp., *Geinitzina splandli*; fish (210–370 cm): Palaeomiscoidei gen. et sp. indet., *Sinohelicoprion changxingensis*, *Sinoplatysomus meishanensis*; ostracods (210-370 cm): *Bairdiacypris fornicata*, *Bairdia wrodeloformis*, *Basslerella firma*, *Eumiraculum changxingensis*, *Petasobairdia bicornuta*, *Silenmites sockakwaformis*; conodonts (215-230 cm): *Clarkina wangi*.

Bed 4b (depth, 158-211 cm). Grey thin- to medium-bedded bioclastic micritic limestone, intercalating light grey thin-bedded calcareous mud rock in the upper part, with slightly wavy beddings. Non-fusulinid foraminifers (158-211 cm): *Geinitzina splandli*., *Pseudoglandulina conicula*; fusulinids (158-211 cm): *Palaeofusulina minima*; fish (158-211 cm): Amblypteridae?, Coelacanthidae gen. et sp. indet., Palaeoniscoidei gen. et sp. indet., *Sinohelicoprion changxingensis*, *Sinoptatysomus meishanensis*; ostracods (158–211 cm): *Basslerella obesa*, *Petasobairdia bicornuta;* conodonts (185-205 cm): *Clarkina orientalis*, *C. wangi*; (174-180 cm): *Clarkina orientalis*, *C. wangi*; (160-167 cm): *Clarkina orientalis*, *C. longicuspidata* transitional to *C. wangi*, *C. wangi*.

Bed 4a (depth, 80.5-158 cm). Grey thick-bedded bioclastic micritic limestone. Fusulinids (85-125 cm): *Palaeofusulina minima, Reichelina changhsingensis*; non-fusulinid foraminifers (125-158 cm): *Frondicularia palmate, Geinitzina splandli, Globivalvulina* sp., *Nodosaria longissma*; (85-125 cm): *Nodosaria delicate*, *Damgarita* sp.; brachiopods (85-158 cm): *Cathaysia chonetoides*, *C. parvalia;* conodonts (141-157 cm): *Clarkina longicuspidata* transitional to *C. wangi*, *C. wangi*; (107-130 cm): *C. longicuspidata*, *C. longicuspidata* transitional to *C. wangi*, *C. wangi*; (88-107 cm): *Clarkina longicuspidata*.

Bed 3 (depth, 56-80.5 cm). Greyish yellow illite-mont-

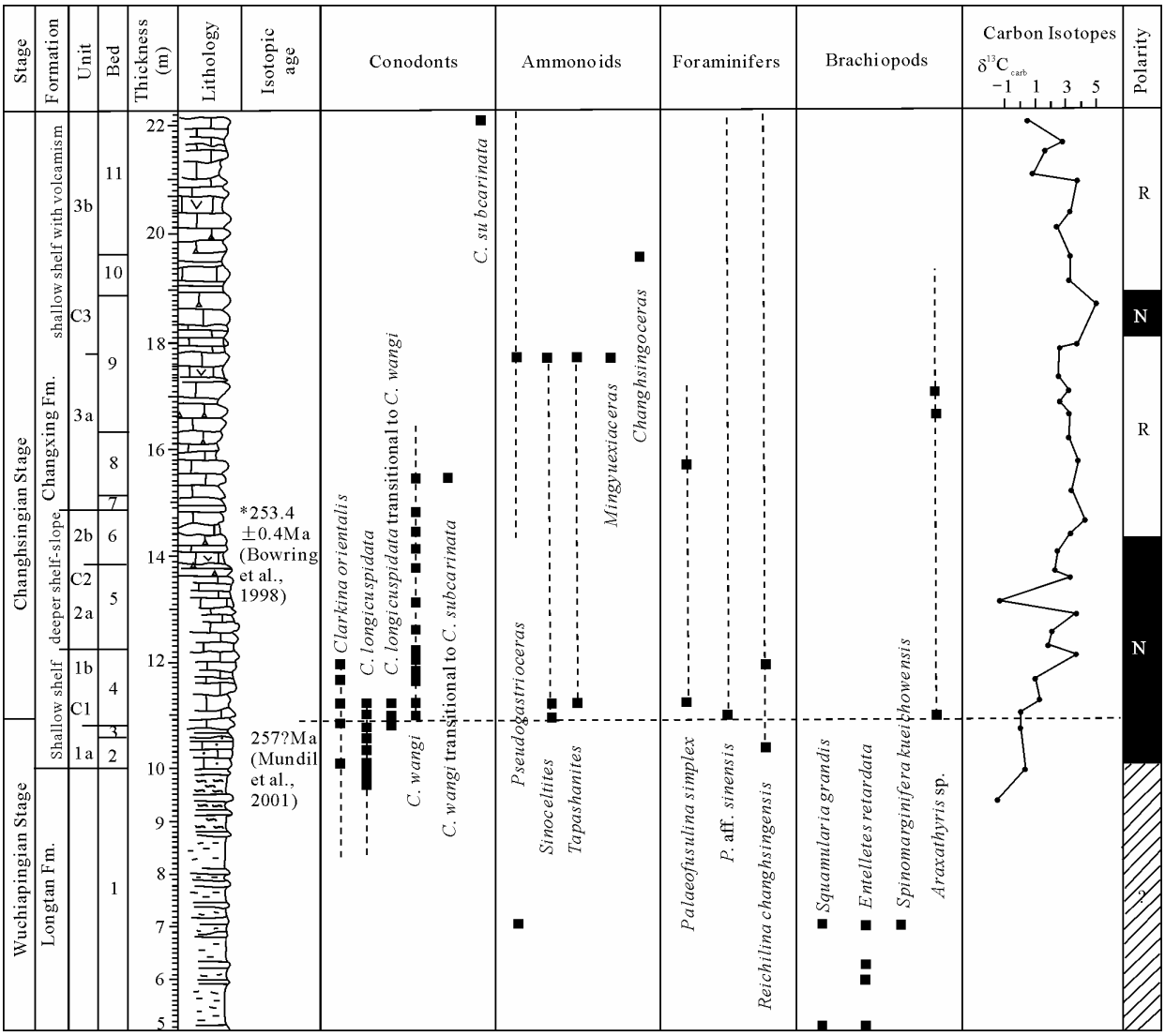

Figure 3. Integrated stratigraphic sequences around the Wuchiapingian-Changhsingian boundary in Meishan and the distribution of various fossil groups, carbon isotopes, geochronologic ages, and magnetic reversals. Note that the lithologic succession is subdivided into both beds and units. The beds are based on historical usage and are depicted to allow comparison with the literature. It is recognized that these beds are actually bedsets or parasequences except in the case of the ash beds, which represent true beds. The units are based on distinctive lithologic changes that reflect interpreted changes in depositional environment.

morillonite clay, U-Pb age: 257 Ma (Mundil *et al*., 2001). (56-82 cm) Greyish black silty and calcareous mud rock intercalating argillaceous mud rock, with horizontal bedding. Conodonts (70-80 cm): *Clarkina longicuspidata*, *C. longicuspidata* transitional to *C. wangi*; (56-70 cm): *Clarkina longicuspidata*.

Bed 2 (depth, 0-56 cm). Dark grey thick-bedded silt-bearing micritic limestone. Non-fusulinid foraminifers (0-55 cm): *Collaniella* sp., *Eacristellaria* sp., *Geinitzina postcarbonica, Pseudoglandulina conica;* conodonts (47-56 cm): *Clarkina longicuspidata*; (32-47 cm): *Clarkina longicuspidata*, *C. orientalis*; (20-30 cm): *Clarkina longicuspidata*; (0-20 cm): *Clarkina longicuspidata*, *C. orientalis*.

----------conformity----------

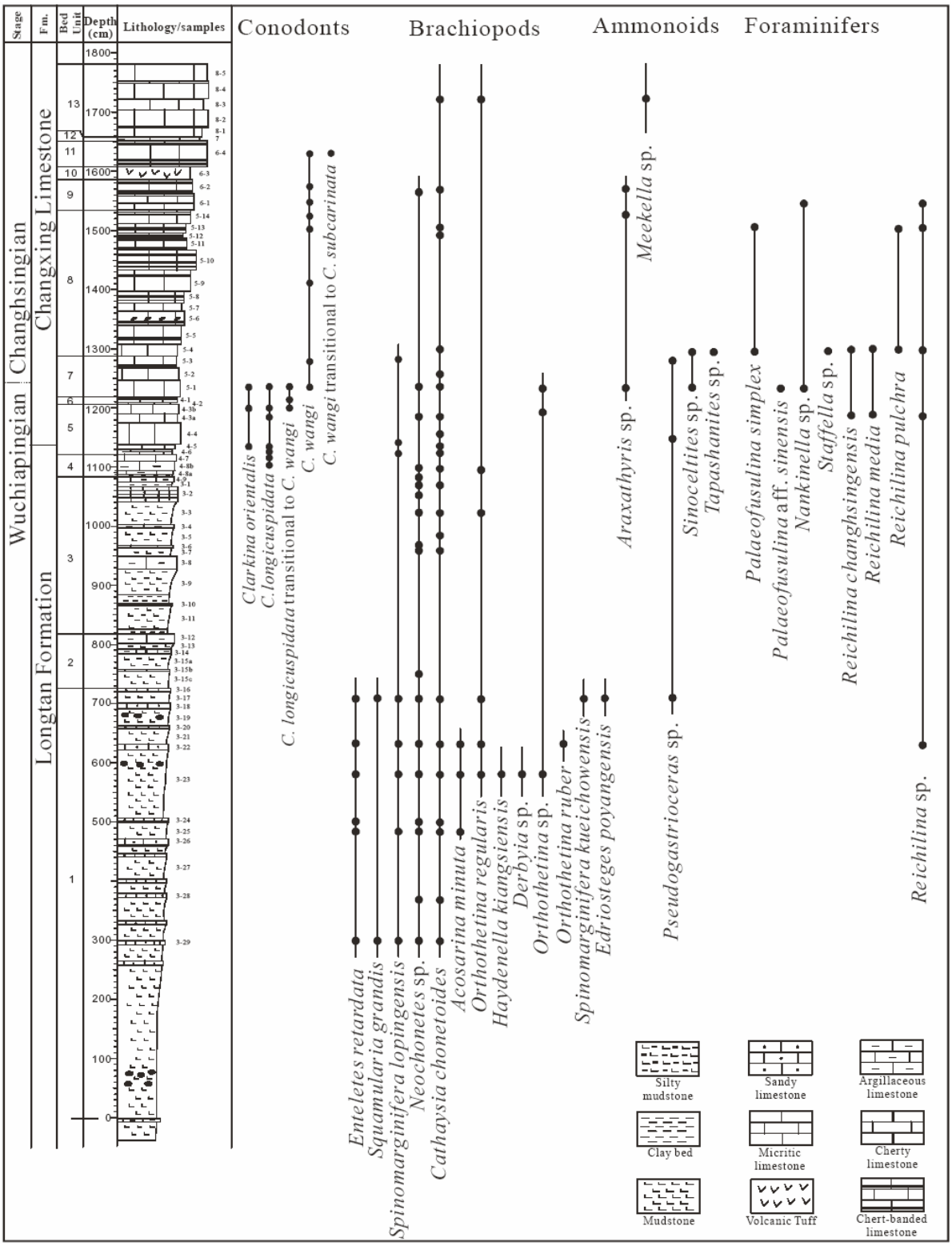

Figure 4. Stratigraphic occurrence of fossils around the Wuchiapingian-Changhsingian interval at Meishan Section C

Figure 5. Picture showing the unit stratotype for the Changxing Limestone prior to construction of the Geopark

Longtan Formation

Bed 1 (depth of upper part, 0 to -30 cm). Dark dolomitized calcirudite with fragments of limestone, siltstone and phosphate. Nonfusulinid foraminifers (0 to -30 cm): *Geinitzina uralica, Hemigardius* sp., brachiopods (0 to -30 cm): *Orbiculoidea* sp., *Cathaysia chonetoides*, *Paryphella gouwaensis*, *Spinomarginifera* sp.; conodonts (-4 to -12 cm): *Clarkina longicuspidata*. (depth of lower part, -30 to -70 cm). Dark medium-bedded calcareous siltstone with horizontal bedding surfaces. Conodonts (-30 to -40 cm): *Clarkina longicuspidata*.

In addition, conodont samples from Meishan Section C have been extensively collected. Meishan section C is a new exposure about 300 metres from Section D that has been studied by Yue Wang and others in which the upper Longtan Formation was excavated (Fig. 4). The value of Section C is that it exposes more of the upper Longtan Formation and that it clearly shows the transitional nature of deposition across the Longtan/Changxing formational boundary. This removes one objection to the proposed stratotype that not enough of the underlying beds were present even though it doesn't have any bearing on the definition, which occurs higher in the lower part of the Changxing Limestone.

Spot 2: Changxing Limestone at Meishan Section D

Since both GSSPs of the top and base of the Changhsingian Stage are very probably at Meishan Section D, the Changxing Limestone at the section becomes the unit stratotype of the Changhsingian Stage (Fig. 5).

The Changxing Limestone is about 40 m thick, composed of lower Baoqing Member and upper Meishan Member. It has received considerable extensive studies since it was named by Grabau in 1931 (Fig. 6).

Spot 3: GSSP of the Permian-Triassic boundary at Meishan Section D

Numerous studies have been performed at the Permian-Triassic boundary of Meishan Section D and involved nearly all aspects dealing with the stratigraphical boundary and related Paleozoic-Mesozoic transitional events. Literatures are vast and we will not iterate here but present only a figure to show the boundary sequence at the section (Fig. 7).

Spot 4: Lower Triassic sequence at Meishan Section D

The Lower Triassic of Meishan is composed of three lithostratigraphical formations in an ascending order: Yinkeng Formation, Helongshan Formation and Nanlinghu Formation. However, the Nanlinghu Formation has only its basal part preserved while the most is eroded in the area. The Meishan quarries exposed only the Yinkeng Formation and the base of the Helongshan Formation and the other part of the Lower Triassic is distributed on the hill slope. At Meishan the Yinkeng Formation is composed mainly of alternations of thin-bedded limestone and mudstone (or shale), which show a marked multiple scales of cycles, corresponding with the Milankovitch periodicity (Tong, 1997) (Fig. 8). The Helongshan and Nanlinghu Formation are mostly limestone. The Induan-Olenekian boundary marked by conodont *Neospathodus waageni* is located at about 280 m above the Permian-Triassic boundary in the upper part of the Helongshan Formation at Meishan Section D (Tong and Yang, 1998).

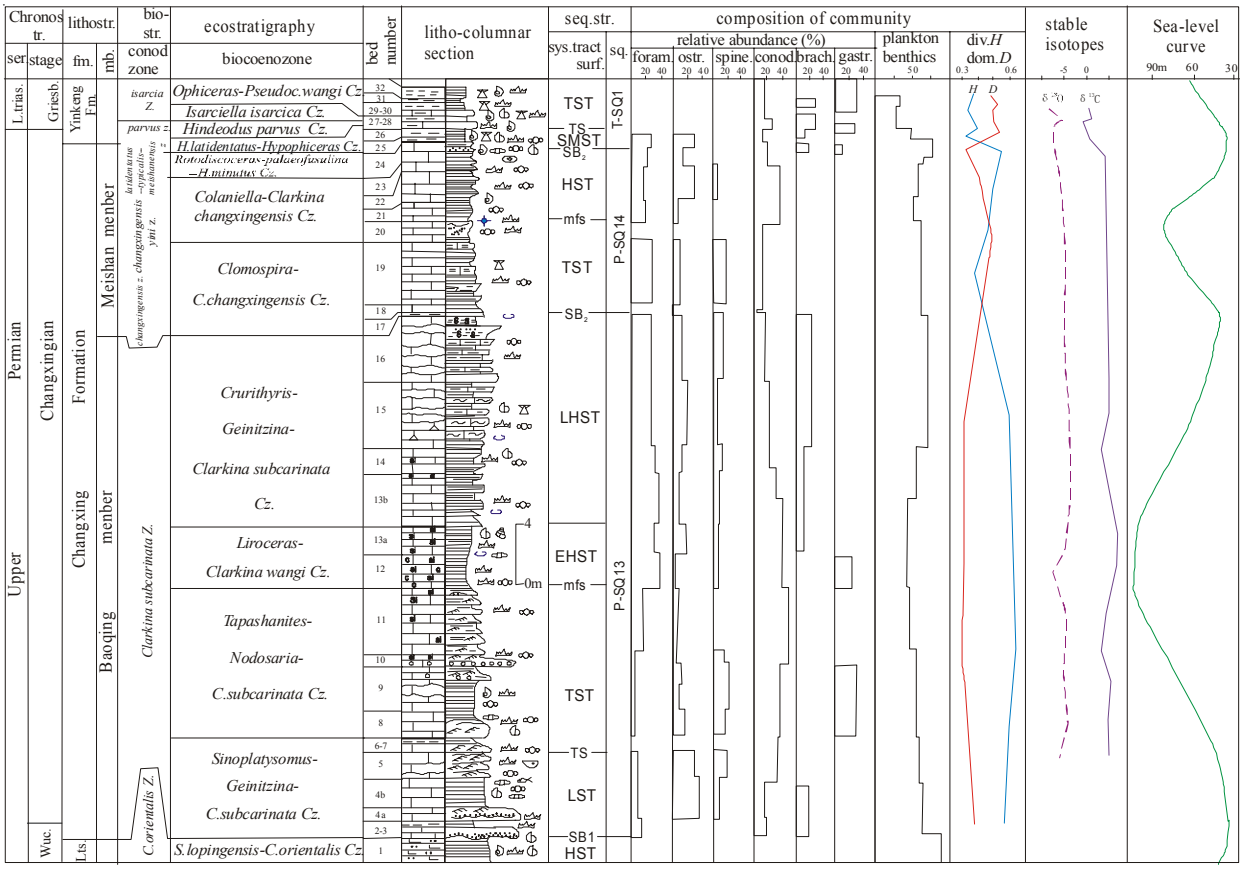

Figure 6. Changhsingian stratigraphical sequence at Meishan Section D

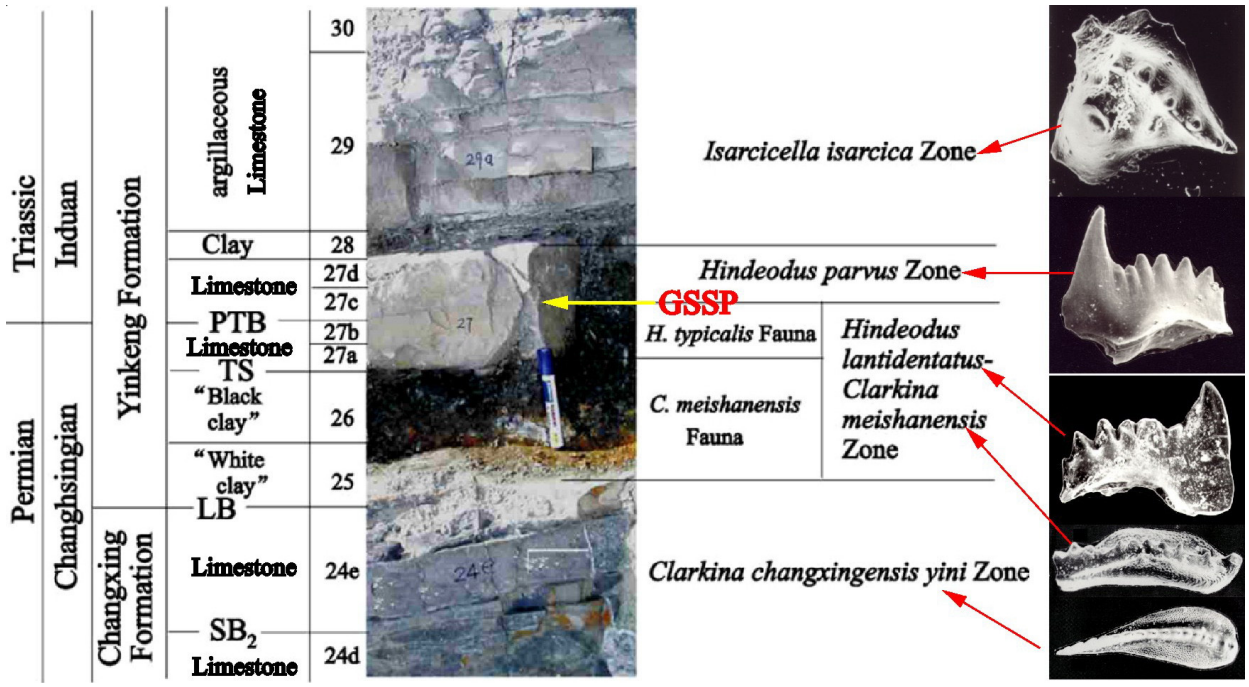

Figure 7. Permian-Triassic boundary sequence at Meishan Section D

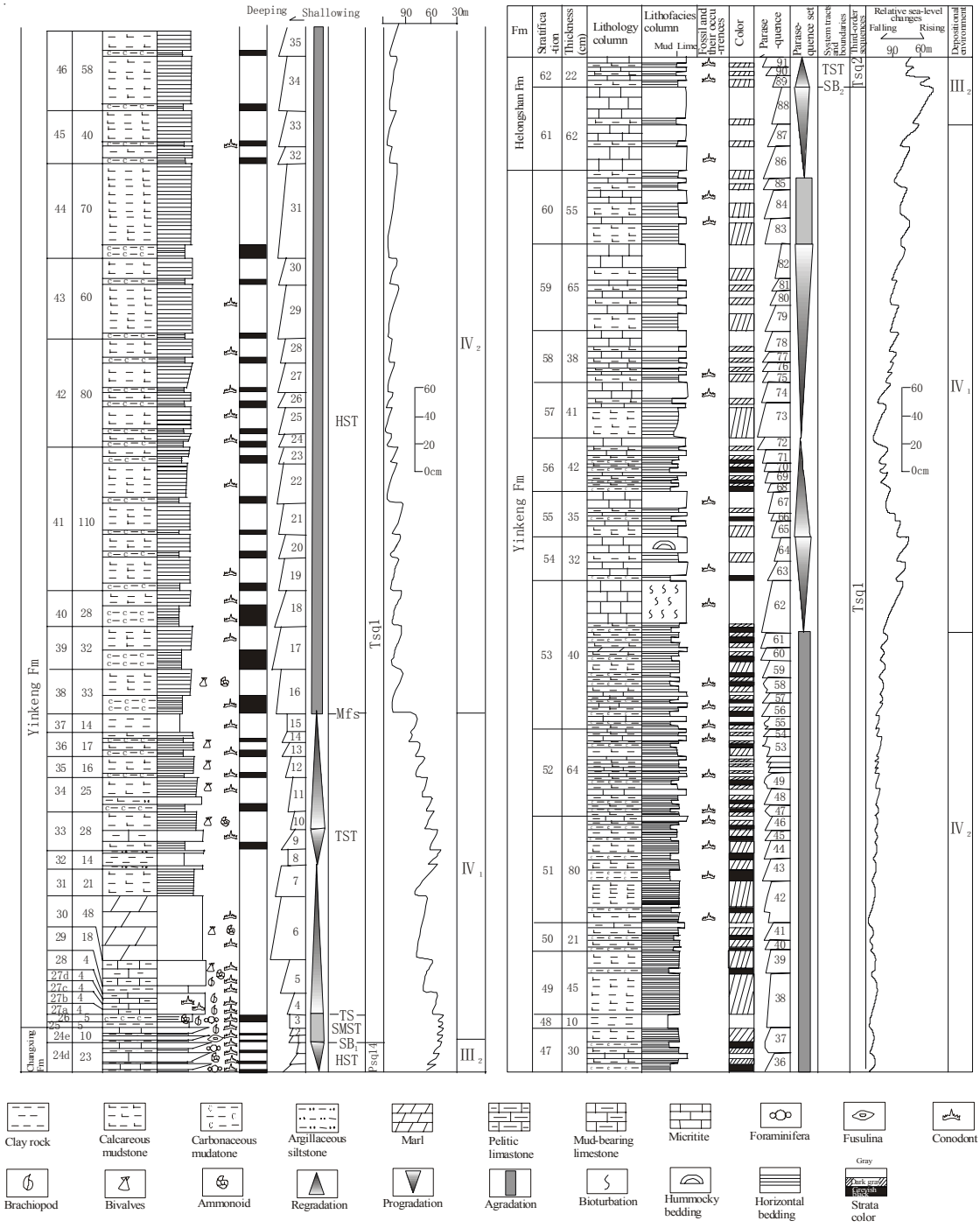

Figure 8. High-frequent cycles and sequence stratigraphy of the Yinkeng Formation at Meishan Section D

Hushan in Nanjing City, Jiangsu Province

Hushan is situated in the eastern suburb of the Nanjing City, Jiangsu Province, about 250 km to Meishan and 130 km to Chaohu (Fig. 1). The area belongs to the north limb of the Tangshan-Lunshan anticlinorium, which split into the Kongshan-Tianwangshan anticline and the Kongshan syncline. From Late Devonian to Early Triassic time, strata are recognized from the Kongshan-Hushan area as for Upper Devonian Wutung Formation and the Lower Carboniferous Kinling Formation, Kaolishan Formation, Hochou Formation and Laohudong Formation; the Upper Carboniferous Huanglung Formation and Carboniferous-Permian Chuanshan Formation; the Lower-Middle Permian Chihsia Formation and Kuhfeng Formation; the Upper Permian to Lower Triassic units which include Longtan Formation, Talung Formation, Xiaqinglong (Lower Qinglong) Formation and Shangqinglong) Upper Qinglong Formation. The Lower Triassic at Hushan is well developed, yielding rich fossils and relatively complete biostratigraphical sequence. It is one of the classic Lower Triassic sequences in South China and received considerable studies. The studies involve the lithostratigraphy, biostratigraphy, carbon and oxygen isotopic stratigraphy, and sedimentology. Special attention has been paid to the strata from the Permian-Triassic boundary to the lower

part of the Olenekian.

The visited Lower Triassic section is situated on the side of a quarry railway of the China Cement Plant, 25 km away from Nanjing City. A 4 km highway connects it with the Nanjing–Shanghai Expressway. It is the upward extension of the Carboniferous–Permian Kongshan section, including the Changhsingian Dalong Formation and Lower Triassic Xiaqinglong (Lower Qinglong) Formation and part of Shangqinglong (Upper Qinglong) Formation. The Dalong Formation was uncovered in a trend while the Lower Triassic is exposed in an abandoned quarry. However, the trend for the Dalong Formation had been filled and leveled up and the strata may not be seen on outcrop now. But the sequence of the Dalong Formation as well as its contact with the overlying Lower Triassic is quite similar to that in Chaohu we will visit during the symposium.

Dalong Formation

The Dalong Formation at the Hushan Section consists of cherty mudrocks with intercalated beds of cherty beds, micritic limestone and silty mudrock. It is the synchronous but heteropic deposits of the Changxing Limestone at the Meishan Section.

A large number of fossils are found at the section. Cephalopods, bivalves and brachiopods are common in the mudrocks, while conodonts are easily obtained in the limestones and the cherty limestone contains abundant radiolarians.

Cephalopods are mainly composed of *Pseudotirolites*, *Pseudogastrioceras*, *Pleuronodoceras*, *Hunanoceras*, etc.

The main bivalves are *Hunanopecten* spp.

Conodonts include *Neogondolella subcarinata* Zone and *N. changxingensis* Zone, which respectively correspond to the two conodont zones in the Changxing Formation at the Meishan Section.

Radiolarians found here comprise 8 species of 6 genera in Spumellina, such as *Copicyntrra akikawaensis*, *Copicyntroides asteriformis*, *Tormentun delicatum*, *Entactinosphaera*? *echinata*, *Quiqueremis robusta*, etc.

Permian and Triassic Boundary

The Permian-Triassic boundary sequence at the Hushan Section is described as follows:

Xiaqinglong (Lower Qinglong) Formation

19. Interbeds of brownish yellow medium-bedded argillaceous limestone and greyish blue thin-bedded mudrock, containing bivalves: *Pseudoclaraia wangi*, *Claraia* cf. *stachei*; ammonoids: *Ophiceras* sp., *Lytophiceras* sp.; and gastropods: (?)*Polygyrina* sp.....not ended

18. Greyish blue thin-bedded mudrock intercalated with marls, yielding bivalves: *Pseudoclaraia wangi*, *Claraia* cf. *stachei*, *Cl*. sp.; ammonoids: *Ophiceras* sp., *Lytophiceras* sp.; brachiopods: *Lingula* sp.; and gastropods: (?)*Polygyrina* sp.....1.71 m

17. Yellowish blue mudrock, containing ammonoids: *Ophiceras* sp.....0.95 m

16. Yellowish blue mudrocks intercalating thin-bedded brownish yellow dolomitic and argillaceous limestones, containing ammonoid *Ophiceras* sp., *Lytophiceras* sp.....0.64 m

15. Greyish yellow dolomitic and argillaceous limestone.....0.22 m

---------- conformity----------

Dalong Formation

14. Greyish blue mudrocks, yielding brachiopods: *Fusichonetes* sp., *Paryphella sulcatifera*, *Paracrurithyris pigmaea* .....0.06-0.08 m

13. Greyish yellow clay .....0.04 m

12. Dark grey and black siliceous mudrocks, yielding cephalopods: *Pseudotirolites* sp., *Hunanoceras* sp., *Qinglongites* sp., *Pseudogastrioceras* sp.; bivalves: *Hunanopecten exilis*, *H. qujingensis*.....not ended

Bed 13 of the section corresponds to the "Boundary Clay", but it is not so well-developed and typical as that at the Meishan Section. No fossils are found so far in the dolomitic and argillaceous limestone of Bed 15. According to the comparison of the lithologic characters of its overlying and underlying strata and the contained fossils, Bed 15 is considered corresponding to the lowest Triassic *I. parva* limestone of the Meishan Section. If so, the Permian-Triassic boundary should be in the middle of Bed 15.

Xiaqinglong Formation (Lower Qinglong Formation)

The Xiaqinglong Formation at this section mainly consists of mudrock and limestone. The relative ratios of the two types of rocks regularly change through the formation. In the lower part the greyish blue and yellowish blue mudrock is the principal rock type, with the intercalated beds of thin-bedded limestone and marl. Limestone increases upwards and its beds become thicker, with the decrease of mudrock. In the upper part the main rocks are the medium-bedded bluish grey limestone, intercalating thin-bedded yellowish grey marl and mudrock. The purplish red nodular limestone is the marker bed of the beginning of Shangqinglong (Upper Qinglong) Formation (Fig. 9).

This formation is about 175 m thick and composed of numerous rhythmic beds of mudrock (and calcareous mudrock) and limestone (or marl), which are combined regularly into a series of cycles of mudrock to limestone. The cycles in the lower part of the formation are mostly mudrock, and every cycle begins with mudrock, generally intercalating few thin beds of argillaceous limestone,

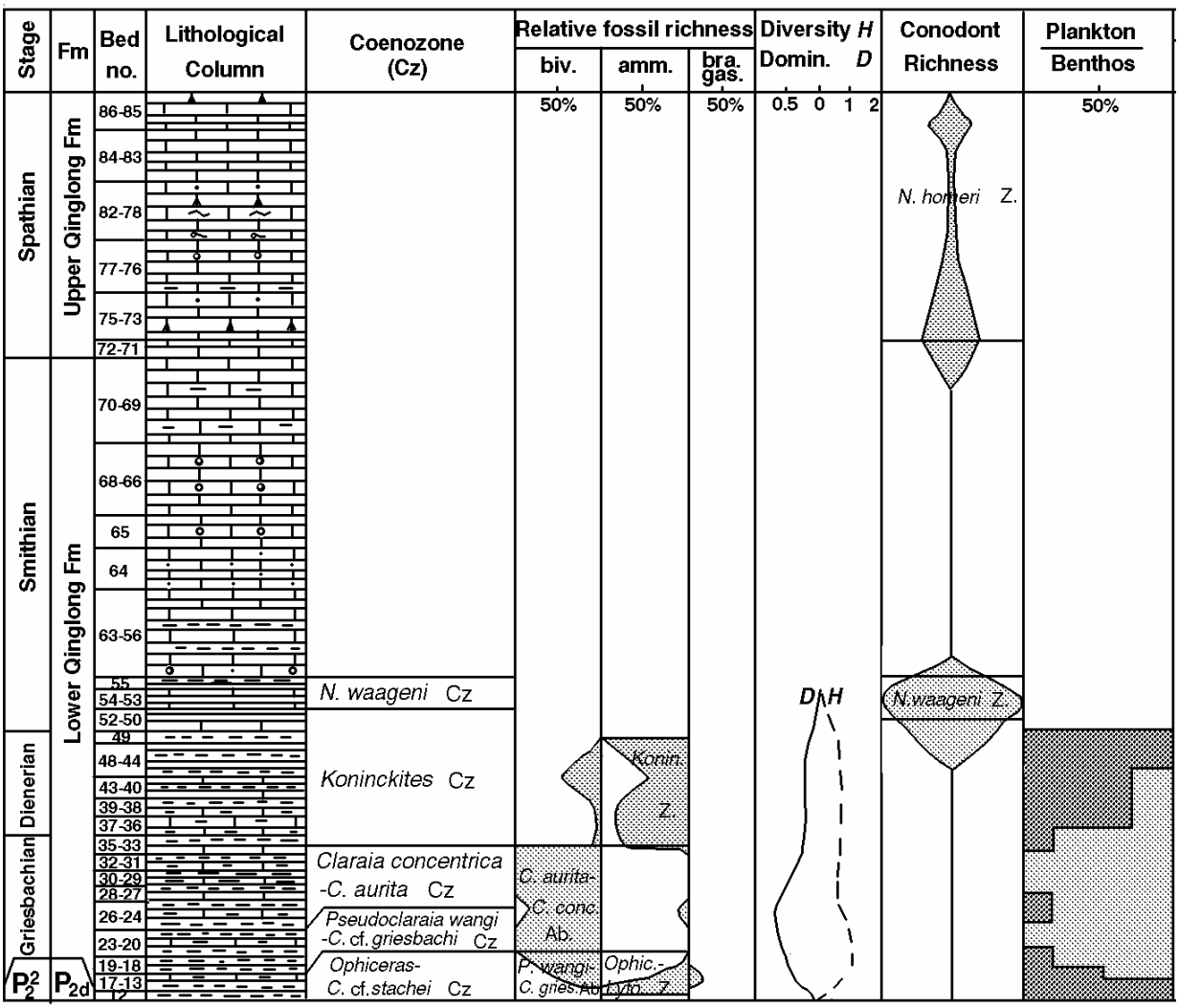

Figure 9. Lower Triassic stratigraphical sequence of the Hushan Section

and ends with interbeds of mudrock and limestone or with thin-bedded limestone intercalating mudrock (Fig. 10a). However, the cycles of the upper part in the formation are mainly composed of limestone, each beginning with mudrock, which is commonly thin, or with marl and ending with medium- to thick-bedded micritic limestone (Fig. 10b). The cycles are usually 0.5 m thick in the lower part but generally over 2m in the upper part. These cycles may correspond to the Milankovitch cyclicity.

The major fossils found in the formation of this section are ammonoids and bivalves in the mudrocks and conodonts in the limestones.

Ammonoids: In the lower part *Ophiceras* and *Lytophiceras* are easily seen; and *Koninckites* and *Flemingites* occur in the middle.

Bivalves: *Pseudoclaraia wangi*, *Claraia* cf. *stachei* and *Cl. griesbachi* are rich in the lower part; *Claraia aurita* and *Cl. concentrica* come later in the middle part; and *Posidonia circularis* and *Guichiella angulata* are mainly found in the upper part of the formation.

Conodonts: So far they are only found in the upper part of Xiaqinglong Formation and the lower part of Shangqinglong Formation at this section, including *Neospathodus waageni*, *N. dieneri*, *N. homeri*, *N. spathi*, *Ellisonia* sp., *etc*.

Induan-Olenekian Boundary

Tong et al. (2003) proposed the West Pingdingshan Section in Chaohu, Anhui Province as a GSSP candidate for the Induan-Olenekian boundary stratotype and the first appearance datum (FAD) of conodont *Neospathodus waageni* as the preferred index to define the boundary. This datum lies 26 cm below the FAD of the ammonoids *Flemingites* and *Euflemingites*, and is located slightly prior to the top of the second Triassic normal magnetozone, and the peak of the first Triassic positive excursion of carbon isotope $\delta^{13}C$.

During the Early Triassic Hushan was on the same carbonate ramp as Chaohu and a correlative Induan-Olenekian boundary sequence defined by conodont *Neospathodus waageni* and ammonoid *Flemingites* can be well identified at the Hushan Section, which is about 45 m above the Permian-Triassic boundary (Fig. 9).

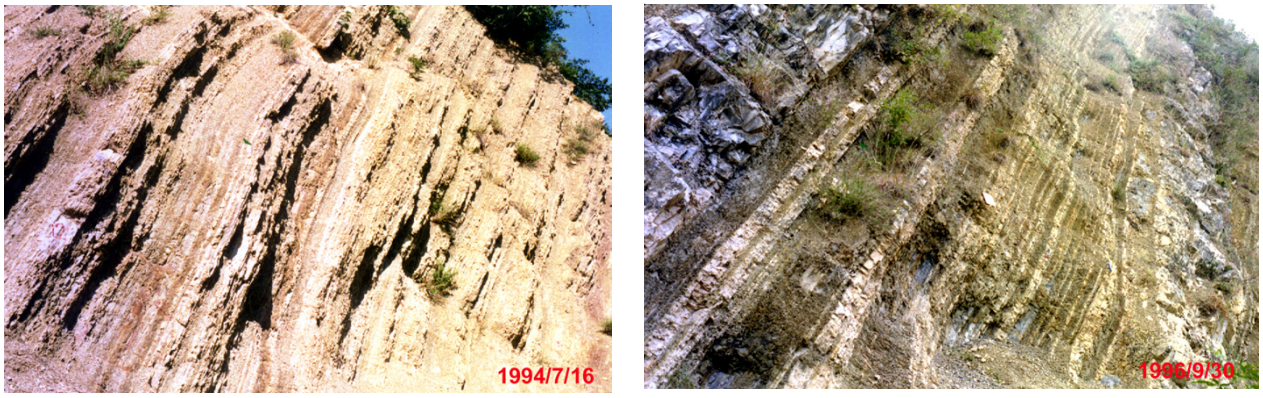

Figure 10. Lithological cycles in the Xiaqinglong Formation at the Hushan Section

Reference

Chen Xu, Wang Haifeng and C.H. Holland, 2000. Geological history of the Nanjing Hills –A guide for overseas geologists. Labortory of Palaeobiology and Stratigraphy, Nanjing.

Jin Y G., Henderson C., Wardlaw B. et al., 2005. Proposal for the Global Stratotype Section and PointGSSPfor the Wuchiapingian-Changhsingian Stage boundary (Upper Permian Lopingian Series). Permophiles, 2005, 1-17.

Sheng Jinzhang, Chen Chuzhen, Wang Yigang, Rui Lin, Liao Zhuoting, Yuji Bando, Ken-ichi Ishii, Keiji Nakazawa and Koji Nakamura, 1984, Permian-Triassic boundary in middle and eastern Tethys: Jour. Fac. Sci. Hokkaido Univ., Ser., 133-181.

Sheng Jinzhang, Chen, C. Z., Wang, Y. G., Rui, L., Liao, Z. T., He, J. W., Jiang, N. Y. and Wang, C. Y., 1987. New advances on the Permian and Triassic boundary of Jiangsu, Zhejiang and Anhui. *In* Nanjing Institute of Geology and Palaeontology, Academia Sinica (ed.), Stratigraphy and Palaeontology of Systemic boundaries in China. Permian-Triassic Boundary, (1): 1-22. Nanjing Univ.

Tong Jinnan, 1997, A study of the Griesbachian cyclostratigraphy of Meishan Section, Changxing, Zhejiang Province. The International Conference on Stratigraphy and Tectonic Evolution of Southeast Asia and South Pacific. Bangkok, Thailand 19-24 August 1997. 158-163.

Tong Jinnan, Yang Yin, 1998, Advance in the Study of the Lower Triassic Conodonts at Meishan Section, Changxing, Zhejiang Province. Chinese Science Bulletin, 43(16): 1350-1353.

Tong Jinnan, Zakharov, Y. D., Orchard, M. J., Yin Hongfu, Hansen, H. J., 2003. A candidate of the Induan-Olenekian boundary stratotype in the Tethyan region. Science in China (Series D), 46(11): 1182-1200.

Yang Zunyi, Yin Hongfu, Wu Shunbao, Yang Fengqing, Ding Meihua, Xu Guirong et al., 1987, Permo-Triassic Boundary Strata and Fauna of South China. Geological Publishing House, Beijing.

Yin H. F., Wu S. B., Ding M. H. et al, 1996. Th Meishan section, candidate of the Global Stratotype Section and Point of Permian-Triassic Boundary. In: Yin, H. F, (ed), The Palaeozoic-Mesozoic Boundary Candidates of Global Stratotype Section and Point of the Permian-Triassic Boundary. China University of Geosciences Press, Wuhan. 31-48.

Yin H., Sweet W. C., Glenister B. F., Kottlyar G., Kozur H., Newell N. D., Sheng J. Yang Z. and Zakharov Y. D., 1996. Recommendation of the Meishan section as Global Stratotype Section and point for basal boundary of Triassic System. Newl. Stratigr. 34(2): 81-108.

Yin Hongfu, Zhang Kexin, Tong Jinnan, Yang Zunyi, Wu Shunbao, 2001. The Global Stratotype Section and Point (GSSP) of the Permian-Triassic boundary. Episodes, 24(2): 102-114.

Triassic in Chaohu, Anhui Province
Guide to the Mid-Symposium Field Excursion of the International Symposium on the Triassic Chronostratigraphy and Biotic Recovery (23-25 May 2005, Chaohu, China)

Tong Jinnan* and Zhao Laishi

*State Key Laboratory of Geological Processes and Mineral Resources, China University of Geosciences, Wuhan 430074, China; *jntong@cug.edu.cn*

1. Location and traffic

Chaohu is located in the southeastern China. It is a mid-size city of Anhui Province with a population of about 840 000. The city town is on the lakeside of Chaohu Lake and the visited Lower Triassic sequences are in the suburb of the city, 5-6 km from the center of the town. Chaohu has a good traffic to connect with some big cities by railway and freeway, within one hundred kilometers to the Hefei City, capital of Anhui Province, and to the Nanjing City, capital of Jiangsu Province, and about 180 km to the northwest of the Meishan Section, where the GSSP of the Permian-Triassic boundary is located.

Geologically, Chaohu was situated in the northern margin of the Lower Yangtze block (Fig. 1). During the Early Triassic it was on a deep part of the Lower Yangtze carbonate ramp in the low-latitude eastern Tethys archipelago (Yin et al., 1999; Tong and Yin, 2001).

2. General geology

In the stratigraphical provincialism Chaohu belongs to the Lower Yangtze Stratigraphical Province. The stratigraphical sequence is preserved from the Upper Sinian (Ediacaran) to Middle Triassic except for the Lower and Middle Devonian though evident parallel unconformities exist between the Silurian and Devonian and between Lower and Upper Carboniferous. Since the area was on a stable platform (Lower Yangtze Block), the total sequence is not very thick, less than 3 000 meters. In lithology the strata from the Upper Sinian to Middle Ordovician and from Carboniferous to Middle Triassic are mainly composed of carbonate rocks while the Silurian and Upper Devonian are predominated by clastic rocks. All the strata were folded synchronously during the Indosinian Movement (Late Triassic). Since the Middle Triassic the marine sedimentation had ended and the area received terrestrial sediments or is eroded.

The Triassic of Chaohu is exposed mainly in Mt.

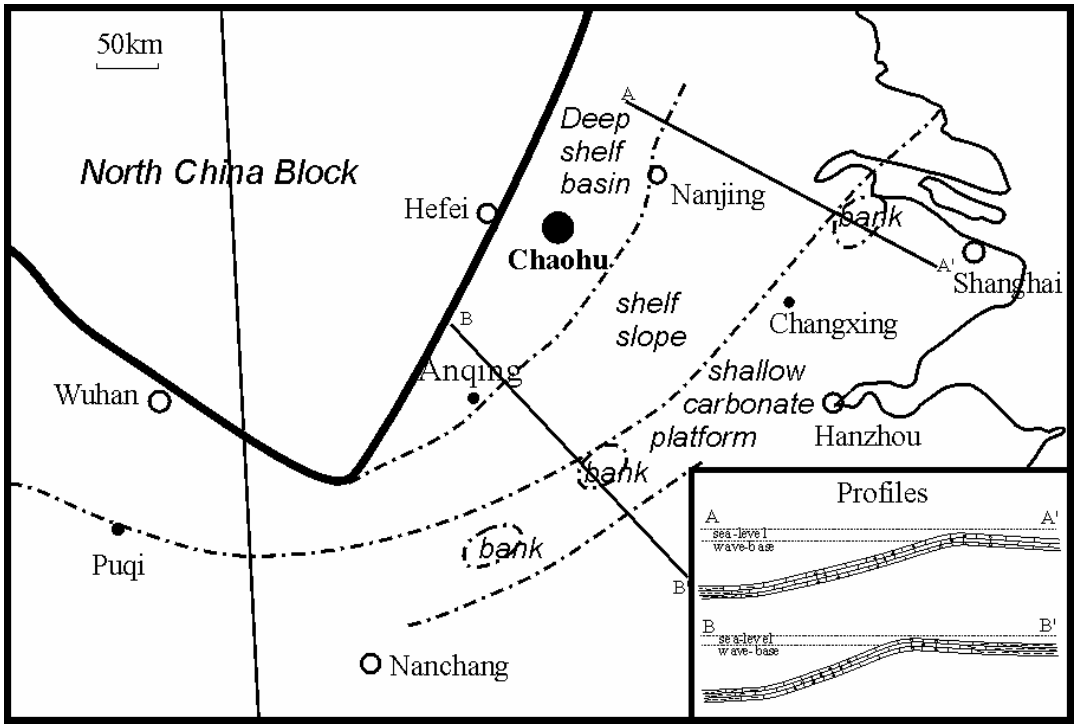

Figure 1. Induan paleogeography of the Lower Yangtze region and location of Chaohu

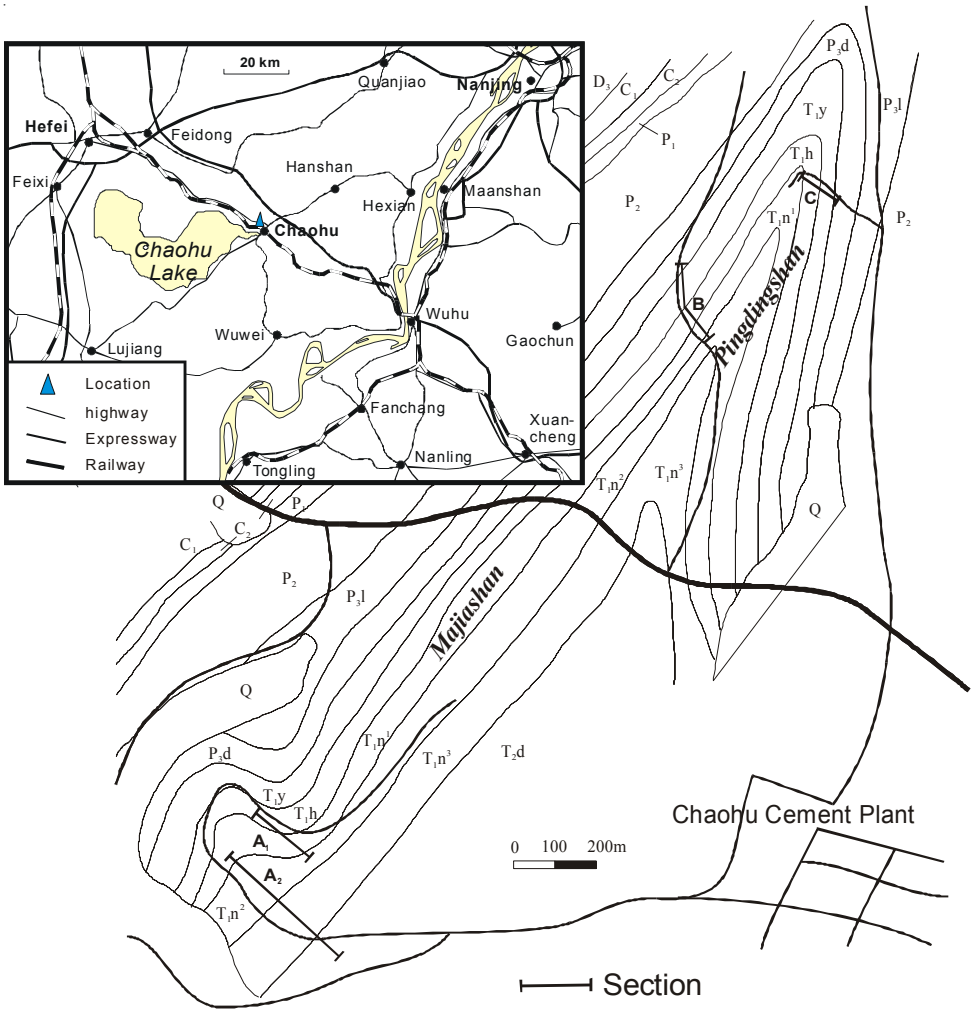

Figure 2. Location map of Chaohu and geological map of Mt. Pingdingshan-Mt. Majiashan
D_3-Upper Devonian, C_1-Lower Carboniferous, C_2-Upper Carboniferous, P_1-Lower Permian, P_2-Middle Permian, P_3l-Upper Permian Longtan Formation, P_3d-Upper Permian Dalong Formation, T_1y-Lower Triassic Yinkeng Formation, T_1h-Lower Triassic Helongshan Formation, T_1n^1, T_1n^2, T_1n^3-Lower, Middle, Upper Member of Lower Triassic Nanlinghu Formation, T_2d-Middle Triassic Dongmaanshan Formation, Q-Quaternary; A_1+A_2-South Majiashan Section, B-West Pingdingshan Section, C-North Pingdingshan Section

Majiashan and Mt. Pingdingshan north to the Chaohu Lake and the Yingping-Qingshuitang area south to the Chaohu Lake and it usually forms the cores of synclines. The best-studied Lower Triassic sections are in the north of the Chaohu Lake (Fig. 2). The Majiashan - Pingdingshan Syncline is a synclinorium with an axis in NE 30°. The syncline becomes broader southwards from Mt. Pingdingshan to Mt. Majiashan. The youngest rock in the core is the Middle Triassic, which exists only in the southern part of the syncline. The limbs are composed of the strata from the Lower Triassic to Lower Silurian with different modes of occurrence. The strata in both limbs incline westward in the southern part of the syncline and the dip angle of the west limb is over 68° while the angle of the east limb is 50-60°. The limbs are of a normal occurrence in the northern part of the syncline. Thus in the studied Triassic sections the complete sequence from the Upper Permian to Middle Triassic occurs only in Mt. Majiashan, the southern part of the syncline, but the Upper Permian-Lower Olenekian sequence is also very excellent in Mt. Pingdingshan.

3. Triassic lithostratigraphical sequence

In lithostratigraphy the Triassic of Chaohu is composed of four formations in an ascending order: Yinkeng Formation, Helongshan Formation, Nanlinghu Formation and Dongmaanshan Formation, among which the former three mainly belong to the Lower Triassic while the latter one is the Middle Triassic but the most upper part of the Dongmaanshan Formation was eroded in the area (Fig. 3). The underlying uppermost Permian unit is the Dalong Formation, which consists of thin-bedded cherty beds and cherty mudstone. The Dalong Formation is the same age with the Changxing Formation but formed in a different facies.

The Triassic of Chaohu was formed in a deeper part of the Lower Yangtze carbonate ramp and composed of carbonate rocks and some fine-grained mudstone and shale. The Yinkeng and Helongshan Formations are mostly interbeds of limestone and mudstone or shale, which form multiple scales of cycles. The condensed and close-spaced thin-bedded alternations of limestone and mudstone usu-

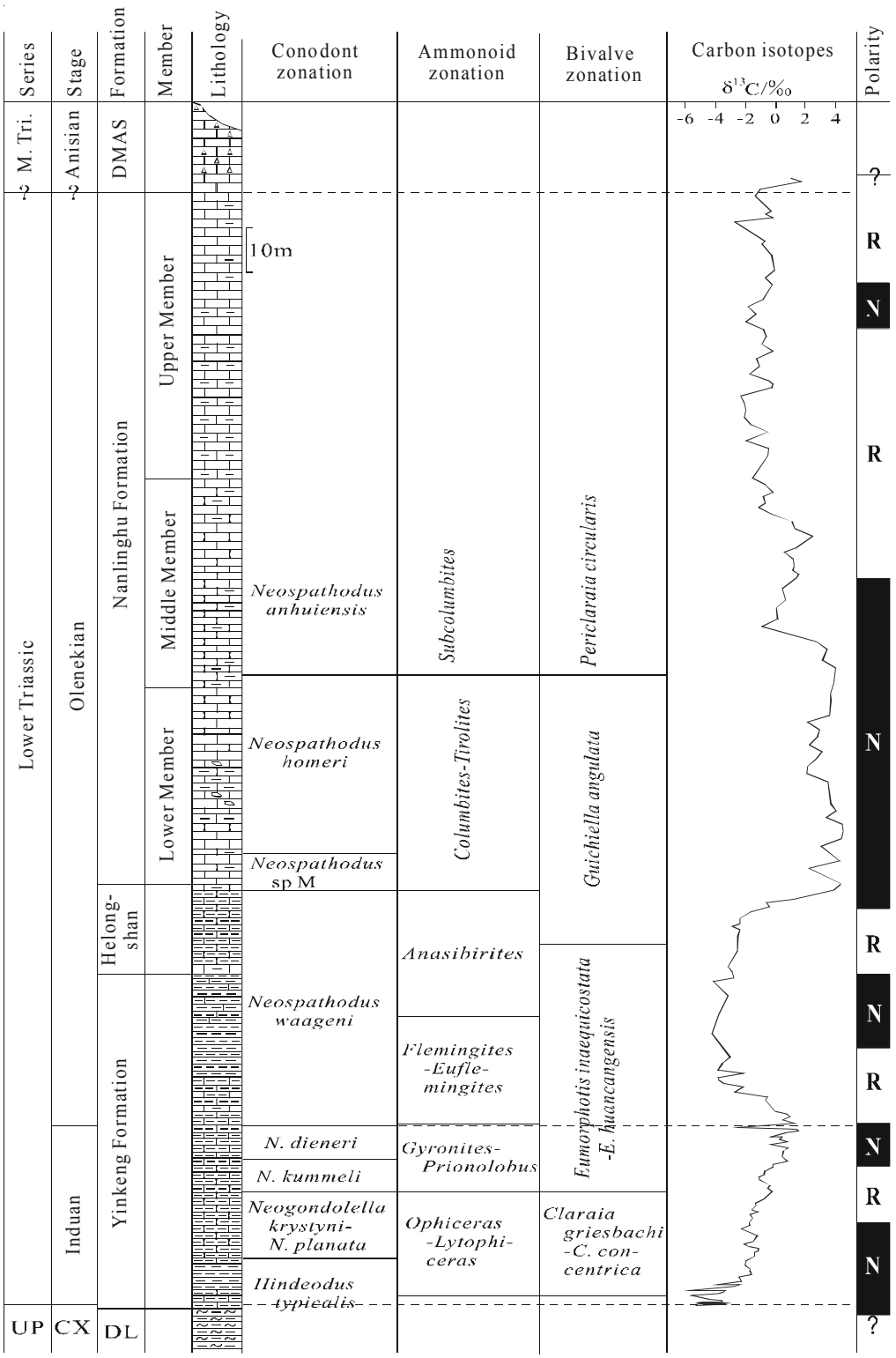

Figure 3. Integrated Lower Triassic sequence of Chaohu, Anhui Province (From Tong et al., 2005b)
UP-Upper Permian, CX-Changhsingian, DL-Dalong Formation, DMAS-Dongmaanshan Formation; N-normal polarity zone, R-reversal polarity zone

ally constitute a specific "nodular limestone". The Nanlinghu Formation is mainly composed of thick-bedded limestone or nodular limestone and intercalated thin-bedded limestone or shale.

Yinkeng Formation: It is mostly composed of alternations of mudrock (shale) and thin-bedded limestone, intercalated by some medium-bedded limestone in the lowest and upper parts and sometimes by some thin beds of marlstone or nodular limestone in the middle and upper parts. The mudrock and limestone usually appear in a series of multiple mudrock-limestone cycles, but the formation is relatively dominated by argillaceous component. The Yinkeng Formation is well exposed at Mt. Pingdingshan, but it is also observable at some quarries in Mt. Majiashan. The formation is about 75 m thick and

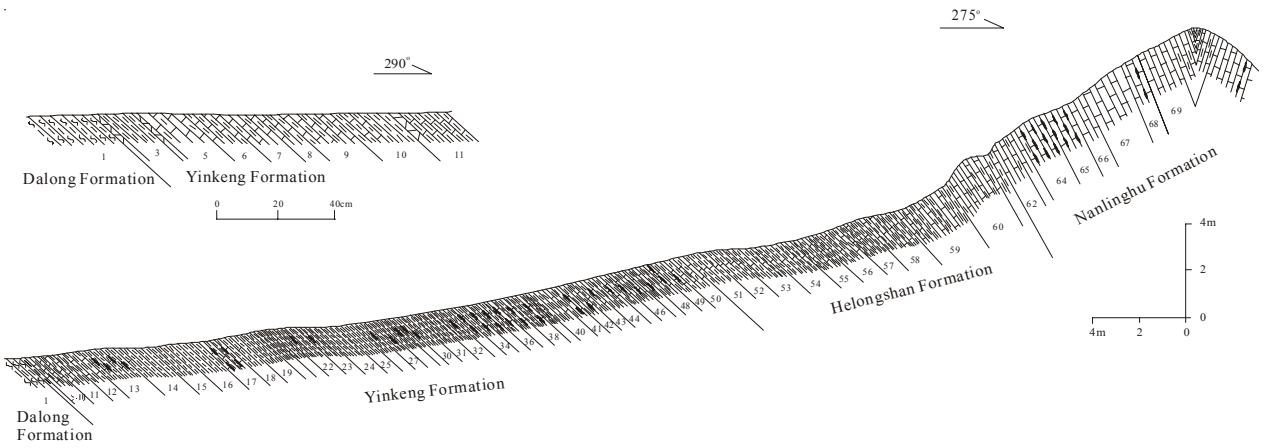

Figure 4. Lower Triassic profile of the North Pingdingshan Section

contains rich ammonoid, bivalve and conodont fossils.

Helongshan Formation: It is chiefly composed of the rhythmic alternations of thin-bedded mudrock and limestone except for two thick beds of limestone at the base which mark the beginning of the formation. The formation is relatively thin, only about 20 m thick, and exposed well at all the sections in Chaohu. It is relatively dominated by an argillaceous component and the rocks are thin-bedded and the thin limestone beds sometimes become lenticular or nodular, thus forming nodular limestones. The fossils are quite rich in this formation, including ammonoids, bivalves, conodonts and bony fishes.

Nanlinghu Formation: It consists mainly of thick-bedded limestone and nodular limestone, interbedded with medium- to thin-bedded limestone and very thin mudrocks. The cyclic bedding is formed by regular sequence of various thicknesses of the limestone beds or by the alternation of limestone and mudrock. This formation is much thicker, about 150 m, than the two lower formations and it is entirely exposed only at the South Majiashan Section. Three members are recognized. The Lower Member is about 44 m thick at the South Majiashan Section and composed of the cycles of medium- to thick-bedded limestone and relatively thin beds of greenish gray mudstone. The Middle Member, about 47 m thick, includes two parts where the lower part consists of interbeds of purplish brown medium- to thick-bedded nodular limestone and relatively thin beds of dark gray mudstone while the upper is of interbeds of dark gray thick-bedded limestone or limestone with argillaceous bands and black mudstone. The Upper Member consists of cyclic beds of grayish thick-bedded limestone and very thin mudrocks. The formation is clearly dominated by limestone with some intercalated beds of fine-grained breccia limestone in the lower part formed by distal storm or turbidite, and some dolomitic beds at the top partly formed due to the closure and evaporation in the basin. The Nanlinghu Formation was obviously formed at a much higher depositional rate but it still contains rich fossils, though not as many as in the two lower formations. It includes ammonoids, bivalves, conodonts, as well as some bony fishes and reptiles.

Dongmaanshan Formation: It is not fully preserved in Chaohu and its preserved thickness is about 100 m. It is composed mainly of evaporites such as dolomite, dolomitic limestone and evaporite-solution breccias; its base is observed in Mt. Majiashan, esp. at the South Majiashan Section.

4. North Pingdingshan Section

At this section observed are the strata from the Upper Permian Longtan Formation to the Lower Member of the Nanlinghu Formation though the coal-measure of the Longtan Formation and the lower part of the Dalong Formation are not fully outcropped. The sequence from the Permian-Triassic boundary to the lower Olenekian (Fig. 4) has been studied since 1990's, mainly covering the biostratigraphy and carbon isotope stratigraphy. The section ends at the core of the syncline and the youngest strata are the early Olenekian Nanlinghu Formation (Lower Member).

Most recent studies on the Permian-Triassic boundary in the area are at this section and the boundary sequence is as follows (Fig. 5):

Yinkeng Formation

14 Yellowish green or yellow thin-bedded calcareous mudstone. Conodonts: *Neogondolella planata*, *N.* sp.; Ammonoids: *Prionolobus* cf. *paralibita*; Bivalves: *Claraia concentrica*, *C.* sp. 2.20m

13 Interbeds of nodular limestone and medium- to thin-bedded calcareous mudstone. Conodonts: *Hindeodus typicalis*, *H.* sp., *Neogondolella planata*, *N.* sp.; Ammonoids: *Lytophiceras* cf. *chamnda*, *L.* sp., *Prionolobus* sp.; Bivalve: *Claraia hunanica*, *C. griesbachi*.....2.10m

12 From bottom to top: gray medium- or thick-bedded argillaceous limestone – yellowish green thin-bedded calcareous mudstone – yellow marl – yellowish green thin-bedded calcareous mudstone. Conodonts: *Hindeodus typicalis*, *H.* sp.; Ammonoids: *Lytophiceras* sp.; Bivalves:

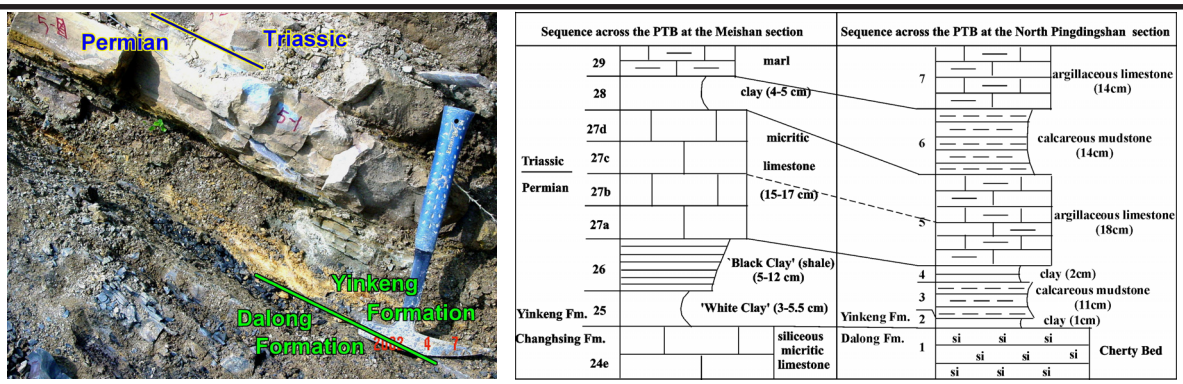

Figure 5. Permian-Triassic boundary at the North Pingdingshan Section and its correlation with that at Meishan Section D

Claraia hunanica, *C. griesbachi*.....0.88m

11 Yellow claystone and yellowish green calcareous mudstone intercalated by medium-bedded marlstone. Conodonts: *Hindeodus typicalis*, *H.* sp.; Ammonoids: *Ophiceras demissum*, *O.* sp.....0.90m

10 Yellowish green thin-bedded calcareous mudstone, intercalated by medium-bedded marlstone.....0.20m

9 Gray medium-bedded marlstone. Conodonts: *Hindeodius* sp.....0.20m

8 Yellowish green thin-bedded calcareous mudstone. Conodonts: *Hindeodus typicalis*, *H.* sp.....0.09m

7 Grayish medium- to thick-bedded argillaceous limestone. Conodonts: *Hindeodus* sp., *Neogondolella planata*, *N. carinata*, *N.* sp.....0.14m

6 Yellowish green thin-bedded calcareous mudstone. Conodonts: *Hindeodus* sp. 0.14m

5 Grey or yellowish brown (weathered) medium-bedded argillaceous limestone. Conodonts: *Hindeodus typicalis*, *H.* sp.....0.18m

4 Grayish brown or yellow claystone.....0.02m

3 Grayish green thin-bedded calcareous mudstone. Conodonts: *Neogondolella changxingensis*, *Hindeodus typicalis*, *H.* sp. 0.11m

2 Yellowish orange claystone.....0.02m

Conformity

Dalong Formation

1 Grayish black thin-bedded cherty mudstone with rich small-sized brachiopods. Ammonoids: *Pleuronodoceras attenuatum*, *Sinoceltites* sp.

Conodont *Hindeodus parvus* has not found at the section yet, but the Permian-Triassic boundary is believed in the middle of Bed 5, which is a medium bed of argillaceous limestone, according to the correlation to the boundary sequence ("Permian-Triassic boundary set") at Meishan Section D (Peng et al., 2001). The study of carbon isotopes indicates that the $\delta^{13}C$ values are very negative in the Permian-Triassic boundary and lowermost Triassic strata at the North Pingdingshan Section (Tong et al., 2002). All the samples from the boundary strata, including those from Bed 5 and the topmost Dalong Formation, show a positive magnetic polarity (Tong et al., 2005b).

5. West Pingdingshan Section

At this section outcropped are the strata from the Gufeng Formation (Middle Permian) to the Middle Member of the Nanlinghu Formation though the continuous sequence is from the upper part of the Longtan Formation (Upper Permian) to the Lower Member of the Nanlinghu Formation. The Lower Triassic sequence (Fig. 6) is well correlative with the North Pingdingshan Section but better studied. The study at this section involves the biostratigraphy, carbon isotope stratigraphy, magnetostratigraphy, cyclostratigraphy, and the major part of the integrated Lower Triassic sequence of Chaohu is based upon the studies at this section (Fig. 3).

There are at least two aspects noticeable and attractive at this section. One is the lithological rhythm and the other is the Induan-Olenekian boundary sequence, which is proposed as the candidate GSSP of the boundary (Tong et al., 2003, 2004).

The lower Triassic at the section shows a persistent rhythmic repetition of couplets composed of ~50 cm mudstone and ~10 cm limestone beds (Fig. 7a). It is impossible not to notice the rhythmic bedding, and the consistency of bed thicknesses is characteristic of orbital forcing. The

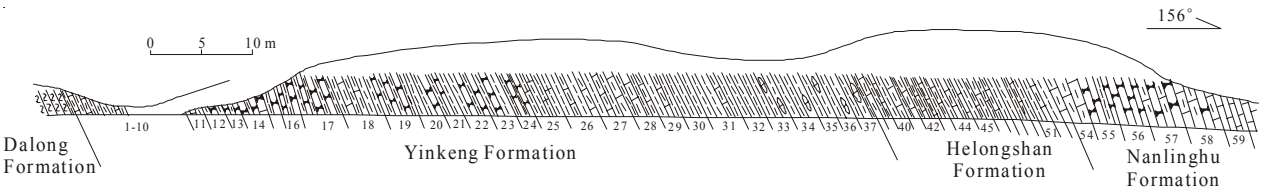

Figure 6. Lower Triassic profile of the West Pingdingshan Section

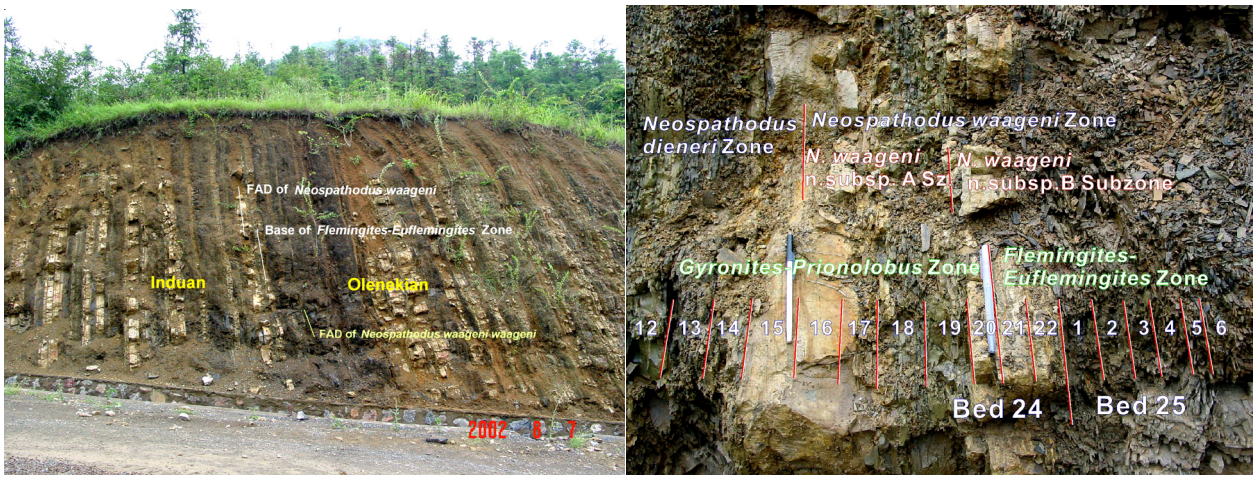

Figure 7. Induan-Olenekian boundary at the West Pingdingshan Section

rhythmic lithologic variations are captured nicely in the magnetic susceptibility record (Cramer, personal comm.) and organic carbon isotopes (see the abstracts for this symposium). Assuming that the ~m-scale lithologic rhythm is the result of precessional forcing, systematic variations in the strength of the mudstone/limestone contrast and in the relative thicknesses of the mudstone versus limestone beds most likely reflect modulation by eccentricity. Both the short and long eccentricity components should be evident, as well as m.y.-scale eccentricity components. There is also a cyclicity in the carbon isotope record that may be consistent with eccentricity (Tong et al., 2005a).

The Induan-Olenekian boundary defined by ammonoid *Flemingites-Euflemingites* Zone and conodont *Neospathodus waageni* is around Bed 24/Bed 25 boundary at the section (Fig. 7). Bed 24 is subdivided into 22 subbeds and Bed 25 is into 33 subbeds. The boundary between ammonoids *Gyronites-Prionolobus* Zone and *Flemingites-Euflemingites* Zone is at the base of Subbed 24-21, while the base of conodont *Neospathodus waageni* Zone is at the base of Subbed 24-16. In the *Neospathodus waageni* group three forms (subspecies or even species) can be well recognized at least in Chaohu (Zhao et al., 2004) and they are herein named *N. waageni* n.subsp.A, *N. waageni* n.subsp.B and *N. waageni waageni*. The three forms occur at the section in an ascending order. The FAD of *N. waageni* n.subsp.A is in Subbed 24-16, 26 cm below the FAD of ammonoid *Flemingites*; the FAD of *N. waageni* n.subsp.B is in Subbed 24-20, 3 cm below the ammonoid boundary; and the FAD of *N. waageni waageni* is in Subbed 25-10, 48 cm above the ammonoid boundary.

In addition, the Smithian-Spathian boundary can be well observed at this section if it is defined by conodont *Neospathodus homeri* or *N.* n. sp. M, which can be correlated with ammonoid *Columbites-Tirolites* Zone. At the West Pingdingshan Section the FAD of *N. homeri* is in Bed 56, about 5 m above the base of the Nanlinghu Formation, while the FAD of *N.* n. sp. M is in Bed 52, about 1.5 m below the lithostratigraphical boundary (Fig. 8a). No typical Spathian ammonoids have been collected at this section but they co-occur at the South Majiashan Section.

6. South Majiashan Section

This is the classic Majiashan Section and a lot of works had been done at this section in early years (see Tong et al., 2001a, b for summary). Since the Permian-Triassic boundary and the lowermost Triassic dominated by

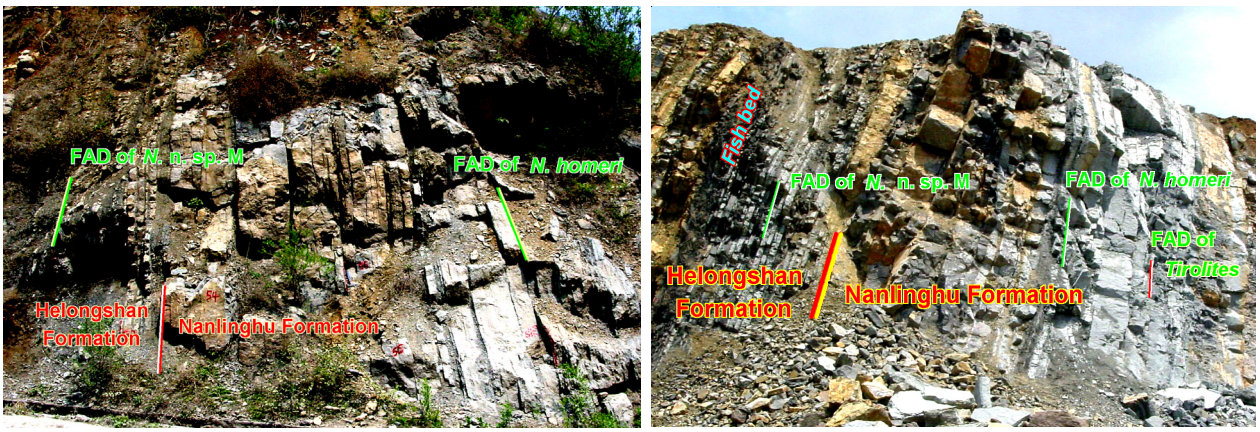

Figure 8. Smithian-Spathian boundary at the West Pingdingshan Section (a) and South Majiashan Section (b)

mudrocks have been heavily covered, studies are mainly in the middle and upper parts at the section recent years. The visited section includes a newly quarried profile, which covers the uppermost Yinkeng Formation, Helongshan Formation and lower Nanlinghu Formation, and some abandoned quarries, which outcrop the most part of the Nanlinghu Formation till the base of the Dongmaanshan Formation (Fig. 9).

The outcropped Yinkeng Formation is about 20 m at the section; the Helongshan Formation is 20 m; and the Nanlinghu Formation composed mainly of limestone is much thicker, about 186 m. The Smithian-Spathian boundary observed at this section (Fig. 8b) is very similar to that at the West Pingdingshan Section. It is noticeable that a black shale bed just below the boundary contains rich lenticular limestone concretions, in which fish fossils are usually found. A same "fish bed" exists at the West Pingdingshan Section, too.

Another well-known marine vertebrate assemblage is also found at this section, that is *Chaohusaurus* sp. (Young and Dong, 1972; Chen, 1985; Motani and You, 1998), which is one of the oldest ichthyosaurs. These marine reptiles are yielded in the upper part of the Nanlinghu Formation.

The Olenekian-Anisian boundary is placed at the base of the Dongmaanshan Formation in the area according to a regional correlation (Li and Ding, 1981). However, no typical Anisian fossils have been observed in Chaohu by now though the uppermost Lower Triassic conodont *Neospathodus anhuinensis* Zone and ammonoid *Subcolumbites* Zone occur early in the Middle Member of the Nanlinghu Formation, which is about 100 m below the top of the Nanlinghu Formation (Fig. 3).

7. Biostratigraphy

The Lower Triassic of Chaohu contains rich ammonoids, conodonts and bivalves throughout the Lower Triassic, which constitute complete biostratigraphical sequences. Marine vertebrates such as bony fishes and ichthyosaurs as well as trace fossils are rich at some horizons. In biostratigraphy Chaohu is one of few areas with both continuous Lower Triassic conodont and ammonoid sequences.

Though ammonoids are very common in many horizons of the Lower Triassic, most fossils are unfortunately preserved in mould without suture lines recognizable, thus an exact specific identification is generally difficult. So the ammonoid biostratigraphy is usually defined at a generic level (Guo and Xu, 1980; Tong et al., 2004; Tong and Zakharov, 2004). Six ammonoid zones can be well defined (Fig. 3) and correlated throughout South China (Tong and Yin, 2002).

Conodonts have been retrieved from most horizons of the Lower Triassic in Chaohu but most fossils, esp. Pa element, are from limestones and they are relatively rare in mudrocks. However, conodonts from the upper part of the Lower Triassic are much less than the lower part though they occur through all the sections. Eight conodont zones can be well defined in the Lower Triassic of Chaohu (Fig. 3), most of which are global conodont zones proposed by Sweet et al. (1971) except for the lower Spathian *Neospathodus* n. sp. M Zone and upper Spathian *N. anhuinensis* Zone established based upon the data from Chaohu. The first conodont *Hindeodus typicalis* Zone across the Permian-Triassic boundary is used here as no *Hindeodus parvus* is found in the boundary strata yet.

Bivalves are very common in the strata, esp. forming "shelly beds" in some mudrocks. They are also preserved in mould and mostly compressed thin-shelled scallops. Four bivalve zones can be recognized (Fig. 3), among which the lower two zones are correlative throughout South China while the upper two are more or less restricted in the Lower Yangtze region.

8. Carbon isotope excursion

All three Lower Triassic sections have been continuously sampled for carbonate carbon isotopes study. All the curves show a very good correlation (Fig. 10). The $\delta^{13}C$ excursion through the Lower Triassic expresses a very close relation to the ecological evolution in the aftermath of the end-Permian mass extinction and environmental

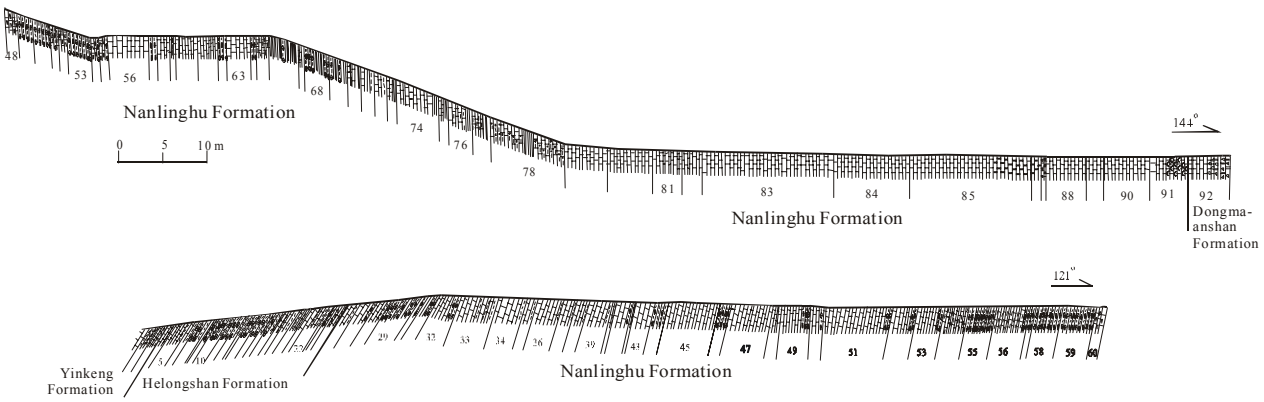

Figure 9. Lower Triassic profile of the South Majiashan Section

catastrophe. As at most Permian-Triassic boundary sections, a big negative anomaly occurs during the Permian-Triassic transition. During the Induan the $\delta^{13}C$ increased steadily with only some small-scale fluctuations in the middle time. This might correspond to a primary recovery of the ecosystems predominated by some opportunistic organisms (or disasters). The positive shift arrives in a highest value around the Induan-Olenekian boundary but the values are just a little higher than zero. Then a big dropping happened in the early Smithian and the negative anomaly occurs in the middle Smithian. This might indicate an extra ecological event, which extended and even enlarged the Permian-Triassic crisis. Following this event occurred the rapid recovery and the $d^{13}C$ excursion shifts positively and firmly. The $d^{13}C$ values arrive high in the early Spathian and keep for a certain time. The gentle decrease in Chaohu during the late Spathian might be resulted from the local tectonic setting with a regression in the region due to the collision between the Lower Yangtze and North China blocks in the Middle and Late Triassic.

9. Magnetostratigraphy

213 plugs for paleomagnetic polarity have been sampled and measured, covering the whole Lower Triassic from the topmost of the Dalong Formation to the base of the Dongmaanshan Formation. The sample interval is generally about 1 m in the lower part and 2 m in the Nanlinghu Formation. However, the samples are taken only in the rocks of certain hardness, so the interval is not constant and the resolution might not be high enough to recognize all the polarity changes. The topmost of the Dalong Formation and the lowermost of the Yinkeng Formation were sampled at the North Pingdingshan Section and the most Yinkeng Formation was sampled at the West Pingdingshan Section while the whole South Majiashan Section from the upper Yinkeng Formation to the base of the Dongmaanshan Formation was drilled.

The Permian-Triassic boundary belongs to a normal polarity interval. It is followed by R-N-R and the suggested Induan-Olenekian boundary is situated close to the top of the second normal polarity interval. The 288 m Lower Triassic sequence is thus composed of five normal inter-

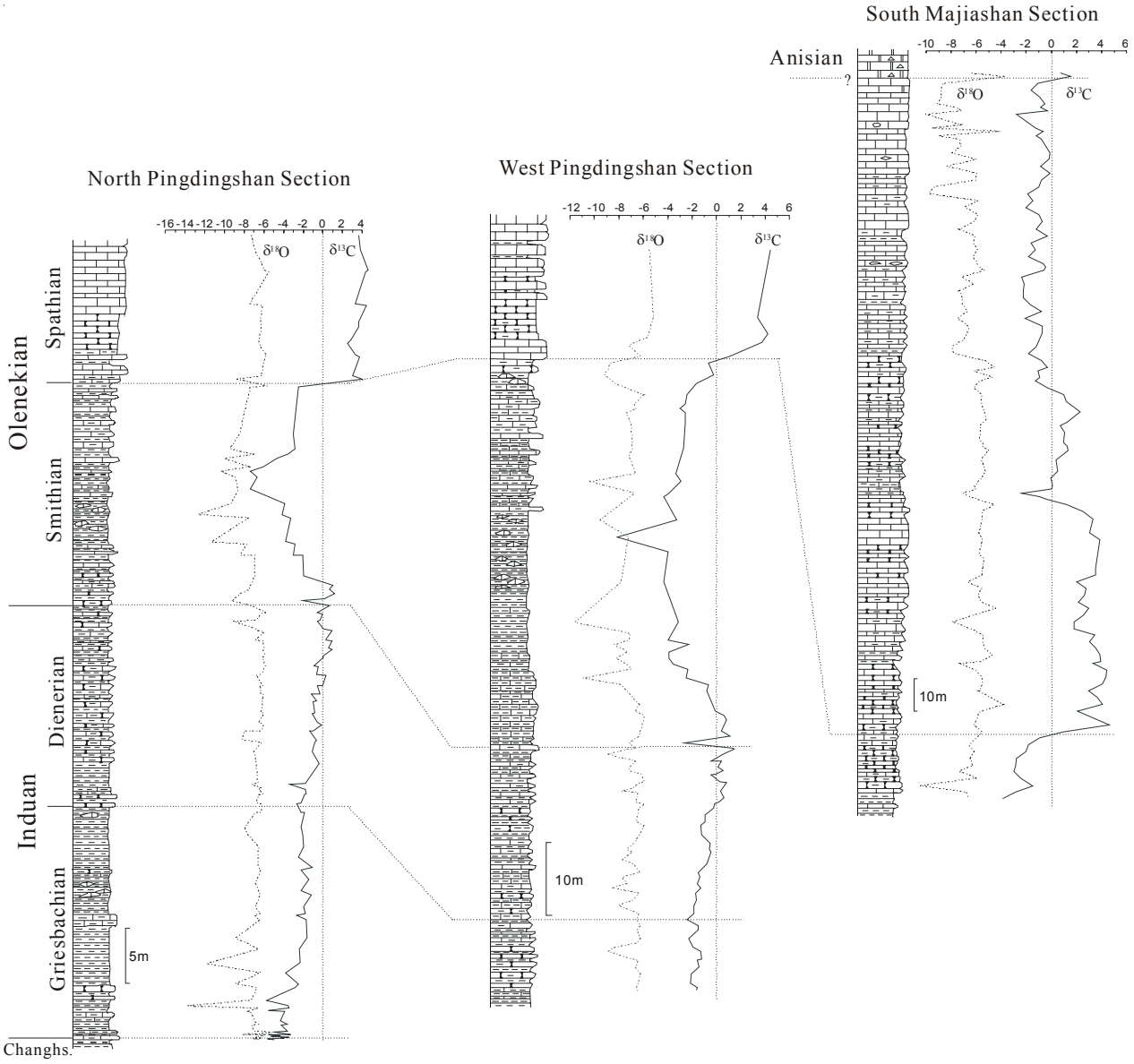

Figure 10. Lower Triassic carbon and oxygen isotopes in Chaohu and the correlation

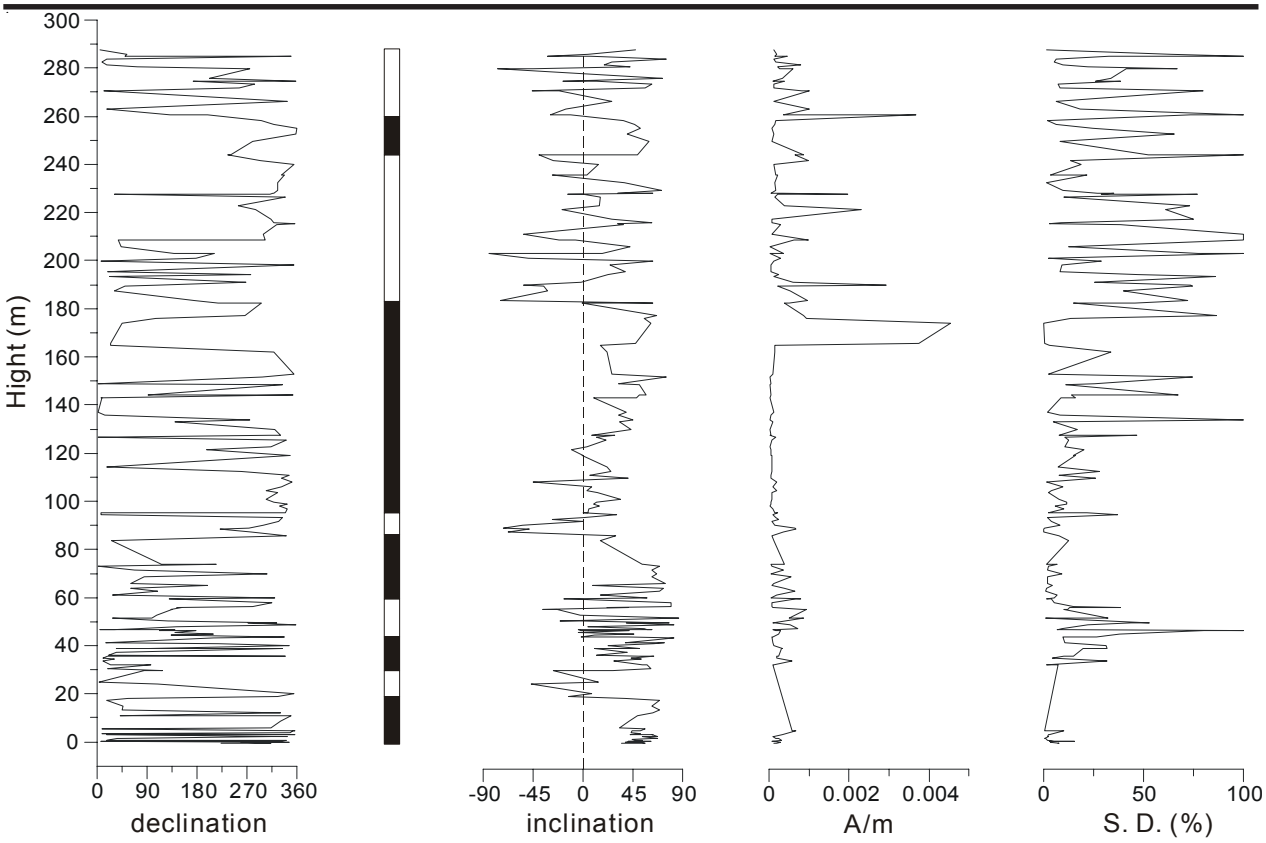

Figure 11. Stratigraphical plot of magnetic vectors and the corresponding interpreted polarity pattern

vals separated by reversed ones, but the uppermost one is not well defined in chronostratigraphy as the very long and apparently continuous section in the upper Nanlinghu Formation and the Dongmaanshan Formation does not have the marine biostratigraphical evidence to demonstrate the presence of the Anisian sediments (Figs. 3, 11). The observed inclination of the magnetic vector in the vicinity of the Permian-Triassic boundary corresponds to a paleolatitude of around 30°N.

Acknowledgements

Most works visited during this field excursion were taken recently under the supports of the National Natural Science Foundation of China Projects (Nos. 40325004, 40232025, 40072011), the Chinese "973 Program" (No. G200007705), the key science project of the Ministry of Education (No. 03033), the basic science project of the Ministry of Science and Technology (No. 2001DEA20020-9), as well as the projects of China Stratigraphical Commission. We are grateful to Dr. Mike Orchard for conodont study, to Dr. Yuri Zakharov for ammonoids, to Prof. Wu Shunbao for bivalves, to Dr. Hans Hansen for paleomagnetic polarity, to Dr. Zuo Jingxun for carbon and oxygen isotopes, and the students at the China University of Geosciences in Wuhan for field works.

References

Chen Liezu, 1985. Early Triassic ichthyosaurs from Chaoxian, Anhui. Regional Geology of China, 15:139-146 (in Chinese).

Guo Peixia and Xu Jiacong, 1980. Knowledge on the age of Qinglong Group in Chaoxian, Anhui Province. Journal of Stratigraphy, 4(4): 310-315 (in Chinese).

Li Jinhua, Ding Baoliang, 1981. Lower and Middle Triassic boundary in Lower Yangtze region. Journal of Stratigraphy, 5(1): 70-75 (in Chinese).

Motani, R., You, H., 1998. The forefin of *Chensaurus chaoxianensis* (Ichthyosauria) shows delayed mesopodial ossification. Journal of Paleontology, 72:133-136.

Peng Yuanqiao, Tong Jinnan, Shi, G. R., Hansen, H. J., 2001. The Permian-Triassic boundary set: characteristics and correlation. Newsletters on Stratigraphy, 39(1): 55-71.

Sweet, W. C., Mosher, L. C., Clark, D. L., Collinson, J. W., Hasenmueller, W. A., 1971. Conodont biostratigraphy of the Triassic. Geological Society of America, Memoir, No.127. 441-465.

Tong Jinnan, Hansen, H. J., Zhao Laishi, Zuo Jingxum, 2005a. A GSSP candidate of the Induan-Olenekian boundary ¾¾ stratigraphic sequence of the West Pingdingshan Section in Chaohu, Anhui Province. Journal of Stratigraphy, 29(2): 205-214 (in Chinese with English abstract).

Tong Jinnan, Hansen, H. J., Zhao Laishi, Zuo Jingxun, 2005b. High-resolution Induan-Olenekian boundary sequence in Chaohu, Anhui Province. Science in China

(Series D), 48(3): 291-297.

Tong Jinnan, Qiu Haiou, Zhao Laishi, Zuo Jingxun, 2002. Lower Triassic inorganic carbon isotope excursion in Chaohu, Anhui Province, China. Journal of China University of Geosciences, 13(2): 98-106.

Tong Jinnan, Yin Hongfu, 2002. The Lower Triassic of South China. Journal of Asian Earth Sciences, 20: 803-815.

Tong Jinnan, Yin Hongfu, Zhang Jianjun, Zhao Laishi, 2001a. Proposed new Lower Triassic stages in South China. Science in China (Series D), 44: 961-967.

Tong Jinnan, Yuri D. Zakharov, Michael J. Orchard, Yin Hongfu, Hans J. Hansen, 2004, Proposal of Chaohu section as the GSSP candidate of the I/O boundary. Albertiana, 29: 13-28.

Tong Jinnan, Zakharov, Y. D., 2004, Lower Triassic Ammonoid Zonation in Chaohu, Anhui Province, China. Albertiana, 31: 65-69.

Tong Jinnan, Zakharov, Y. D., Orchard, M. J., Yin Hongfu, Hansen, H. J., 2003. A candidate of the Induan-Olenekian boundary stratotype in the Tethyan region. Science in China (Series D), 46(11): 1182-1200.

Tong Jinnan, Zhang Jianjun, Zhao Laishi, 2001b. Report on the Lower Triassic of Chaohu, Anhui Province, China. Albertiana, No.25, 23-27.

Yin Hongfu, Wu Shunbao, Du Yuanshen, Peng Yuanqiao, 1999. South China defined as part of Tethyan archipelagic ocean system. Earth Science ¾ Journal of China University of Geosciences, 24(1): 1-12 (in Chinese with English abstract).

Young Chongchiang, Dong Zhiming, 1972. On the Aquatic Triassic Reptilia in China: *Chaohusaurus geishanensis* in Anhui. Institute of Vertebrate Paleontology and Paleoanthropology, CAS, Memoir A, 9:11-15, Science Press, Beijing (in Chinese).

Zhao Laishi, Orchard, M. J., Tong Jinnan, 2004. Lower Triassic conodont biostratigraphy and speciation of *Neospathodus waageni* around the Induan-Olenekian boundary of Chaohu, Anhui Province, China. Albertiana, 29: 41-43.

Permian-Triassic Sequences from Marine to Terrestrial Facies in Western Guizhou
Guide to the Post-Symposium Field Excursion of the International Symposium on the Triassic Chronostratigraphy and Biotic Recovery (23-25 May 2005, Chaohu, China)

Yu Jianxin*, Yang Fengqing, Peng Yuanqiao, Zhang Suoxin and Yin Hongfu

*Faculty of Earth Sciences, China University of Geosciences, Wuhan 430074, China; *yujx_cug@yahoo.com.cn*

Introduction

This field excursion is designed to provide the participants to examine some Permian-Triassic boundary (PTB) sections from marine neritic facies to terrestrial facies. One neritic clastic PTB section, different from the neritic carbonate facies such as the Meishan section, and two terrestrial Permian-Triassic boundary (TPTB) sections will be observed. A previously suggested section in a paralic facies may not be visited in this excursion owing to a bad traffic condition and the limited duration of the excursion (Fig. 1).

General Geology

The western Guizhou (and eastern Yunnan area) was situated in the southwestern part of the Upper Yangtze Block but close to the Kan-Dian Old-land. The sediments from the Middle Proterozoic to the Quaternary were accumulated in the area. The Middle and Late Proterozoic were dominated by marine terrigenous clastic rocks, interbedded with volcano-clastic and carbonate rocks, while the strata from the Paleozoic to Upper Triassic were mainly composed of marine carbonate rocks, occasionally interbedded with clastic beds. The area has been occupied by terrestrial sediments since the late Triassic.

During the Permian-Triassic transition, the area differen-

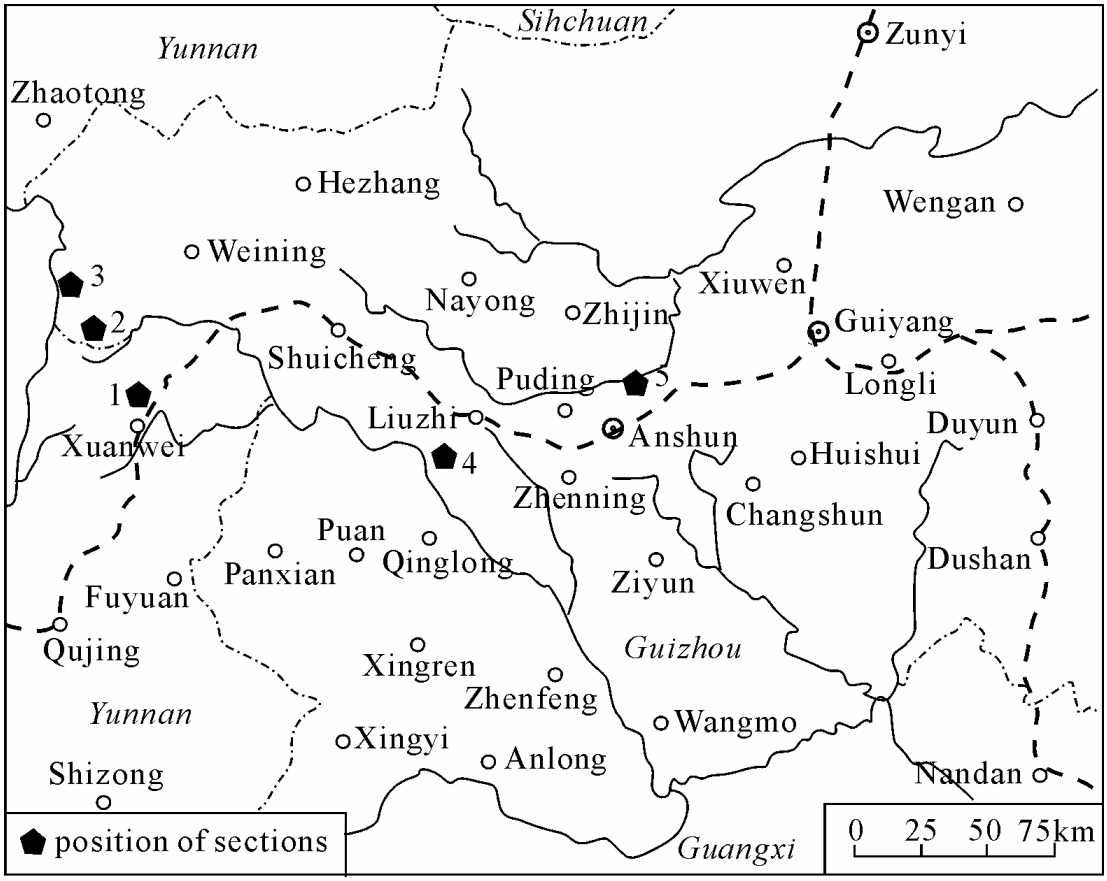

Figure 1. Location map of the field excursion and PTB sections 1-Laibin section, 2-Zhejue section, 3-Chahe section, 4-Zhongzai section, 5-Jiaozishan section; Sections 1, 2 and 3- terrestrial facies, Section 4-neritic clastic faceis, Section 5-nertic carbonate facies. Sections 3 and 4 will be examined in this field excursion.

tiated in geography from marine in the east to terrestrial in the west via a paralic facies (Fig. 2). A series of the Permian-Triassic boundary (PTB) sections from the marine to terrestrial facies can be well observed and investigated in the area.

Description of Excursion Stops

Though we may not be able to visit all the sites listed below during this field excursion, a full list of sites is provided here in the eventuality that sufficient time is available or that excursion participants may wish to visit some sites at a later date. These sites also provide adequate options to study the various aspects related to the PTB. The order of the stops described below may not necessarily be the same as that visited during the excursion, which will very much depend on weather and other natural conditions.

Stop 1: Zhongzai Section in Liuzhi, Guizhou Province ¾ neritic clastic PTB section

This stop is designed to allow participants to examine a PTB sequence in neritic clastic facies, which are different from the PTB sequence in carbonate facies, such as the Meishan Section — the Global Stratotype Section and Point (GSSP) of the PTB.

The Zhongzai Section is located at the north part of the Zhongzai village (or Heilaga village), Langdai, Liuzhi County, Guizhou Province. It is exposed by a highway from Langdai to Zhongzai. The Upper Permian and Lower Triassic outcrop well and the Permian-Triassic boundary sequence is very clear. Fossils are abundant and the Permian-Triassic sequence is divided into the Longtan Formation and Yelang Formation.

The Permian-Triassic boundary sequence at the section is as follows:

Yelang Formation

11. Grayish green thin-bedded argillaceous-bearing siltstone.....0.70 m

10. Grayish green thin-bedded shale.....0.14 m

9. Brown (weathering color) thin-bedded arenaceous limestone with abundant fossils. Containing bivalves: *Claraia wangi*, *C. wangi minior*; gastropods: *Polygyrina depressa*; ostracods: *Hollinella tingi*, *Langdaia suboblonga*; brachiopods: *Crurithyris* cf. *speciosa*, *Orbiculoidea elegans* .....0.06 m

8. Yellow thin-bedded montmorillonite claystone...0.03m

7. Yellow (weathering color) medium- to thin-bedded arenaceous limestone with abundant fossils, and some gray lenticular limestone beds. Containing bivalves: *Pteria* ussurica *variabilis*; brachiopods: *Waagenites* sp.; ostracods: *Hollinella tingi*, *Langdaia suboblonga*.....0.22 m

6. Yellowish white thin-bedded montmorillonite claystone.....0.05 m

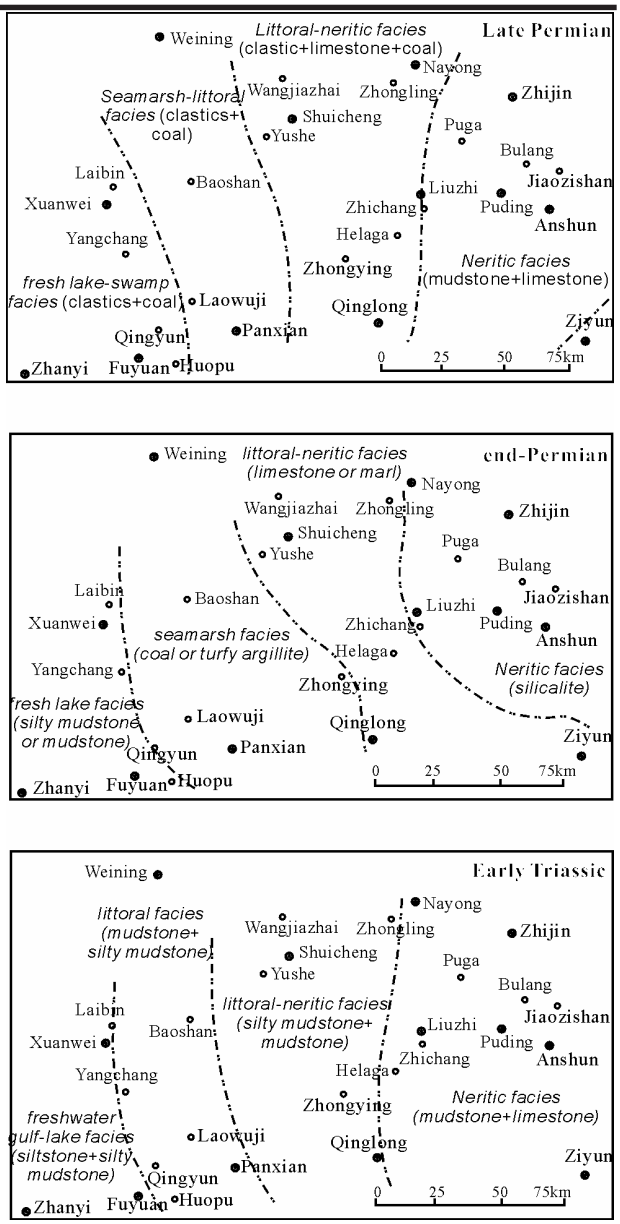

Figure 2. Lithofacies and paleogeography in the western Guizhou and eastern Yunnan during the Permian-Triassic transition time

conformity

Longtan Formation

5. Gray thin-bedded argillaceous limestone. Containing brachiopods: *Lingula* sp.....0.20 m

4. Yellowish green and grayish green thin-bedded calcareous-bearing siltstone and silty mudstone, interbedded with thin-bedded limestone in the upper part. Upper part containing cephalopods: *Pseudotirolites* sp., *Lopingoceras lopingense*; bivalves: *Pernopecten guizhouensis*, *P.* cf. *piriformis*, *Streblochondria*? sp.; gastropods: *Bellerophon* sp.; brachiopods: *Haydenella kiangsiensis*, *Orthotetina frechi*, *Spinomarginifera alphea*, *Waagenites barusiensis*; ostracods: *Fabalicypris parva*, *Healdia subcircinantis*, *Hollinella capacilacuna*, *Knoxiella langdaiensis*, *K.*

xinhuaensis .....8.93 m

3. Grayish green thick-bedded fine sandstone. Middle part containing bivalves: *Tambanella subquadrata*; brachiopods: *Orthotetina* sp.....9.15 m

2. Green and grayish green thin-bedded calcareous siltstone and silty mudstone. Top part containing bivalves: *Ensipteria intermedia*, *Leptodesma* (*Leiopteria*) *guizhouensis*, *Palaeolima* cf. *dieneri*, *Streblochondria zhongyingensis*, *Tambanella oblique*, *Towapteria equicosta*, *T. minima*.....6.53 m

1. Gray thick-bedded limestone, interbedded with yellowish green and grayish green thin-bedded marl. Containing foraminifers: *Palaeofusulina fusiformis*, *P. guizhouensis*, *P. typicalis*, *Colaniella* sp., *Monogenerina* sp.....3.60 m

Stop 2: Chahe Section in Weining, Guizhou Province ¾ Terrestrial PTB section

This stop is designed to allow participants to examine a terrestrial Permian-Triassic boundary (TPTB) sequence. At this section, a claystone bed at the Permian-Triassic eventostratigraphical boundary was found, in which many zircons are selected. These zircons may provide us excellent materials to date the TPTB, plant fossils are abundant in the Upper Permian.

The Chahe section (E 103.8°; N26.7N°) is located between milestones of 31st km and 32nd km of the highway from the Heishitou Town to Haila in Weining County (Fig. 1). The section includes the upper part of the Xuanwei Formation (Beds 1-70, Upper Permian to lowest Triassic), the whole Kayitou Formation (Beds 71-89, lowest Triassic) and the lower part of the Dongchuan Formation (Beds 90-93, Lower Triassic) (Fig. 3). The Permian-Triassic boundary sequence is described as follows:

Dongchuan Formation

83. Gray (purplish when weathered) thick-bedded siltstone, interbedded with thin-bedded argillaceous siltstone, bearing horizontal beddings and sandy laminations.....9.50 m

82. Gray thin-bedded fine sandstone and siltstone interbedded with purplish thin-bedded argillaceous siltstone and silty mudstone, fine sandstone and siltstone spheroidally weathered.....4.50 m

81. Purplish thin-bedded silty mudstone interbedded with gray laminar-bedding siltstone, with mini-scale sandy laminations and cross-beddings.....1.50 m

conformity

Kayitou Formation(Fm)

80. Light yellowish green thin-bedded siltstone with fine sandstone lens.....140 cm

79. Greyish green thin- to medium-bedded siltstone and fine sandstone.....80 cm

78. Greyish green thin- to medium-bedded siltstone and fine sandstone, yielding sporopollen: *Gleicheniidites* sp., *Periplecotriletes* sp., *Aratrisporites* sp., *Protopinus* sp., *Protohaploxypinus samoiloichiae*, *P.* sp., *Limitisporites* sp., *Pityosporites* sp., *Taeniaesporites* sp., *Cycadopites* sp.; fungi spores: *Inapertisporites* cf. *rotundus*, *Diporisporites communis*, *Lacrimasporonites* sp....55 cm

77. Yellowish green to yellow thick-bedded siltstone, finely striated, with a few fine sandstone lens, containing estheriid: *Palaeolimnadia xuanweiensis;* sporopollen: *Calamospora* cf. *microrugosa l*, *Striatites* sp., *Multicellaesporites ramiform*.....110 cm

76. Yellowish green to yellow thick-bedded, fine- to medium-grained lithic arkose, fining upwards gradually into fine sandstone.....80 cm

75. Light yellow thick-bedded siltstone, coarsening to fine sandstone at bottom.....150 cm

74. Purplish thin-bedded siltstone, yielding fungi spore: *Diporicellaesporites* sp.....30 cm

73. Yellow thick-bedded fine lithic arkose, with fine horizontal striae which are more conspicuous on transection.....65 cm

72. Yellow fine arkose intercalated by thin bands of siltston, containing purple thin-bedded siltstone at top.....75 cm

71. Yellow thick-bedded fine lithic arkose in the lower part, gradually altering upward into intercalations of fine bands of yellow siltstone and fine sandstone, containing purple siltstone bands at top.....185 cm

Conformity

Xuanwei Formation

70. Bluish grey to yellowish thin-bedded siltstone, yielding sporopollen: *Cyathidites* sp., *Cyclogranisporites* sp., *Limatulasporites* sp., *Lundbladispora* sp., *Lunzisporites lunzensis*, *Converrucosis- porites* sp., *Triquitrites* sp., *Yunnanospora radiata*, *Periplecotriletes* sp., *Polypodiidites* sp., *Aratrisporites* sp., *Verrucosisporites* sp., *Limitisporites* sp., *Minutosaccus potoniei*, *Lueckisporites* sp., *Protohaploxypinus samoilovichiae*, *P. perfectus*, *P.* sp., *Protopinus* sp., *Pityosporites*? sp., *Alisporites* sp., *Podocarpidites multesimus*, *Taeniaesporites pellucidus*, *Cycadopites* sp., *Perinopollenites* sp.; fungi spore: *Inapertisporites rotundus*.....50 cm

69. Lower part: bluish grey medium-bedded argillaceous siltstone; upper part: yellowish grey medium-bedded fine arkose, with bedding striation at millimeter interval. Large quantity of carbonaceous clasts distributes along bedding planes; more than half of the plane area is occupied by black carbonaceous fragments of various sizes and irregular shapes. It contains plants: *Gigantonoclea* sp., *Neuropteridium* sp., *Rajahia guizhouensis* Zhang;

sporopollens: *Punctatisporites pistilus* Ouyang, *Lophotriletes mictus*, *Pluricellaesporites* sp.; fern spore: *Punctatisporites pistilus* Ouyang; fungi spore: *Pluricellaesporites* sp.....70 cm

68c. Yellowish green claystone.....3 cm

68b. Black and dark brown claystone, yielding sporopollens: *Triquitrites* sp., *Alisporites* sp.; fungi spores: *Inapertisporites rotundus*, *I.* sp., *Multicellaesporites* sp., *Reticulatasporites* sp.....5 cm

68a. Yellowish green claystone with reddish brown and yellow speckles. It yields fungi spores: *Inapertisporites rotundus*, *I.* sp., *Multicellaesporites* sp.....5 cm

67b. Yellowish green silty mudstone with remarkable sphaeroidal weathering. The lower 20cm ($67b^{1-3}$) yields sporopollens: *Punctatisporites* sp., *Toroisporis* sp. The upper 60cm ($67b^{4}$) yields no fossil.....80 cm

67a. Lower part: bluish grey-yellowish green medium- to thick-bedded silty mudstone; upper part: yellowish green medium- to thick-bedded muddy siltstone with sporopollen: *Leiotriletes* sp., *Punctatisporites* sp., *Toroisporis infundibulus*, *Triquitrites stenosis*, *T.* sp., *Thymospora* sp., *Cyclogranisporites staplin*, *Kraeuselisporites* sp., *Aratrisporites* sp., *Laevigatosporites* sp., *Samoilovitchisaccites sinensis*, *Alisporites communis* Ouyang, *Colpectopollis pseudostriatus*, *Protohaploxypinus* sp.; fungi spores: *Inapertisporites* sp., *Multicellaesporites* sp.....4 cm

66h. Bluish grey claystone.....15 cm

66g. Black claystone, yielding plant fragments and sporopollen: *Leiotriletes* sp., *Punctatisporites* sp.; fungi spores: *Pluricellaesporites* sp., *Reticulatasporites* sp., *Inapertisporites* sp.....8 cm

66f. Grey silty claystone, yielding plant fragments and sporopollens: *Leiotriletes pulvinulus*, *L. concavus*, *L.* sp., *Gulisporites cochlearius*, *Punctatisporites* sp., *Apiculatisporites variocorneus*, *A.* sp., *Thymospora mesozoica*, *Yunnanospora radiata*, *Converrucosisporites capitatus*, *C. confractus*, *C. mictus*, *Verrucosisporites* sp., *Protohaploxypinus* sp., *Alisporites* sp., *Platysaccus* sp., *Lueckeisporites virkkiae*.....10 cm

66e. Light greenish yellow thin- to medium-bedded argillaceous siltstone and silty mudstone, yielding plant fragments.....30 cm

66d. Greyish green medium-bedded medium-coarse sandstone with black fragments and yellow claystone pebbles. It yields sporopollen: *Leiotriletes pulvinulus* Ouyang, *Converrucosisporites* sp., *Striatopinites* sp., *Protohaploxypinus* sp.....22 cm

66c. Greyish green thin-medium bedded fine

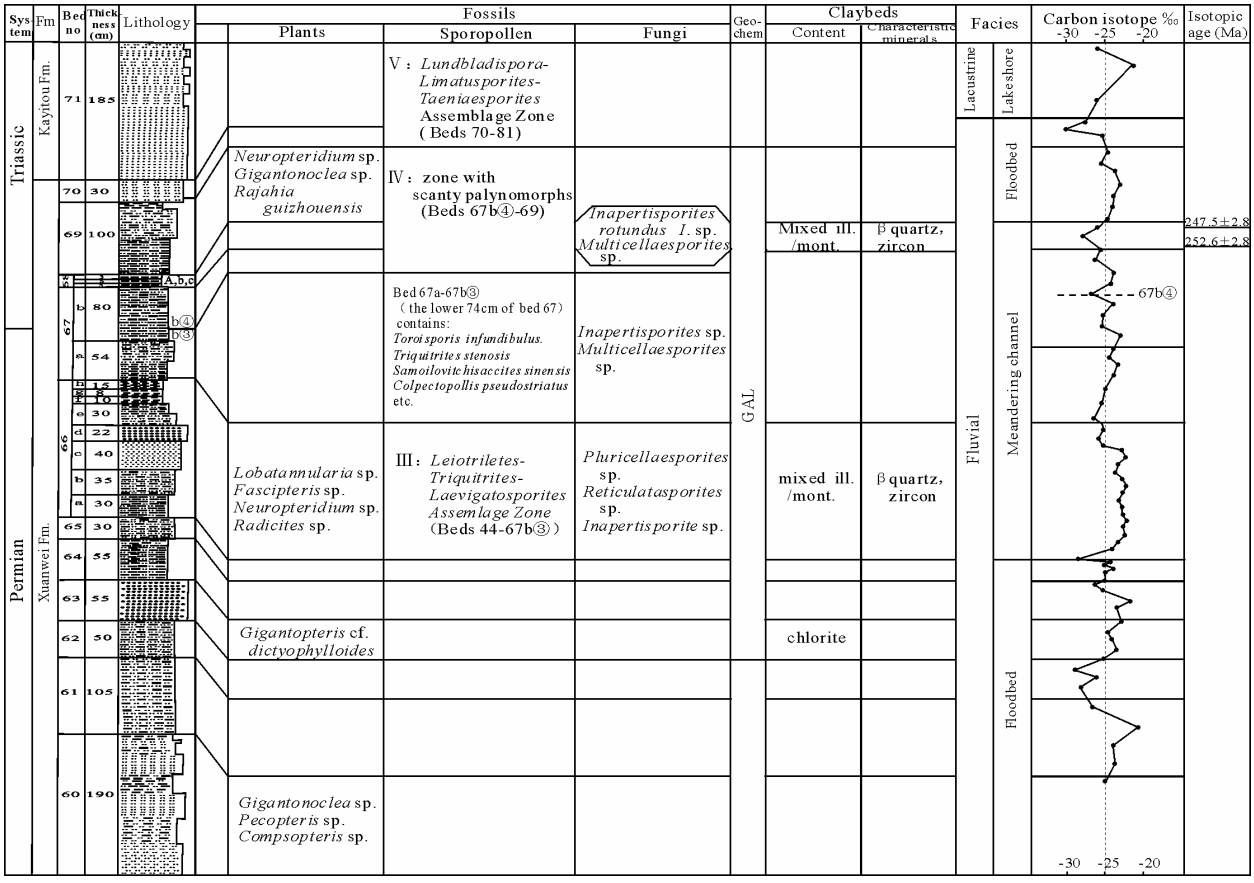

Figure 3. Upper Permian to Lower Triassic stratigraphical column of the Chahe Section
ass. assemblage, F. fluvial, Fm. formation, L. lacustrine, Ls. lake shore, no. number, Pm. palynomorph assemblage, Seq. sequence, Sl. shallow lake, Ss. sandstone, strat. stratigraphy,

graywacke.....40 cm

66b. Dark greyish green medium-bedded siltstone with horizontal worm-tubes.....35 cm

66a. Dark greyish green thin-medium bedded silty mudstone intercalated by irregularly distributed and elliptical light grey claystone, yielding plants: *Lobatannularia* sp., *Fascipteris* sp., *Neuropteridium* sp., *Radicites* sp.; sporopollen: *Leiotriletes pulvinulus*, *L. concavus*, *L.* sp., *Gulisporites cochlearius*, *Dictyophyllidites discretus*, *D. intercrassus*, *D.* sp., *Calamospora pusilla*, *Leschikisporites* sp., *Laevigatosporites lineolatus*, *L.* sp., *Polypodiidites fuyuanensis*, *P. reticuloides*, *P.* sp., *Punctatisporites* sp., *Apiculatisporites variocorneus*, *A.* sp., *Thymospora mesozoica*, *Yunnanospora radiata*, *Converrucosisporites capitatus*, *C. confractus*, *C. mictus*, *Verrucosisporites* sp., *Convolutispora* sp., *Neoraistrickia*? *spanis*, *Reticulatisporites* sp., *Dictyotriletes* sp., *Lophotriletes* sp., *Lycospora* sp., *Densosporites paranulatus*, *Torispora securis*, *Lundbladispora* sp., *Aratrisporites* sp., *Protohaploxypinus* sp., *Umbilisaccites medius*, *Striatopinites* sp., *Cycadopites eupunctatus*, *C.* sp., *Anticapipollis tornatilis*, *Gardenasporites meniscatus*, *Vittatina* cf. *cincinata*.....30 cm

65. Greyish green medium-bedded argillaceous siltstone, gradually altered into silty mudstone upwards, intercalated by black coal seams and purple argillaceous bands at top, yielding sporopollen: *Leiotriletes* sp., *Punctatisporites* sp., *Polypodiidites fuyuanensis*, *Thymospora* sp., *Abietineaepollenites* sp.....30 cm

64. Yellowish green-yellow thick-bedded argillaceous siltstone, and grey-greyish yellow mudstone at top
55 cm

63. Bluish grey-yellowish, medium-bedded argillaceous siltstone, and dark grey-greyish green silty mudstone at top, yielding plant: *Gigantopteris* cf. *dictyophylloides*; sporopollen: *Macrotorispora gigantea*.....55 cm

62. Bluish grey—light muddy yellow, thick-bedded argillaceous siltstone, and bluish grey-greyish white mudstone at top, yielding sporopollen: *Punctatisporites* sp., *Cyclogranisporites* sp. .....50 cm

61. Bluish grey-yellowish, thick-bedded argillaceous siltstone, and bluish grey-greyish white mudstone at top, yielding sporollens: *Leiotriletes* sp., *Laevigatosporites vulgaris*, *Protohaploxypinus* sp.....105 cm

60. Composed of four cycles in ascending order. (1): greyish yellow-bluish grey, thick-bedded siltstone with black carbonaceous fragments in the lower part and bluish grey thin-bedded argillaceous siltstone with more carbonaceous fragments in the upper; (2) greyish yellow thick-bedded fine-grained lithic arkose with small scale wedge-shape cross bedding in the lower part, and yellow-greyish white silty mudstone in the upper; (3) yellow thick-bedded siltstone with plant fragments in the lower part, and grey silty mudstone in the upper; and (4) bluish grey thin-bedded siltstone in the lower part and grey silty mudstonein the upper. Yielding plants: *Compsopteris* sp., *Gigantonoclea* sp., *Pecopteris* sp.; sporopollen: *Leiotriletes* sp., *Gulisporites cochlearius*, *Dictyophyllidites mortoni*, *D.* sp., *Densosporites playfordii*, *Punctatisporites latilus*, *P.* sp., *Cyclogranisporites* cf. *congestus*, *Acanthotriletes microspinosus*, *Apiculatisporis variocorneus*, *A.* sp., *Apicalatasporites nanus*, *Verrucosisporites* sp., *Converrucosisporites* sp., *Torispora* sp., *Thymospora* cf. *mesozoica*, *T.* sp., *Yunnanospora radiata*, *Cycadopite*s sp., *Lueckisporites* sp., *Ephedripites* sp., *Cordaitina uralensis*, *Alisporites* sp.....190 cm

59. Composed of two cycles. Lower cycle: bluish grey-yellow thick-bedded fine-grained arkose in the lower part, andbluish grey-yellow thick-bedded siltstone in the upper with rich plant fragments; and Upper cycle: dark green thin-bedded fine-grained lithic sandstone with large quantity of black carbonaceous fragments of irregular shapes and various sizes, and greyish yellow thin-bedded mudstone in the upper.....135 cm

58. Greyish yellow thick-bedded fine-grained arkose, and greyish yellow thin-bedded argillaceous siltstone at top, with fine horizontal bedding, containing plant: *Compsopteris contracta*.....40 cm

57. Composed of two similar cycles. Lower part: greyish yellow medium- to thick-bedded fine- to medium- grained arkose; upper part, bluish grey thin-bedded siltstone, yielding sporopollen: *Tuberculatosporites impistus*, *Polypodiidites* sp.....255 cm

56. Bluish grey to greyish yellow medium- to thick-bedded siltstone, yielding plant: *Stigmaria* sp., fungi spores: *Inapertisporites rotundus*, *Pluricellaesporites* sp....270 cm

Biostratigraphy of fossil plants

33 species of 19 genera of fossil plants have been discovered at the Chahe Section, distributed in 19 beds from Bed 1 to Bed 69, all belonging to upper Xuanwei Formation. Percentage of different groups is shown in Table 1. It is noteworthy from Table 1 that plant diversity and its stratigraphic distribution of both Chahe and nearby (ca. 20km SE) Zhejue Sections (Fig.1) are almost the same, which implies that the plant diversity and distribution at the Chahe Section may be somewhat representative of the P-T interval in this area. Main elements are *Annularia shirakii, Cladophlebis permica, C. fuyuanensis, Compsopteris contracta. Lobatannularia multifolia, L. heianensis, Lepidodendron lepidophloides, Gigantonoclea guizhouensis, Gigantopteris dictyophylloides, G. nicotianaefolia, G. guizhouensis, Neuropteridium coreanicum, Pecopteris guizhouensis, Rajahia guizhouensis*. They are attributed to the South China Subregion of the Late Cathaysian Flora, which is a typical Late Permian littoral swamp flora under humid tropical weather, similar to recent tropical forest (Li et Wu, 1994; Li, 1995).

Stratigraphical distribution of the plant fossils of both Chahe and Zhejue Sections shows a tripartite pattern (Fig.3). In ascending order, the first assemblage (Beds 1-

Table 1. Fossil distribution in the Permian-Triassic boundary strata at the Chahe Section

Age	Fm	Bed no.	Plant fossil, Sporopollen, Fungi
Triassic	Kayitou	81	Sporo-pollen: *Bactrosporites* sp., *Lacrimasporonites* sp.
		78	Sporo-pollen: *Gleicheniidites* sp., *Periplecotriletes* sp., *Aratrisporites* sp., *Protopinus* sp., *Protohaploxypinus samoilovichii*, *Limitisporites* sp., *Pityosporites* sp., *Taeniaesporites* sp., *Cycadopites* sp. Fungi: *Inapertisporites* cf. *rotundus*, *Diporisporites communis*, *Lacrimasporonites* sp.
		77	Sporo-pollen: *Calamospora* cf. *microrugosa*, *Striatites* sp. *Fungi: Multicellaesporites ramiform*
		74	Fungi: *Diporicellaesporites* sp.
	Xuanwei	70	Sporo-pollen: *Cyathidites* sp., *Cyclogranisporites* sp., *Limatulasporites* sp., *Lundbladispora* sp., *Lunzisporites lunzensis, Converrucosisporites* sp., *Triquitrites* sp., *Yunnanospora radiata*, *Periplecotriletes* sp., *Polypodiidites* sp., *Aratrisporites* sp., *Verrucosisporites* sp., *Limitisporites* sp., *Minutosaccus potoniei* Mädler, *Lueckisporites* sp., *Protohaploxypinus samoilovichiae*, *P. perfectus, P.* sp., *Protopinus* sp., *Pityosporites*?sp., *Alisporites* sp., *Podocarpidites multesimus*, *Taeniaesporites pellucidus*, *Cycadopites* sp., *Perinopollenites* sp. Fungi: *Inapertisporites rotundus*
		69	Plant fossil: *Gigantonoclea* sp., *Neuropteridium* sp., *Rajahia guizhouensis* Sporo-pollen: *Punctatisporites pistilus Lophotriletes mictus* Fungi: *Pluricellaesporites* sp.
		68b	Fungi: *Inapertisporites rotundus, I.* sp., *Multicellaesporites* sp., *Reticulatasporites* sp.
		68a	Fungi: *Inapertisporites rotundus, I.* sp., *Multicellaesporites* sp.
Permian		67b[1-3]	Sporo-pollen: *Punctatisporites* sp., *Toroisporis* sp.
		67a	Sporo-pollen: *Leiotriletes* sp., *Toroisporis infundibulus*, *Punctatisporites* sp., *Triquitrites stenosis T.* sp., *Thymospora* sp., *Aratrisporites* sp., *Cyclogranisporites stapling*, *Kraeuselisporites* sp., *Laevigatosporites* sp., *Samoilovitchisaccites sinensis*, *Alisporites communis*, *Colpectopollis pseudostriatus*, *Protohaploxypinus* sp. Fungi: *Inapertisporites* sp., *Multicellaesporites* sp.
		66g	Sporo-pollen: *Leiotriletes* sp., *Punctatisporites* sp. Fungi: *Pluricellaesporites* sp., *Reticulatasporites* sp., *Inapertisporites* sp
		66f	Sporo-pollen: *Leiotriletes pulvinulus*, *L. concavus*, *Gulisporites cochlearius*, *Punctatisporites* sp., *Apiculatisporites variocorneus*, *Thymospora mesozoica*, *Yunnanospora radiata*, *Converrucosisporites capitatus*, *C. confractus*,, *C. mictus, Verrucosisporites* sp., *Protohaploxypinus* sp., *Alisporites* sp., *Platysaccus* sp., *Lueckeisporites virkkiae*,
		66d	Sporo-pollen: *Leiotriletes pulvinulus*, *Converrucosisporites* sp., *Striatopinites* sp., *Protohaploxypinus* sp.
		66a	Plant fossil: *Lobatannularia* sp. *Fascipteris* sp. *Neuropteridium* sp. *Radicites* sp. Sporo-pollen: *Leiotriletes pulvinulus*, *L. concavus*, *Gulisporites cochlearius*, *Dictyophyllidites discretus*, *D. intercrassus*, *Calamospora pusilla*, *Leschikisporites* sp., *Laevigatosporites lineolatus*, *Polypodiidites fuyuanensis*, *P. reticuloides*, *Punctatisporites* sp., *Apiculatisporites variocorneus*, *Thymospora mesozoica*, *Yunnanospora radiata*, *Converrucosisporites capitatus*, *C. confractus*, *C. mictus, Verrucosisporites* sp., *Convolutispora* sp., *Neoraistrickia? spanis*,*Reticulatisporites* sp., *Dictyotriletes* sp., *Lophotriletes* sp., *Lycospora* sp., *Densosporites paranulatus*, *Torispora securis*, *Lundbladispora* sp., *Aratrisporites* sp., *Protohaploxypinus* sp., *Umbilisaccites medius*, *Striatopinites* sp., *Cycadopites eupunctatus*, *Anticapipollis tornatilis*, *Gardenasporites meniscatus*, *Vittatina* cf. *cincinata*
		65	Sporo-pollen: *Leiotriletes* sp., *Punctatisporites* sp., *Polypodiidites fuyuanensis*, *Thymospora* sp., *Abietineaepollenites* sp.
		63	Plant fossil: *Gigantopteris dictyophylloides*, *Macrotorispora gigantea*
		62	Sporo-pollen: *Punctatisporites* sp., *Cyclogranisporites* sp.
		61	Sporo-pollen: *Leiotriletes* sp., *Laevigatosporites vulgaris Protohaploxypinus* sp.
		60	Plant fossil: *Compsopteris* sp., *Gigantonoclea* sp., *Pecopteris* sp. Sporo-pollen: *Leiotriletes* sp., *Gulisporites cochlearius Dictyophyllidites mortoni, Densosporites playfordii*, *Punctatisporites latilus*, *Cyclogranisporites* cf. *congestus*, *Acanthotriletes microspinosus Apiculatisporis variocorneus*, *Apicalatasporites nanus*, *Verrucosisporites* sp., *Converrucosisporites* sp., *Torispora* sp., *Thymospora* cf. *mesozoica*, *Yunnanospora radiata*, *Cycadopite*s sp., *Lueckisporites* sp., *Ephedripites* sp., *Cordaitina uralensis*, *Alisporites* sp.
		58-57	Plant fossil: *Compsopteris contracta* Sporo-pollen: *Tuberculatosporites impistus*, *Polypodiidites* sp.

38 of Chahe, Beds 1-23 of Zhejue) yields the most diversified flora (28 species at Chahe; 21 species at Zhejue), dominated by filices and pteridosperms. Lycopsids and sphenopsids played considerable role. In the second assemblage (Beds 39-69 of Chahe; Beds 24-49 of Zhejue) the dominants were the same but floral diversity decreased (11 species at Chahe; 20 species at Zhejue) and sphenopsids almost disappeared. It is notable that in both sections, the upper part of first assemblage and the lower part of second assemblage constituted an interval with least diversity while lycopsids played considerable role. Li (1995) subdivided the Late Cathaysian (Late Permian) Flora of South China into an early (Longtanian = Wuchiapingian) *Gigantopteris nicotianaefolia-Lobatannularia multifolia-Schizoneura manchuriensis* Assemblage and a late (Changhsingian) *Gigantonoclea guizhouensis-Ullmannia* cf. *bronnii-Annularia pingloensis* Assemblage. Locally in the Wumongshan region of western Guizhou where the Chahe and Zhejue Sections are located, the late (Changhsingian) plant assemblage was named the *Ullmannia bronii-Gigantopteris dictyophylloides* Assemblage (Bureau of Geol. Min. Res. Guizhou Prov., 1987). Fossil plants at Chahe and Zhejue belong to this late assemblage, which differs from the early

one by remarkably decreased diversity. *G. dictyophylloides* is quite abundant at these two sections, while *U. bronnii* usually appears at more littoral sections. Noteworthy is that the members of this flora appear up to Bed 69 at Chahe, above the presumed PTB (Bed 67b^3).

In the third assemblage (Beds 70-93 of Chahe; Beds 50-56 of Zhejue), the Cathaysian Flora has already become extinct. No identifiable plant remains have been discovered at Chahe. However at Zhejue, in Bed 56 of the lower Kayitou Fm have been revealed *Compsopteris* cf. *contracta, Gigantonoclea* sp., *Pecopteris* sp., *Cordaites principalis* and *Taeniopteris* sp. In Yunnan-Guizhou region, relicts of *Gigantopteris* flora have been reported to survive onto earliest Triassic (Nanjing Institute of Geology and Paleontology, 1980), which is reconfirmed by our work as well. Occurrence of these relicts of the Cathaysian Flora in Kayitou Fm indicates that, unlike most marine biota, relicts of paleophytes could survive into Mesozoic.

Biostratigraphy of palynomorphs

Of the total 93 beds of Chahe section, 55 beds yield palynomorphs. 5 assemblage zones of palynomorphs have been subdivided in ascending order (Fig. 3), of which the described Beds 58-78 contain three (Table1). They are indicated as follows:

The 1st Assemblage Zone (Beds 1-34): *Cyclogranisporites-Thymospora-Punctatisporites* Assemblage Zone (abbreviated).

The 2nd Assemblage Zone (Beds 35-43): Assemblage zone of abundant fungi spores (abbreviated).

The 3rd Assemblage Zone (Beds 44-67b^3): *Leiotriletes-Triquitrites- Laevigatosporites* Assemblage Zone.

The 4th Zone with scanty palynomorphs (Beds 67b^4-69): characterized by low plants as shown by molecular fossil analysis.

The 5th Assemblage Zone (Beds70-81): *Lundbladispora-Limatusporites-Taeniaesporites* Assemblage Zone.

In brief comparison with the megaphyte sequence, the 1st palynomorph assemblage corresponds to the 1st plant assemblage, the 2nd or fungi spore assemblage corresponds to the less diversified interval characterized by lycopsids, the 3rd palynomorph assemblage corresponds to the 2nd plant assemblage, the short-lived 4th palynomorph assemblage has no reflection in plant, and the 5th one corresponds to the 3rd plant assemblage.

Although the fungi-flourishing 2nd Assemblage Zone implies somewhat peculiar environment, the three lower zones below Bed 67b^3 together denote a Late Permian age with index fossil *Lueckisporites*. Assemblage Zones 1 and 3 have much in common and represent normal and abundant plant community. The late Permian spore-dominated assemblage extends up to Bed 67a and 67b^3 and then disappear. Like the 1st zone, the 3rd zone is dominated by spores of filices and pteridosperms (>70%), with gymnosperm pollens ca. 10% and fungi spores <10%. Such taxonomic proportion is identical with corresponding fossil plant assemblages and both denote paleophytic rather that mesophytic aspect.

In the 4th zone at Chahe (Beds 67b^4-69), both sporopollen and fungi spores are only sparsely discovered. However at the nearby Zhejue section, the same interval (boundary beds of Beds 47-50) contains abundant fungi spores, accounting for more than 90% of the total palynomorph grains discovered therein, and thus comprises a fungi-dominated assemblage zone (Peng et al., 2003). Main fungi spores at Zhejue are *Reduviasporonites (Tympanicysta), Inapertisporites, Dicellaesporites, Multicellaesporites* and *Staphlosporonites*. This corresponds to the PTB fungi spike discovered throughout the world and represents the PTB (Eshet et al., 1995), although at Meishan fungi distributed much wider in stratigraphic column and did not show such a spike (Ouyang and Utting, 1990). Research on molecular fossils accords with palynomorph results. Beds 67-69 at Chahe are characterized by the dominance of low-carbon-numbered alkanes ($<C_{21}$) against high-carbon- numbered alkanes ($>C_{22}$), higher $C_{21\text{-}24}/C_{21\text{-}33}$ alkanes ratio and strengthened vibration of STN/HP ratio (Xie Shucheng, pers. comm.). Low-carbon-numbered alkanes mainly derive from low plants such as fungi and algae. Higher $C_{21\text{-}24}/C_{21\text{-}33}$ ratio may reflect existence of submerged macrophytes or bryophytes (Xie et al., 2001). ATN mainly relate to eucaryotes while hopanes (HP) mainly relate to prokaryotes, so vibration of STN/HP ratio implies alternation between eucaryotes-prevailing and prokaryotes-prevailing environments. Hence, molecular record of the 4th Assemblage Zone of Chahe tells the abundance of procarya, low plants and probably bryophytes instead of higher plants.

The Assemblage Zone 5 (Beds 70-81) displays disparate pattern of palynomorphs from Assemblage Zones 1 and 3. Contents of its gymnosperm pollens exceeds those of fern spores and becomes the dominate elements, and Early Triassic index fossils *Aratrisporites* (Bed 78), *Lundbladispora* and *Taeniaesporites* (Beds 70 and 78) appear, which indicate that this zone belongs to Early Triassic and can be correlated with synchronous assemblage in Junggar Basin (Ouyang and Norris, 1999).

According to palynomorphs, the PTB should be located between Assemblages 3 and 5, i.e., at the level of Assemblage 4. Similar palynomorph assemblages have been described in Fuyuan County of the adjacent Yunnan Province (Ouyang, 1986). Together they comprise a flora typical of the P/T interval of Sichuan-Yunnan Oldland. Palynomorphs of the Chahe Section are also correlatable with those from the P/T transitional beds of the Junggar Basin, Xinjiang (Ouyang and Norris, 1999). An alternative boundary could be the base of Bed 71, i.e. the boundary between Kayitou and Xuanwei Fms. This was the traditional P/T boundary and the *Gigantopteris* flora extended up to Bed 69. However this alternative does not accord with the palynomorph zonation, isotope age and PTBST character stated above.

Table 2. Clay mineral and their contents in the clay beds of the Chahe Section

Bed	Sample no.	Clay mineral and their contents (ill., illite; mont., montmorillonite)	Zircon and β - quartz
68c	GWC-68c	Mixed ill./mont.(85%) + mont.(10%) + chlorite（5%）	no
68a	GWC-68a	Mixed ill./mont.（70%）+ mont.（25%）+ chlorite (5%)	yes
66f	GWC-66f	Mixed ill./mont.（70%）+ mont.（25%）+ chlorite（5%）	yes
63	GWC-63	chlorite（100%）	no
30	GWC-30	kaolinite（80%）+ chlorite（20%）	no
28	GWC-28	kaolinite（60%）+ chlorite（40%）	no
22	GWC-22	kaolinite（55%）+ chlorite（45%）	no
21	GWC-21	kaolinite（55%）+ chlorite（45%）	no

Boundary Clay Beds

Analysis of clay minerals (Fig. 4): Eight claystone beds at the Chahe Section have been investigated (Zhang et al., 2004). They are Beds 21, 21, 30, 63, 66f, 68a and 68c. Results are listed in Table 2.

From Table 2 the following conclusions can be drawn:

1. Only Beds 66f and 68a, c yield zircon and ˜-quartz, which are typical volcanogenic minerals especially in the PTB strata of South China. But they are not found in the other clay beds.

2. As in other PTB sections of South China, the volcanogenic clay beds, notably Beds 66f and 68a, c, are mainly composed of mixed layers of illite and montmorillonite.

Besides, among these beds Beds 66f, 68a and 68c show peculiar oxide and trace element contents: for Bed 66f highest TFe_2O_3, SiO_2, Cr, and lowest Al_2O_3, Zr; for Beds 68a and 68c highest K_2O, MgO, MnO and lowest TiO_2, Cr, Co (Zhang et al., 2004). Geochemical anomalies were also detected in the boundary clay beds of Meishan (Chai et al., 1992).

The similarity of PTB clay bed composition and origin between Chahe and Meishan, as well as other sections in South China, provides a convincing evidence for accurately locating the PTB level at the Chahe Section.

Carbon isotope ($\delta^{13}C_{org}$)

The $\delta^{13}C_{org}$ curve around the Permian-Triassic interval of Chahe section is shown on the right column of Fig. 3. The samples were collected at 10 cm interval, but densified to 2-5 cm interval at the boundary—Bed 67. Analysis was made by the MAT-251 Mass Spectrometer at the Isotope Laboratory of China University of Geosciences. Analysis precision of the MAT-251 MS: σ ±0.03‰; sample preparation precision: σ ±0.1‰; standard error of the sample analysis: σ ±0.1‰. Unlike in marine sequences, the result does not show a general decrease of $\delta^{13}C_{org}$ value near the boundary. Rather the whole curve is relatively smooth with minor oscillations around -25‰. There are four small (2-3‰) negative excursions in Bed 67 and 68 (upper clay bed), but the strong excursions happen at the two ends of the curve (Beds 61 and 71).

Previous researches in terrestrial PTB sequences of Gondwana show large multiple negative excursions of $\delta^{13}C_{org}$ separated by sharp positive excursions and distributed in a thickness of 20 m or more (de Wit et al., 2002). On the other hand, a $\delta^{13}C_{carb}$ curve in Karoo Basin shows a single negative excursion down to near -16‰ (McLeod et al., 2000). The Chahe curve is dissimilar with either of them. However there is the possibility that the curve length (thickness) may be not long enough to display these spikes. Its mean value around -25‰, like that of the Gondwanan sequences, is within the range of modern C_3 plants. Anyway, no single $\delta^{13}C$ excursion occurs at the PTB of Chahe. We agree with de Wit et al. (2002) that we should caution against models of the P/T extinction based on singular event (Jin et al., 2000; Becker et al., 2001).

Isotope Dating

Samples of zircon were collected from the two PTBST volcanogenic clay beds (Beds 66 and 68) of Chahe, but only two samples, from Bed 68a (GWC68-xia) and 68c (GWC68-shang) respectively, can be dated. The 5 zircon grains from 68a were all light yellow transparent automorphic crystals, 2 short columnar, 1 long columnar and 2 finely elongated columnar; the 4 zircon grains from 68c were also light yellow transparent automorphic, 1 short columnar and 2 finely elongated columnar, while the 4th grain obtained a deviated age and was not taken into account. They are all formed under magmatic crystallization (Zhang et al., 2004).

Pb/U isotope dating of the zircons were measured by Dr. Li Huiming at the Tianjin Institute of Geology and Mineral Resources, using a VG534 TIMS (Thermo-Ionization Mass Spectrometer). Chemical and ID (Isotope Dilution TIMS) procedures are conventional. Data processing and chart plotting were made with software ISOPLOT of the Berkeley Geochronological Center. Results of both samples (except the 4th one of 68c) fall within the $^{206}Pb/^{238}U$-$^{207}Pb/^{235}U$ Concordia, which mean that enclosed system sustained since the formation of zircons without Pb

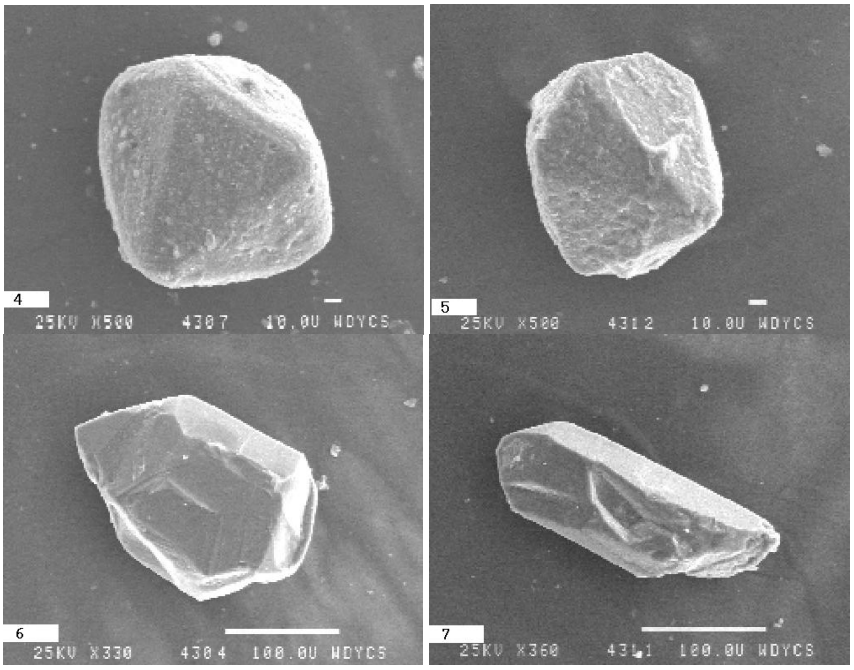

Figure 4 Volcanogenic minerals of the boundary claybeds
4 GWC-66f, ß quartz; 5 GWC-68a, ß quartz; 6 GWC-66f, zircon; 7 GWC-68a, zircon

loss or gain. The results were convincing. Five zircon grains of Bed 68a yield an Pb/U isochron age of 252.6±2.8 Ma, while three zircon grains of Bed 68c yield an Pb/U isochron age of 247.5±2.8 Ma. The average age for Bed 68 is 250.0±2.8 Ma. This age accords with the upper claybed (Bed 28) age of Meishan and the eruption age of Tunguss Basalt, and is so far the most accurate age obtained from terrestrial PTB.

Conclusions

1. The PTBST, characteristic of the GSSP section of Meishan and widespread in marine PTB sequences of South China, is also recognized at Chahe (Beds 66f—68c). As in the marine sequences, this PTBST is a tripartite set, lithologically consisting of an underlying (Bed 66f) and an overlying (Bed 68c) volcanogenic clay bed and a sandwiched bed (Bed 67). At the terrestrial Chahe section this sandwiched Bed 67 is siltstone instead of limestone at Meishan (Bed 27). The gradual replacement from limestone (Anshun, central Guizhou) to sandy limestone (Zhongzai, littoral facies in centro-western Guizhou) and finally to terrestrial siltstone at Chahe has been traced. This event boundary is also confirmed by isotope age, sedimentary, floral and molecular fossil changes. Thus in comparison, Bed 67 of Chahe corresponds to Bed 27 of Meishan, and the terrestrial PTB should lie somewhere within Bed 67b. Accurately speaking, the PTB should be above Bed 67b[3], the LAD of Permian palynomorph zone III, and below Bed 68a, c, the upper volcanogenic claybed. The interval is less than 80cm, which is so far the highest accuracy in terrestrial PTB. The boundary is tentatively set at the base of Bed 67b[4]. Age of the PTB should be between 247 and 253 ma, averaged as 250 Ma.

2. Biostratigraphic research confirms the above statement. Plant fossils show high diversity and abundance below the PTBST, and both abruptly decrease above the PTBST. Relicts of *Gigantopteris* flora survived up to Bed 69 and then became wholly extinct. Sporopollens are dominated by fern spores of Permian nature below the PTBST, and replaced by gymnosperm pollens of Triassic nature above the PTBST. At Chahe the PTBST itself bears rare fern and fungi spores, but at the nearby Zhejue Section, the same PTBST is characterized by the abundance of fungi spores, which constitutes the special 4th zone inserted between the underlying spore and overlying pollen zones, corresponding to the fungi spike widespread over the world.

3. Based on X-ray diffraction analysis, electronic scanning analysis and X-fluorescent spectrometer analysis, it has been proved that the boundary clay beds (66f and 68a,c) are composed of mixed illite-montmorillonite layers analogous with the boundary clay beds at Meishan, and that they contains typical volcanogenic minerals such as bipyramid γ-quartz and zircon just as at Meishan. Sphaerules has been reported at PTB of the nearby Zhejue section (Wang and Yin, 2001b).

4. The Changhsingian-Lower Triassic sequence of Chahe accords with those at Meishan and in whole Yangtze, which means that the whole South China experienced same sea level change during that interval. Different from Xingjiang and South Africa, the facies sequence of Chahe Section at Permian-Triassic transition (Beds 56-80) deepened and fined upward. This warns us that shallowing and coarsening upward is not a generalized case at Permian-Triassic transition.

Reference

Becker, L., Poreda, R. J., Junt, A. G., Bunch, T. E. Rampino, M., 2001. Impact event at the Permian-Triassic Boundary: evidence from extra-terrestrial noble gasses in fullerenes. Science, 291:1530-1533.

Bureau of Geology and Mineral Resources of Guizhou Province, 1987. Regional geology of Guizhou Province. Geological Memoirs of Ministray of Geology and Mineral Resources, China, Ser. 1, no. 7, 698pp., Beijing, Geological Publishing House [in Chinese with English summary].

Chai Chifang, Zhou Yaoqi, Mao Xueying, Ma Shulan, Ma Jianguo, Kong Ping, He Jingwen, 1992. Geochemical constraints on the Permo-Triassic boundary event in South China. *in* Sweet, W. C., Yang Zunyi, Dickins, J. M., Yin Hongfu (eds.) Permo-Triassic events in the eastern Tethys: Cambridge, Cambridge University Press, 158-168.

de Wit, M. J., Ghosh, J. G., de Villiers, S. C., Rakotosolofo, N., Alexander, J., Tripathi, S., Looy, C., 2002. Multiple organic carbon isotope reversals across the Permo-Triassic Boundary of terrestrial Gondwana sequences: clues to extinction patterns and delayed ecosystem recovery. Jour. Geol., Univ. Chicago, 110: 227-240.

Eshet, Y., Rampino, M. R., Visscher, H., 1995. Fungal event and palynological record of ecological crisis and recovery across the Permian-Triassic boundary. Geology, 23(11): 967-970.

Jin, Y. G., Wang, Y., Wang, W., Shang, Q. H., Cao, C. Q., Erwin, D. H., 2000. Pattern of marine mass extinction near the P-T boundary in South China. Science, 289: 432-436.

Li Xingxue (ed.), 1995. Floras in the geological periods of China. Guangzhou: Science and Technology Press of Guangdong, 539pp +144 pls. [in Chinese].

Li Xingxue, Wu Xiuyuan, 1994. The Cathaysian and Gondwana floras:their contribution to determining the boundary between eastern Gondwana and Laurasia. Jour. SE Asian Earth Sci., 9(4): 309-317.

MacLeod, K. G., Smith, R. M. H., Koch, P. L. Ward, D. P., 2000. Timing of mammal-like reptile extinction across the Permian-Triassic boundary in South Africa. Geology, 28: 227-230.

Nanjing Institute of Geology and Palaeontology, Academia Sinica, 1980. Late Permian coal-bearing strata and palaeontology fauna in western Guizhou and easternYunna. Beijing: Science Press, 1-277 [in Chinese].

Ouyang Shu, 1986. Late Permian and Early Triassic palynological assemblages in Fuyan of Yunnan. Beijing: Science Press, 1-122 [in Chinese].

Ouyang Shu, Norris, G., 1999. Earliest Triassic (Induan) spores and pollen from the Junggar Basin, Xinjiang, northwestern China. Review of Palaeobotany and Palynology, 106(1-2): 1-56.

Ouyang Shu, Utting, J., 1990. Palynology of Upper Permian and Lower Triassic rocks, Meishan, Changxing county, Zhejiang Province, China. Review of Palaeobotany and Palynology, 66(1-2): 65-103.

Peng Yuanqiao, Yang Fengqing, Shi, G. R., Gao Yongqun, 2003. Correlating marine and non-marine Permian-Triassic boundary sections using high-resolution event-stratigratigraphy and biostratigraphy: an example from South China. Proc. XVth International Congress on Carboniferous and Permian Stratigraphy, Utrecht, The Netherlands, 395-396.

Wang Shangyan, Yin Hongfu, 2001a. Study on terrestrial Permian-Triassic boundary in Eastern Yunnan and Western Guizhou. Wuhan: China University of Geoscience Press, 87 pp.[in Chinese with English summary].

Wang Shangyan, Yin Hongfu, 2001b. Discovery of microspherules in claystone near the terrestrial Permian-Triassic Boundary. Geol. Rev., 47(4): 411-414 [in Chinese with English abstract].

Xie, S. C., Evershed, R. P., 2001. Peat molecular fossils recording paleoclimatic change and organism replacement. Chinese Science Bulletin, 46: 1749-1752.

Permian and Triassic depositional history of the Yangtze platform and Great Bank of Guizhou in the Nanpanjiang basin of Guizhou and Guangxi, south China

Daniel J. Lehrmann[1], Paul Enos[2], Jonathan L. Payne[3], Paul Montgomery[4], Jiayong Wei[5], Youyi Yu[5], Jiafei Xiao[5], and Michael J. Orchard[6].

[1]University of Wisconsin, Oshkosh, WI, U.S.A., lehrmann@uwosh.edu;
[2]University of Kansas, Lawrence, KS, U.S.A.;
[3]Harvard University, Cambridge, MA, U.S.A;
[4]ChevronTexaco, Bellaire, TX, U.S.A.
[5]Guizhou Bureau of Geology, Guiyang, Guizhou, P.R.C.;
[6]Geological Survey of Canada, Vancouver, B.C., Canada;

Abstract - The Nanpanjiang basin occurs in the southern margin of the south China plate. Marine sedimentation dominated from the Late Proterozoic to the Late Triassic when siliciclastic turbidites filled the basin and sedimentation regionally shifted to fluvial deposition. Permian and Triassic carbonate strata record a long history of platform evolution and include diverse architectures and evolutionary histories that reflect the impact of local depositional environments, rates of siliciclastic flux and accelerating tectonic subsidence as the basin experienced tectonic convergence and foreland basin development in the Triassic.

The Triassic margin of the Yangtze platform that rims the basin extends in a sigmoidal SW/NE trend from Yunnan through Guizhou. Several isolated platforms, including the Great Bank of Guizhou and the Chongzuo-Pingguo platform, occur within the basin in southern Guizhou and Guangxi. The basin expanded in the Late Permian during a regional transgression. The Yangtze platform and isolated platforms evolved from low-angle ramps with oolite margins in the Early Triassic to steepening *Tubiphytes* reef margins in the Middle Triassic (Anisian). Basin-wide shift from ramp to steepening-margins was stimulated by the evolution of *Tubiphytes* and other organisms that stabilized platform margins. The western Yangtze platform (Guanling and Zhenfeng) and the northernmost isolated platform (the Great Bank of Guizhou) aggraded in the Anisian and developed high-relief escarpments during the Ladinian. At the same time the eastern sector of the Yangtze platform (Guiyang) evolved from an erosionally collapsed margin to a progradational margin that advanced basinward at least 600 m over basin filling clastics. The western Yangtze platform was drowned and buried by turbidites in the Late Triassic (Carnian) whereas shallow-water carbonate sedimentation continued until burial by siliciclastics in the eastern sector. The isolated platforms exhibit a north to south pattern of greater longevity in the north, step-backed margins and pinnacle development in the south, and earlier drowning and burial by siliciclastics in the south. These differences resulted from faster subsidence rates in the southern part of the basin caused by tectonic convergence along the southern margin of the south China plate.

The Great Bank of Guizhou has the longest history of the isolated carbonate platforms in the basin. A faulted syncline exposes a continuous two-dimensional cross section through the platform interior and margins, thus facilitating a detailed assessment of its architecture and depositional history. Conformable Permian-Triassic boundary sections, and thick, continuously exposed sections through the Early to Middle Triassic biotic recovery interval make this platform an ideal area for evaluating the marine environments and biotic conditions that operated during the end-Permian extinction and its aftermath.

Figures 11-18 are found in the guide for field excursion 2 p. 167-184 this volume

Tectonic setting of south China

The Nanpanjiang basin has the longest marine history of any basin in China, having been the site of marine sedimentation during most of the Late Proterozoic through Late Triassic (Enos, 1995). During the Permian and Triassic the Nanpanjiang basin formed a deep-marine embayment in the southern margin of the south China block (fig.1).

The south China block includes the Yangtze craton and south China fold system (fig. 1). Most authors have considered the south China block a single continental plate that stabilized in the Proterozoic or Early Paleozoic (Huang, 1978; Lin et al., 1985; Yang et al., 1986; Chen et al. 1991; Gilder et al., 1995; Metcalfe, 1996; Li, 1998; Tan et al., 2000). In contrast Hsu et al. (1988, 1990) proposed that the south China fold system is a separate tectonic block, the Huanan terrane that united with the Yangtze craton during the Late Triassic Indosinian orogeny. This hypothesis has received a great deal of criticism (Gupta, 1989; Rodgers, 1989; Rowley et al., 1989;

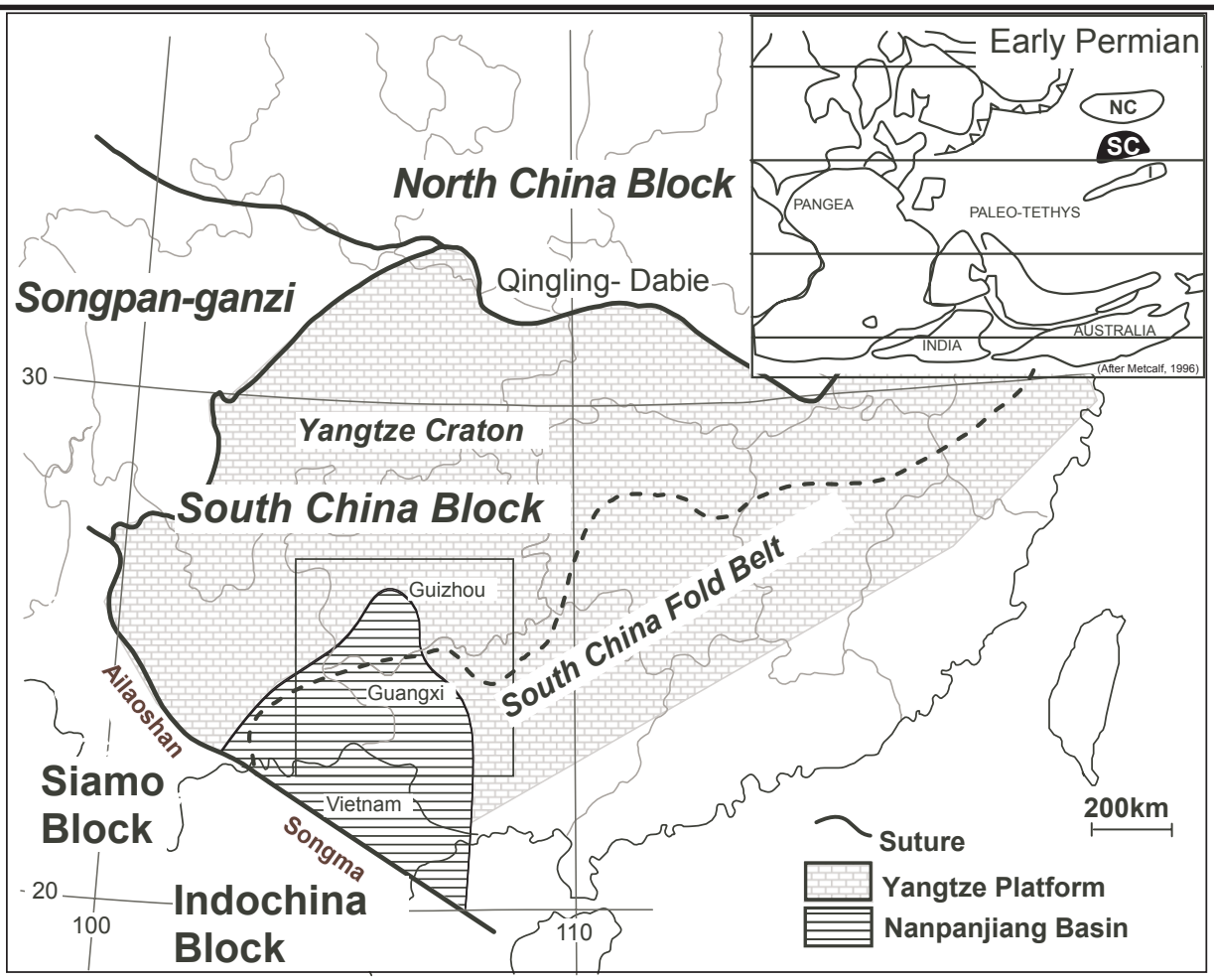

Figure 1: Tectonic map illustrating cratonic blocks (plates) of south China, interpreted suture zones and extent of the Nanpanjiang basin and Yangtze platform. South China block includes Yangtze craton and south China fold belt. Modified from Sun Shu et al., 1989. Inset, upper right illustrates global plate reconstruction and position of south China block (SC) in Early Permian. Modified from Metcalfe, 1996.

Tan et al., 2000) and would imply that a suture runs through the northern part of the Nanpanjiang basin (fig. 1). The stratigraphic similarities among carbonate platforms developed across the basin as well as similarities in subsidence histories (Koenig et al., 2001) support the interpretation of a south China block that has been unified since the Early Paleozoic and argue against Triassic suturing of the south China fold system.

The south China block is bordered on the north by the Qingling-Dabie orogenic belt, a suture between the north and south China blocks (fig. 1; Metcalf, 1996; among many others). To the northwest it is bounded by the Songpan-Ganzi fold system interpreted to be a remnant oceanic basin filled with Triassic flysch during suturing of the south and north China blocks (Ingersoll et al., 2003). The south China block is bordered on the south and southwest by the Ailaoshan and Songma/Songda faults which have been interpreted as suture zones bounding the Siamo-Sibumasu and Indochina plates respectively (fig. 1; Klimetz, 1983; Zhang et al., 1984; Wang, 1988; Metcalf, 1996).

Plate reconstructions indicate that the south China block rifted from the northeast margin of Gondwanaland probably adjacent to Australia during the Devonian (Metcalf, 1996), drifted northward across the Eastern Tethys, crossing the equator during the Permian to approximately 12^0 N latitude by the beginning of the Middle Triassic, and eventually docked with the north China plate along the Qinling suture during the Late Triassic (Klimetz, 1983; Sengör, 1987; Enkin et al., 1992; Van-der-Voo, 1993, Enos, 1995; Li, 1998; Paul Montgomery, 2002, unpublished paleomagnetic results from southern Guizhou). Controversy regarding whether the north and south China blocks docked instead during the Early Paleozoic (cf. Mattauer et al., 1985; Zhang et al., 1997) seems to have been reconciled with a tectonic model that includes earlier docking of a terrane along the northern Qinling followed by Late Triassic docking of south China along the southern Qinling (cf. Sun and Li, 1998 and Meng and Zhang, 1999).

The Siamo-Sibumasu and Indochina blocks converged upon and collided with the southern margin of the south China block sometime during the Late Paleozoic or Triassic (Klimetz, 1983; Zhang et al., 1984; Wang, 1988; Fan and Zhang, 1994; Metcalf, 1996, 2002). There has been controversy as to the timing of suturing of Indochina and the Siamo-Sibumasu blocks to south China and as to

whether the Songma/Songda fault zone represents a suture (Findlay and Trinh, 1997). Most authors have interpreted suturing and collision along the Ailaoshan and or Songma/Songda zones during the Triassic Indosinian orogeny (Klimetz, 1983; Zhang et al., 1984; Wang, 1988; Sengör et al., 1987; Fan and Zhang, 1994; Carter et al., 2001). Others have interpreted Paleozoic docking of Indochina and south China (Hutchinson, 1989; Metcalf, 1996, 2002; Findlay and Trinh, 1997). The Ailaoshan and Songma/Songda zones are exceedingly complex. They may include a history of docking of smaller Late Paleozoic terranes (cf. Metcalfe, 2002), as well as having been involved in Triassic convergent tectonism and metamorphism (cf. Lepvrier et al., 1997; Lacassin et al., 1998); finally they were overprinted by extensive Cretaceous-Tertiary shearing and metamorphism associated with India-Asia collision (cf. Tapponier et al., 1990; Lepvrier et al., 1997). Although Indosinian convergence and arc development along the Songma/Songda in the south remains controversial, several observations in the Triassic record support this interpretation: 1) The patterns of greater longevity of carbonate platforms in the northern part of the basin (e.g. Permian-Carnian of the Great Bank of Guizhou) and shorter history, earlier drowning and stepback of platforms in the southern part of the basin (fig. 2-5), 2) earlier onset of accelerating subsidence and greater subsidence rates in the southern part of the basin (fig. 6; Koenig et al., 2001) and 3) thickening felsic volcanics in the southern part of the basin (Newkirk et al., 2002).

The Nanpanjiang basin is embayed by the Yangtze platform, a vast platform of primarily shallow-marine deposition that stretches across much of the south China block (fig. 1) (Wang, 1985; Yang et al., 1986; Liu and Xu, 1994; Enos, 1995; Xu Qiang, et al., 1996; Xu Xiaosong, et al., 1996). During the long history of marine sedimentation from Proterozoic to Late Triassic, the Yangtze platform-Nanpanjiang basin system of Guizhou and Guangxi underwent several important phases of tectonic reorganization.

The south China block (Yangtze Craton) stabilized as a cratonic block during the Neoproterozoic ***Yangtze orogeny,*** which was followed by stable cratonic sedimentation during the end of the Proterozoic (Sinian) and Early Paleozoic (fig. 6; Huang, 1978; Ren et al., 1987; Metcalf, 1996). In Guizhou and Guangxi the Proterozoic basement is unconformably overlain by Neoproterozoic (Early Sinian) glacial and glacial-marine deposits followed in the Late Sinian and Cambrian by shallow and deep marine clastics marking transgression and initiation of passive margin development (Guangxi Bureau, 1985; Guizhou Bureau, 1987). Early Paleozoic facies are dominated by mature clastics and shallow-marine carbonates, indicating the development of a vast and longstanding passive continental margin (fig. 6; Wang, 1985).

The region became tectonically active during the Early Devonian ***Guangxi orogeny,*** resulting in development of a basinwide unconformity and the regional absence of basal Devonian sediments (fig. 6; Guangxi Bureau, 1985; Guizhou Bureau, 1987; Xie et al., 1984). The unconformity bevels strata down to the Cambrian in southern Guangxi (unpublished regional stratigraphic data; Geological Survey of Guangxi). Regional tectonic syntheses have inferred extensional block faulting associated with the Devonian orogeny. The Guangxi orogeny has been widely attributed to a phase of extensional deformation impacting the region (Guangxi Bureau, 1985; Guizhou Bureau, 1987; Xie et al., 1984; Huang, 1978; Qing et al. 1991; Xu Xiaosong, et al., 1996). Plate reconstructions indicate the Early Devonian deformation and uplift probably resulted from the rifting of the south China block from Gondwanna (cf. Metcalf, 1996).

Passive-margin conditions resumed in the Late Paleozoic with widespread development of shallow-marine carbonate sedimentation in the Yangtze platform in Guizhou and around the eastern periphery of the Nanpanjiang basin in Guangxi (Wang, 1985; Enos, 1995; Xu Xiaosong, et al., 1996). Regional paleogeographic reconstructions have indicated the existence of isolated carbonate platforms developed within the basin in Guangxi during the Devonian (Xie et al., 1984; Wang 1985; Xu Xiaosong, et al., 1996).

Several authors have speculated that horst blocks formed in the Devonian set up the structural grain for the nucleation of isolated carbonate platforms that developed in Guizhou and Guangxi (cf. Xie et al., 1984; Qing et al., 1991). Regional mapping demonstrates that the margin of at least one of the isolated Triassic platforms, the Chongzuo platform in the southern part of the basin, was controlled by a fault and that another, the Great Bank of Guizhou in the northern part of the basin, nucleated on antecedent topography inherited from an Upper Permian reef margin rather than a fault block (fig. 2, 3; Lehrmann et al., 1998).

The Lower-Upper Permian transition is marked by a period of renewed tectonic activity with extensional faults, eruption of the Emeishan Basalt along the western margin of the basin, and development of a disconformity that extends across the entire basin (Guangxi Bureau, 1985; Guizhou Bureau, 1987). This period of activity is commonly referred to as the "***Dongwu movement***" in the Chinese literature (fig. 6; Dai et al., 1978; Zhang, 1984; Guizhou Bureau, 1987; Huang and Chen, 1987). The most dramatic expression of this tectonism is vast outpourings of Emeishan Basalt. Eruption of the Emeishan flood basalt was apparently centered in southern Sichuan and eastern Yunnan, where maximum reported thicknesses exceed 2 km (Luo et al., 1990; Chung and Jahn, 1995). Emeishan tectonism has been variously interpreted to have resulted from rifting, back arc spreading, or development of a mantle plume (Yang et al., 1986; Guizhou Bureau, 1987; Qing et al., 1991; Luo et al., 1990; Xu Xiaosong, et al., 1996; Thompson et al., 2001; Song et al., 2004). The Emeishan basalt thins eastward and extends into western Guizhou where it has a maximum thickness of 500 m. The basalt thins and pinches out to the southeast and is found only within the westernmost part of the Nanpanjiang

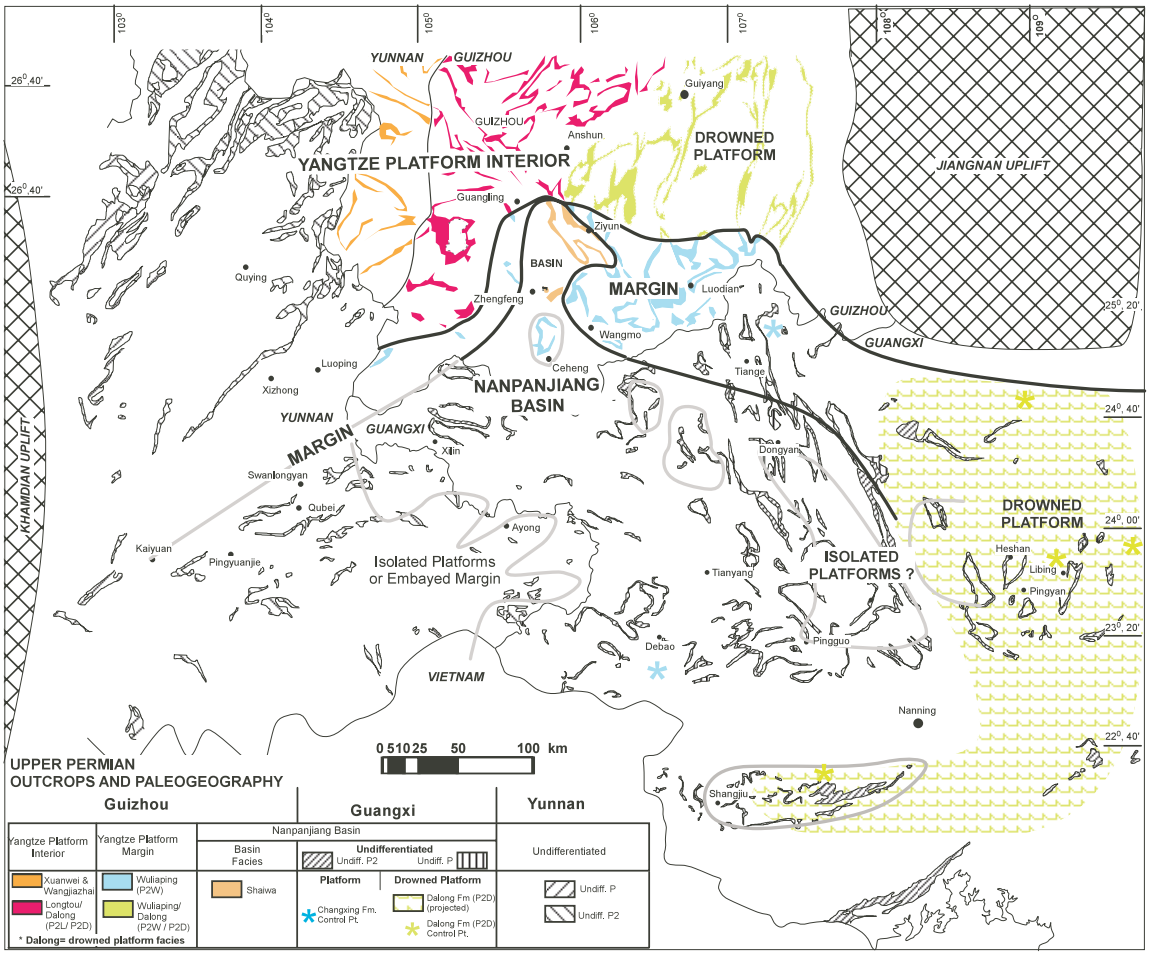

Figure 2: Upper Permian lithofacies and interpreted paleogeography of the Nanpanjiang basin and Yangtze platform in Guizhou, Guangxi, and Yunnan. Compiled from regional geologic maps of the Yunnan Bureau of Geology, 1984; Guangxi Bureau of Geology, 1985, and Guizhou Bureau of Geology, 1987. Maps have been modified and updated with results from our regional mapping. Data control (colored facies polygons) is the distribution of surface exposure of various facies (Formations) indicated in the legend.

basin, suggesting that the Dongwu movement may have had its greatest impact in the western part of the basin.

From the Late Permian through Middle Triassic the Yangtze platform was the site of a thick and expansive succession of shallow-marine carbonates with intermittent siliciclastic flux onto the platform from the west and with a variety of reef, ramp and collapsed type platform margins (Enos, 1995, Enos et al., 1997, 1998). Isolated carbonate platforms developed within the basin during the Triassic (fig. 3; Lehrmann et al., 1998). Deep-marine sedimentation in the Early Triassic basin was dominated by relatively thin "starved" pelagic carbonate and shale of the Luolou Formation (fig. 3) indicating relatively quiet tectonic conditions.

Conditions changed dramatically during the Middle and Late Triassic ***Indosinian orogeny***. During the Middle and Late Triassic the basin rapidly subsided and was eventually filled with siliciclastic turbidites (fig. 4, 5, 6). Carbonate platforms were progressively drowned and buried with siliciclastics from the beginning of the Middle Triassic Anisian (in southern basin) to the beginning of the Late Triassic (northern basin) (fig. 3, 4, 5). Marine turbidites changed upward to fluvial clastics marking the end of marine sedimentation in the Late Triassic (fig. 7). The Indosinian orogeny marks the termination of marine conditions across the south China block. Although the Indosinian orogeny is an important turning point in the evolution of the Nanpanjiang basin, the specific tectonic cause is still unclear.

During the Triassic, the Nanpanjiang basin has been variously interpreted as a back arc or foreland basin with an arc developed in southern Guangxi or within a southerly continent (He, 1986; Xia et al., 1993), as a back arc extensional basin (Hou and Huang, 1984), as a foreland basin developed along the eastern side of collision zone along the Ailaoshan suture (Qing et al., 1991), and as a flysch nappe thrust over a suture zone from the Huanan block onto the Yangtze craton (Hsu et al., 1990). The Middle Triassic history adequately classifies the Nanpanjiang basin as a foreland basin as a perisutural basin developed on continental lithosphere associated with compressional tectonics (Allen et al., 1986), as south China was involved in convergence and collision potentially along its north-

ern, western and southern sides.

Enos et al. (1998) noted that the facies succession formed during Late Triassic termination of the Yangtze platform in southern Guizhou forms a classic flysch to mollasse sequence typical of a foreland basin (fig. 7). However, the directions of the source areas and the timing of siliciclastic flux are complex and poorly understood. The flysch in southern Guizhou (Bianyang Formation) seems to have been derived from the east based on paleocurrents (Sun et al., 1989; Chaikin, 2004). The sandstone petrology and heavy mineral suite are consistent with derivation from the Jiangnan massif (fig. 5; Chaikin, 2004). The rapid rate of supply (Carnian, adjacent to the Great Bank of Guizhou) is surprising, however, and indicates uplift and rejuvenation. Siliciclastics in the southern part of the basin must have arrived earlier as evidenced by the Anisian and Ladinian burial of isolated carbonate platforms in Guangxi (fig. 3, 4, 5). On the other hand, the mollasse (Bannan, Houbachong and Erqiao Formations; fig. 7) in Guizhou thins and fines rapidly eastward and more slowly northward (Enos et al., 1998). A source to the west, likely the Khamdian massif, is indicated (fig. 5).

Permian-Triassic stratigraphy and depositional setting of the Yangtze platform and Nanpanjiang basin

Permian and Triassic stratigraphy of the Yangtze platform in Guizhou

The Yangtze Platform of south China formed a stable paleogeographic element from late Proterozoic to the end of Middle Triassic. Mature sedimentary facies, in particular shallow-water carbonates, accumulated during much of this time. The Yangtze Platform bordered or surrounded several persistent massifs ("oldlands"), notably the Jiangnan massif in southeast Guizhou and adjacent provinces and the Khamdian massif in eastern Yunnan (fig. 2). The southern margin of the platform was embayed by the Nanpanjiang Basin that extended into central Guizhou (fig. 2). Persistent deep-water deposits surrounded various isolated carbonate platforms within the basin.

The Early Permian deposits on the platform in southern Guizhou were dominated by fossiliferous limestone with minor dolostone (the upper part of Maping Formation and lower Houziguan Formation; table 1). The Lower Permian platform-interior strata are capped by a regional subaerial exposure surface. The Nanpanjiang basin was broad, although rather shallow, but in southern Guizhou it was confined to a narrow gulf (Liu and Xu, 1994). The Early Permian deposits in the basin were dark-gray to black thin-bedded limestone, chert and mudstone, intercalated with debris-flow breccia (Nandan Formation; 300 – 500 m thick, table 1). Within in a very limited area of the platform in western Guizhou**,** at the transition belt between platform and basin, argillaceous limestone, sandstone, mudstone (Longyin Formation) and black shale (Baomoshan Formation; table 1) were conformably deposited over the top of the shallow-water limestone (Maping Formation; table 2).

The Middle Permian deposits in the basin were claystone and marl with subordinate limestone and shale (Sidazhai Formation; 350-650 m thick table 1, fig. 7). The initial Middle Permian deposits on the platform were well differentiated. Argillaceous sandstone and claystone with some coal flanked the Khamdian massif in the west (Liangshan Formation; table 1). Shale layers with brachiopods record marine incursions. Eastward, in southern Guizhou, the shore zone produced cleaner sandstone and siltstone that interfinger with coal, shale, marl and fossiliferous marine limestone, and finally graded into limestone. Later on, cherty, nodular lime mudstone (Qixia Formation; table 1) and fossiliferous limestone, locally cherty (Maokou Formation; table 1) dominated across the entire platform. The carbonate content and energy increased seaward to produce pure bioclastic limestone and *Tubiphytes*-sponge boundstone at the platform margin (Houziguan Formation, table 1, fig. 7). The Jiangnan massif was submerged essentially throughout the Permian, as witnessed by scattered outcrops of marine limestone across the massif, a lack of facies differentiation, and overstepping of older formations by Permian deposits around the massif (Guizhou Bureau, 1987; Liu and Xu, 1994; Enos, 1995). Deposition was interrupted in mid-Permian by a great outpouring of tholeiitic lava, the Emeishan Basalt, that extended across the Yangtze Platform from the Khamdian area (table 1, fig. 7).

Facies distributions and migrations in the Late Permian were similar to those of the Middle Permian. The Nanpanjiang Basin in Guizhou became even narrower, presumably because of gradual progradation of the platform rimmed by reefs and bioclastics (fig. 2). Basinal deposits are claystone and bedded chert that enclose carbonate breccias and bioclastic limestones, probably turbidites (Shaiwa Formation, table 1, figs. 2, 7). Cherty, bioclastic limestone with sponge and coral reefs at the platform margin pass into cherty, micritic and argillaceous limestones, calcareous siltstones and claystones in the platform interior (Wujiaping and Changxing Formations, respectively; table 1, figs. 2, 7). These interfinger toward the Khamdian massif with claystone and coal and finally with alluvial sandstone (Longtan, Wangjiazhai and Xuanwei Formations; table 1, figs. 2, 7). Terrestrial deposition persisted in the Khamdian massif throughout the Late Permian, indicating less extensive flooding than in the Middle Permian. Eventually the carbonate platform was covered by chert and spiculitic mudrock, a deepening phase that marked the permanent drowning of large areas of the Yangtze platform (Dalong Formation, table 1, figs. 2, 7).

Deposition continued uninterrupted into the Early Triassic in most areas. The drowning event toward the end of the Permian (Dalong Formation; table 1, fig. 2) resulted in a reconfiguration of the platform margin to a sigmoidal SW/NE trend involving more than 100 km of retreat of the eastern margin in southern Guizhou (Luodian, Guiyang; fig. 3). Following initial deposition of bivalve-

TABLE 1. STRATIGRAPHIC UNITS AND DEPOSTIONAL ENVIRONMENTS OF THE PERMIAN SYSTEM SOUTHWESTERN GUIZHOU

<table>
<tr><th></th><th>STAGE*</th><th>TERRESTRIAL</th><th>PARALIC</th><th>PLATFORM INTERIOR</th><th>PLATFORM MARGIN</th><th>BASIN</th></tr>
<tr><td rowspan="3">Upper Permian</td><td rowspan="2">CHANGXING</td><td rowspan="3">XUANWEI FM.
Alluvial & lacustrine sandstone, shale & coal</td><td rowspan="2">WANGJIAZHAI FM.
Interfingering marine & continental siliciclastics

& coal</td><td colspan="2">DALONG FM.
Dark, spiculitic mudrock & chert
Moderately deep water</td><td rowspan="3">SHAIWA FM. and LINGHAO FM
Shale, thin siltstone, lime mudstone & breccia</td></tr>
<tr><td>CHANGXING FM.
Bioclastic limestone, locally cherty</td><td rowspan="2">WUJIAPING FM.
Cherty bioclastic limestone, coral/ sponge reefs</td></tr>
<tr><td>LEPING</td><td>LONGTAN FM.
Interbedded continental sandstone, mudrock, coal & marine limestone</td><td>WUJIAPING FM.
Cherty limestone, local coral/sponge reefs, some shale, coal</td></tr>
<tr><td rowspan="5">Middle Permian</td><td rowspan="2">MAOKOU</td><td colspan="3">EMEISHAN BASALT Tholeiitic basalt & tuff, to 800 m thick</td><td rowspan="5">HOUZIGUAN FM.
Bioclastic packstone sponge boundstone
Bioclastic packstone Tubiphytes boundstone</td><td rowspan="5">SIDAZHAI FM.
Cherty lime mudstone & shale.</td></tr>
<tr><td colspan="2">No record</td><td>MAOKOU FM.
Fossiliferous, micritic & dolomitic limestone</td></tr>
<tr><td>QIXIA</td><td colspan="2">No record</td><td>QIXIA FM.
Fossiliferous, micritic cherty limestone</td></tr>
<tr><td rowspan="2"></td><td>LIANGSHAN FM.
Argillaceous sandstone, claystone, coal, & shale with brachiopods</td><td>HUAGOANG FM.
Quartz arenite, siltstone, shale, bioclastic limestone, marl & coal</td><td>SAZHI FM
Argillaceous & bioclastic limestones, silty claystone & shale</td></tr>
<tr><td rowspan="2">Lower Permian</td><td rowspan="2">LONGYIN</td><td colspan="2" rowspan="2">No record</td><td>BAOMOSHAN FM</td><td rowspan="2">NANDAN FM</td></tr>
<tr><td>LONGYIN FM</td></tr>
<tr><td></td><td>MAPING</td><td colspan="3">MAPING FM</td><td></td></tr>
<tr><td>Carboniferous</td><td></td><td colspan="3"></td><td>WEINING FM</td><td></td></tr>
</table>

ADAPTED FROM GUIZHOU BUREAU (1987), ENOS (1995).

* Designation of Permian stage names in China is still in flux (cf. Enos, 1995; International Union of Geological Sciences, 2000). Guizhou stage names are used here. Changxing (Changshingian) and Wujiaping (Wuchiapinian) are recognized as semiformal stages by IUGS (2000), although the formations on which they are based are considered partially time equivalent in Guizhou (Guizhou Bureau, 1987, p. 271).

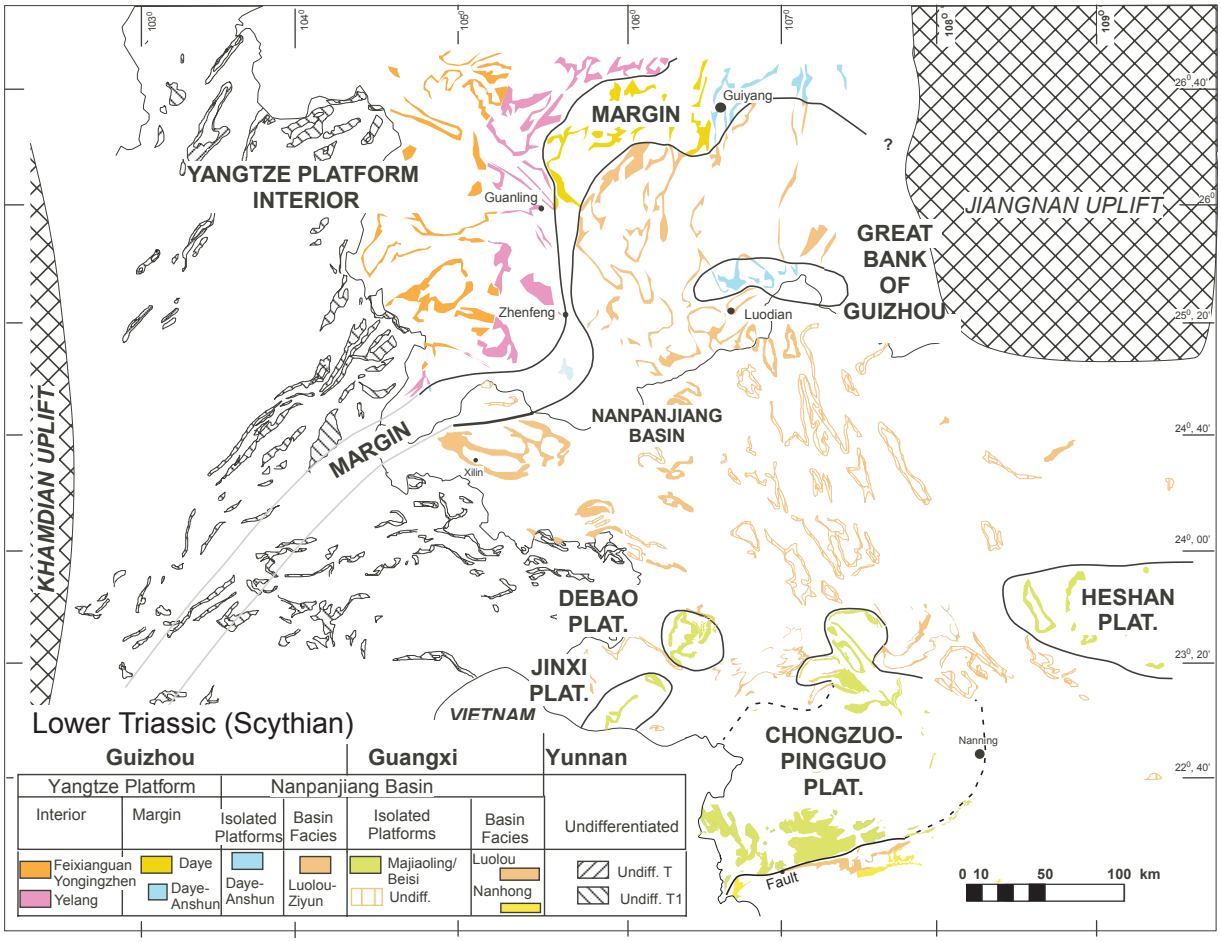

Figure 3: Lower Triassic (Scythian) lithofacies and interpreted paleogeography of the Nanpanjiang basin and Yangtze platform in Guizhou, Guangxi, and Yunnan. Compilation data and methods are given in caption for figure 2.

bearing mudrock, a carbonate ramp developed in the Induan across the flat top of the Permian platform. Distal ramp deposits are thin, commonly laminated, beds of dark-gray lime mudstone with ammonoids and thin-shelled bivalves (Luolou Formation; table 2, fig. 3, 7). Interspersed carbonate breccias reflect intrabasinal slumps and debris flows from shallower environments to the northwest. Thin-bedded lime mudstones with prominent burrowed horizons formed on the mid-ramp (Daye Formation; table 2, fig. 3, 7). Updip, three to five thick intervals of oolite are interspersed within mudrock and lime mudstone (Yelang Formation; table 2, fig. 3). Mudrock and sandstone predominate westward toward the Khamdian massif. Basinal deposits in the Olenekian are alternating lime mudstone and terrigenous mudrock totaling only 100 m thick (upper Luolou Formation; table 2, fig. 3, 7). Peritidal carbonate cycles capped by tepee structures mark the platform margin (Anshun Formation; table 2, fig. 3). Subtidal lime mudstone in the platform interior indicates a lagoon behind a raised rim (Yongingzhen Formation; table 2, fig. 3). The lagoon became very restricted toward the end of the Olenekian with the deposition of evaporites, represented by extensive solution-collapse breccias.

The Early-Middle Triassic boundary in Guizhou is demarcated by a widespread acid tuff layer, dated at 247 Ma (Martin et al., 2001). Anisian deposits in the Nanpanjiang basin are predominately siliciclastic mudrocks, only 250 m thick in central Guizhou, but more than 1000 m thick to the southwest (Xinyuan and Zuman Formations; table 2, fig. 4, 7). Platform-interior deposits are subtidal lime mudstones with sparse but widespread molds of gypsum crystals and rosettes. Peritidal cycles are confined to near the platform margin (Guanling Formation; table 2, fig. 4). Numerous thin shale interbeds that give a ledged appearance to outcrops were probably derived from the east, where red mudrock and sandstone signal the emergence of the Jiangnan massif. The first well-developed reefs of the Triassic formed a narrow, elevated rim on the platform. *Tubiphytes*, *Plexoramea*, arborescent corals, and sponges formed a framework with copious encrustation by other problematic fossils and cements (Poduan Formation; table 2, fig. 4, 7). Episodic collapse of the reef margin produced an apron of bioclasts and debris at the basin margin that includes reef blocks up to 100 m long (Qingyan Formation; table 2, fig. 4; Enos et al., 1997). The total absence of reef facies, except in the transported blocks, along most of the 175-km-long debris apron in the northeast (Guiyang area, fig. 4) suggests a uniform retreat of at least 3 to 7 km, the average width of the reef belt elsewhere.

The platform margin apparently grew higher and steeper

TABLE 2. STRATIGRAPHIC UNITS AND DEPOSTIONAL ENVIRONMENTS OF THE TRIASSIC SYSTEM SOUTHWESTERN GUIZHOU

STAGE	PLATFORM INTERIOR	PLATFORM MARGIN	BASIN	GUIYANG AREA (PLATFORM)
RHAETIAN	ERQIAO FM. Braided-stream gravel to mudstone		NO STRATA PRESERVED	ERQIAO FM. Thinner sandstone and mudstone. Distal stream deposits
NORIAN	HUOBACHONG FM. Cyclic braided-stream deposits; marine mudstone incursions; paralic coals			HIATUS
CARNIAN	BANAN FM. Cyclic sandstone and mudstone; shallow-shelf to coastal			HIATUS?
	LAISHIKE FM. Flysch; turbidite sandstone & mudrock		LAISHIKE FM. (very local)	SANQIAO FM. Shallow-marine sandstone, mudstone, limestone
	WAYAO FM. Condensed black shale & mudrock		BIANYANG FM. Partly or entirely Carnian?	GAICHA FM. Peritidal limestone with minor sandstone & mudrock
	ZHUGANPO FM. Deep-water, nodular lime mudstone			
LADINIAN	YANGLIUJING FM. Cyclic peritidal dolostone tepees common	LONGTOU FM. Cyclic peritidal limestone tepees common	BIANYANG FM. Flysch; turbidite sand-stone & mudrock	LONGTOU FM. Cyclic peritidal limestone tepees common
ANISIAN	GUANLING FM. Subtidal argillaceous limestone; evaporite molds	PODUAN FM. Framework reefs of *Tubiphytes* & arborescent corals; breccia	XINYUAN FM. (thin) ZUMAN FM. (v. thick) Distal turbidites & mudrock, ± calcareous	PODUAN FM. (Same) QINGYAN FM. (basin margin) Lime breccias, calci-turbidites, lime mudstone
OLENKIAN	YONGNINGZHEN FM. Subtidal muddy limestone; evaporites in top	ANSHUN FM. Cyclic peritidal dolostone, oolite.	UPPER LUOLOU (ZIYUN) FM. Mudrock ± calcareous; Lime mudstone	ANSHUN FM. Cyclic peritidal dolostone, Tepees common
INDUAN	YELANG FM. Limestone & oolite; red weathering typical	DAYE FM. Mid-ramp; interbedded laminated & burrowed lime mudstone	LUOLOU FM. Distal ramp; mudrock (base); laminated lime mudstone (top)	DAYE FM. Mid-ramp; interbedded laminated & burrowed lime mudstone

*ADAPTED FROM GUIZHOU BUREAU (1987) AND YANG SHOUREN ET AL., 1995.
FEIXIANGUAN FM. (Induan, western Guizhou): sandstone & mudrock, fluvial and littoral deposits
BADONG FM. (Middle Triassic, eastern Guizhou): sandstone and red shale

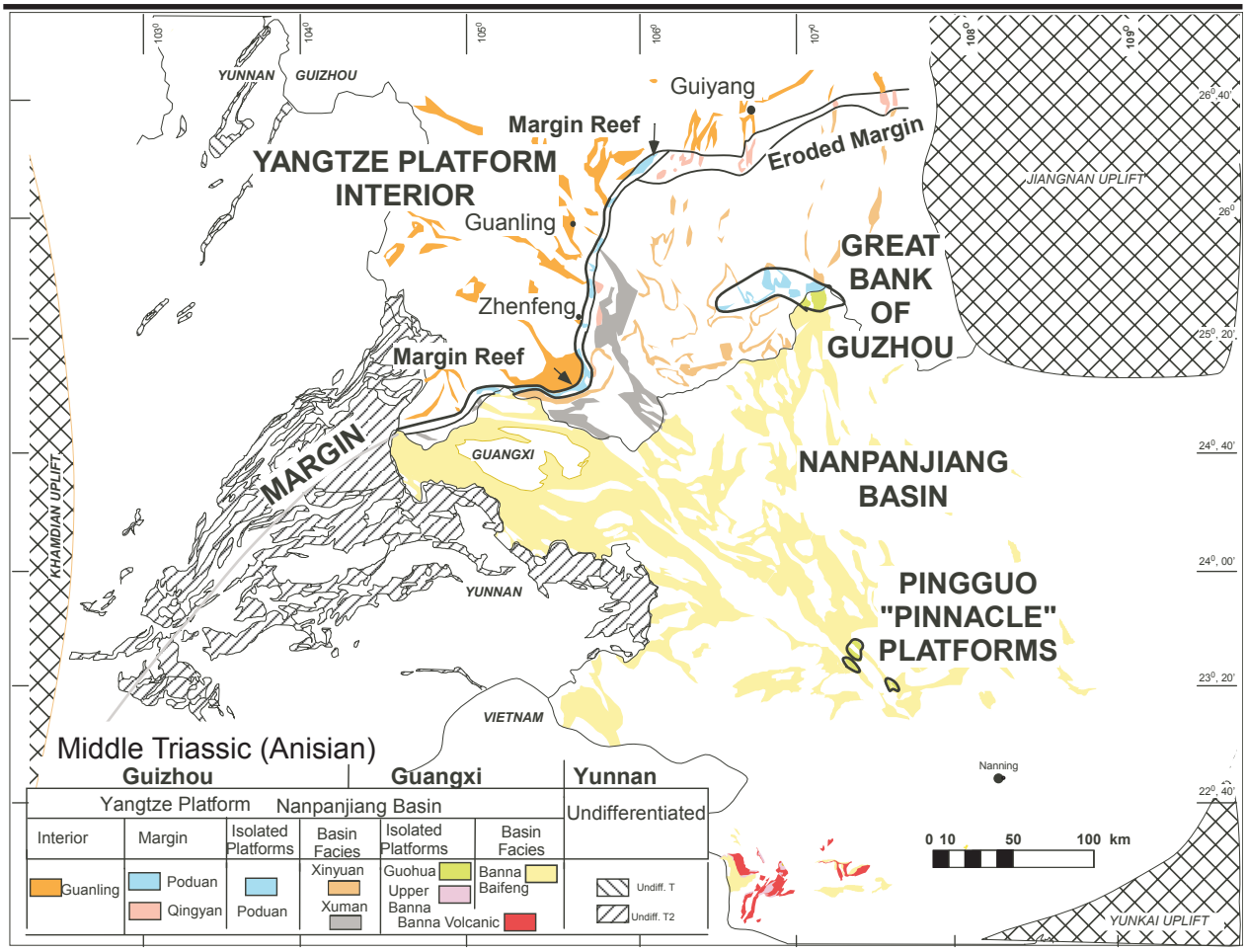

Figure 4: Middle Triassic (Anisian) lithofacies and interpreted paleogeography of the Nanpanjiang basin and Yangtze platform in Guizhou, Guangxi, and Yunnan. Compilation data and methods are given in caption for figure 2.

in the Ladinian, although sands of bioclasts and grapestone formed the margin, whereas reefs were confined to small patches (Longtou Formation; table 2, fig. 5, 7). Peritidal cycles capped by tepee structures are ubiquitous and extend far into the platform interior, indicating a flat top to the platform. This package, around 1000 m thick, of limestone at the margin and dolostone in the interior forms the most prominent ridges in the landscape of southwestern Guizhou (Longtou and Yangliujing Formations; table 2, fig. 5). The Ladinian platform margin prograded at least 600 m over Anisian basinal deposits south of Guiyang (Xinyuan Formation, table 2, fig. 7), but backstepped and aggraded in the Zhenfeng area (fig. 5). The basin was eventually filled with flysch deposits, hemipelagic mudrock and fine-grained turbidite sandstones about 2000 m thick (Bianyang Formation; table 2, fig. 5, 7). Filling may have accompanied platform aggradation, but the detailed conodont record at the north slope of the Great Bank of Guizhou indicates that the basin was starved until early Carnian and then filled with extreme rapidity (Lehrmann, 1993; Lehrmann et al., 1998, 2002), an end-member example of reciprocal sedimentation.

Shallow-water carbonate deposition continued on the Yangtze platform into the Carnian in the Guiyang area. Some shale and sandstone are interspersed with peritidal limestone about 100 m thick (Gaicha Formation; table 2). Later the balance shifts strongly to sandstone and shale with shallow-water biota (Sanqiao Formation; table 2). In contrast, Carnian deposition in the Zhenfeng and Guanling areas begins with nodular-bedded, ammonoid-bearing, dark-gray lime mudstone that records abrupt drowning of the Yangtze platform (Zhuganpo Formation; table 2; Enos et al., 1998). Carbonate deposition soon ceased, resulting in a condensed sequence characterized by black shale and marl with concentrations of manganese, iron and organic carbon (Wayao Formation; table 2). The Wayao Formation is gaining fame for its spectacular crinoid and marine reptile lagerstätte developed in the Guanling area (fig., 5; Yin et al., 2000). Accommodation space created during drowning was subsequently filled by up to 800 m of turbiditic sandstone and mudrock and 465 m of shallow-shelf sandstone during the Carnian (Laishike and Banan Formations; table 2). Thinning- and fining-upward cycles of conglomerate and cross-bedded sandstone of the Norian are interpreted as braided-stream deposits with interspersed paralic coals and mudrocks bearing fresh-water, brackish, or marine fossils (Huobachong Formation; table 2, fig. 7). Still coarser grained deposits of the Rhaetian indicate rejuvenation of braided streams to form a clastic wedge that thins and fines rapidly to the east and slowly to the north as it spread across a surface that beveled platform deposits as old as Anisian (Erqiao Formation; table 2, fig. 7). Thus, the

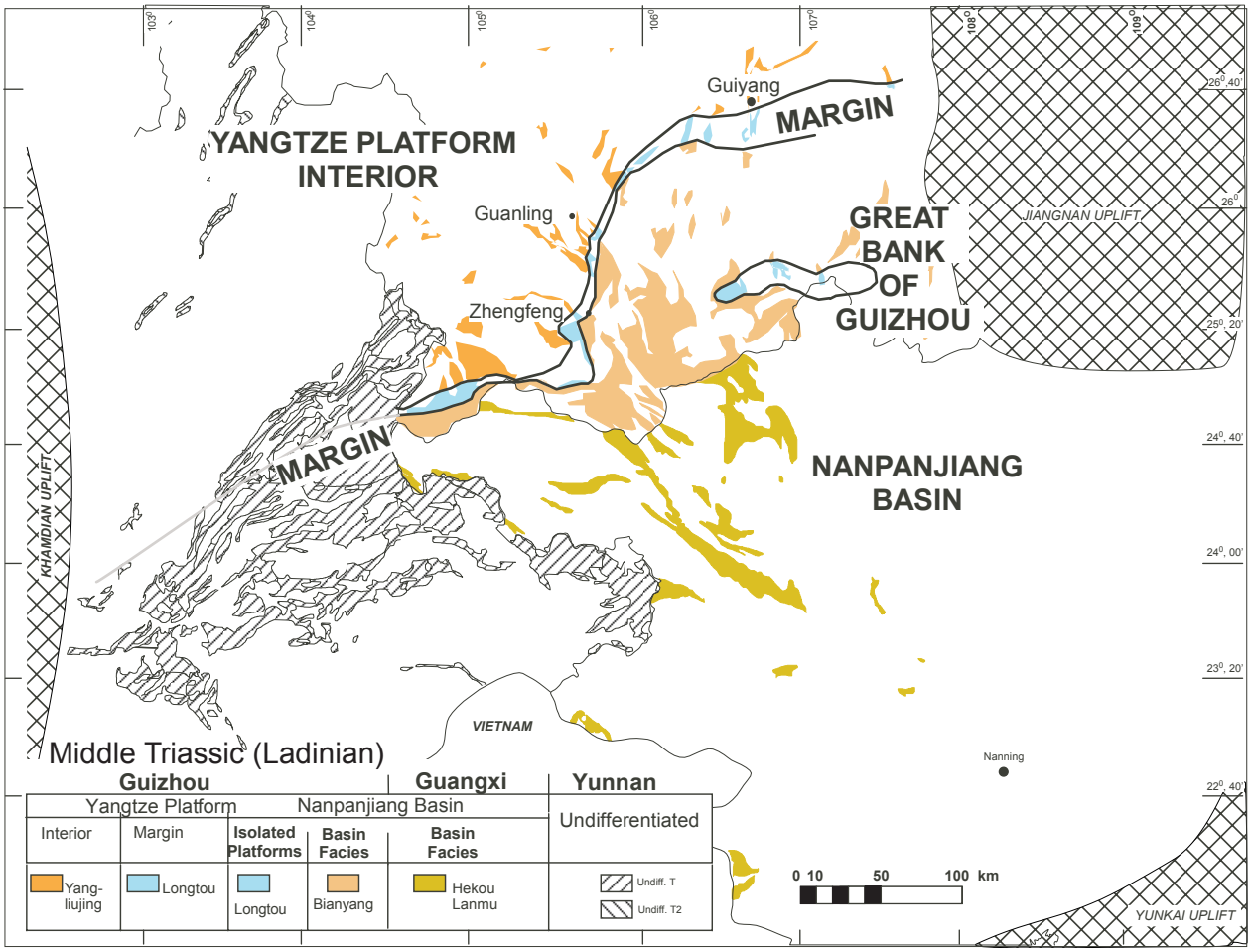

Figure 5: Middle Triassic (Ladinian) lithofacies and interpreted paleogeography of the Nanpanjiang basin and Yangtze platform in Guizhou, Guangxi, and Yunnan. Compilation data and methods are given in caption for figure 2.

long and impressive history of the Yangtze carbonate platform ended in the Carnian throughout Guizhou.

Isolated carbonate platforms of the Nanpanjiang basin in Guizhou and Guangxi

During the Triassic several isolated platforms developed within the Nanpanjiang basin including the Great Bank of Guizhou in southern Guizhou Province, and the Debao, Jinxi, Heshan and Chongzuo-Pingguo platforms in southern Guangxi (fig. 3). Each of the platforms is delineated from regional mapping of the distribution of shallow-marine carbonate platform facies and deep-water basinal carbonate and clastic facies. The Great Bank of Guizhou nucleated on antecedent topography inherited from the Late Permian Yangtze platform margin (fig. 2, 3). The isolated platforms in southern Guangxi may represent continued accumulation of shallow-marine carbonate sediments atop older isolated platforms that existed already in the Late Permian, although regional mapping in Guangxi does not differentiate facies sufficiently to delineate platform distribution (fig. 2). The southern margin of the Chongzuo-Pingguo platform was controlled by a regional fault for much of its length (fig. 2, 3). The north wall of the fault was elevated in the Late Permian.

Regional maps delineate the Great Bank of Guizhou to be composed of shallow-marine carbonate platform facies of the Lower Triassic Daye and Anshun Formations, and the Middle Triassic Poduan and Longtou Formations surrounded by basinal facies of the Lower Triassic Luolou Formation and the Middle Triassic Xinyuan and Bianyang Formations (fig. 3, 4, 5, 7). Like the Yangtze platform, the Great Bank of Guizhou evolved from a ramp (or low relief bank) profile in the Early Triassic through a progressively steepening reef-rimmed profile in the Middle Triassic and was terminated and buried with clastics in the Late Triassic Carnian (fig. 7). Details of the lithofacies and depositional environments of the Great Bank of Guizhou are provided in the following section.

The Debao, Jinxi, Heshan and Chongzuo-Pingguo platforms in Guangxi are delineated in regional geological maps as shallow-marine carbonate facies of the Majiaoling and Beisi Formations surrounded by basinal carbonates and clastics of the Luolou and Nanhong Formations respectively (fig. 3). The Majiaoling Formation consists of thin-bedded and burrowed lime mudstone with thin lenses of oolite. The Beisi Formation, in contrast, contains a number of thick beds of oolite grainstone, and contains restricted molluscan biota, supratidal fabrics and dolostone in its upper part. In the Chongzuo-Pingguo platform the Majiaoling and Beisi Formations are 140 m and 750 m thick respectively. Oolite intervals in the Beisi Formation at Chongzuo are typically cross-bedded and occur in mas-

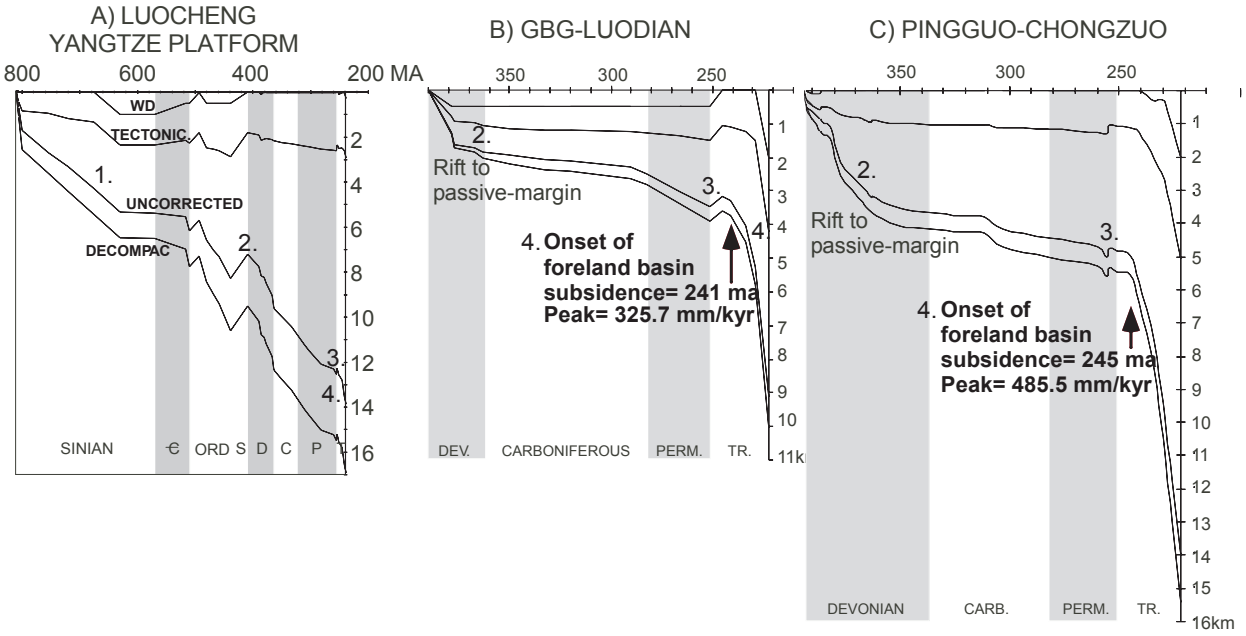

Figure 6: Subsidence histories. Subsidence curves were compiled from unpublished composite stratigraphic sections, biostratigraphy, lithofacies and interpreted water depths provided by the Guizhou Bureau of Geology and Geological Survey of Guangxi. Subsidence analyses (backstripping) were performed with a program provided by M. A. Kominz using the decompaction and tectonic subsidence algorithms of Bond and Kominz (1984). A) Proterozoic through Triassic subsidence history from Loucheng of central Guangxi. B) Devonian through Triassic subsidence history from GBG-Luodian area southern Guizhou. C) Devonian through Triassic subsidence history from Chongzuo-Pingguo platform, southern Guangxi. Tectonic events indicated numerically: 1 - Late Proterozoic to Early Paleozoic stabilization of Yangtze craton and passive-margin development. 2 -Guangxi orogeny, Devonian rifting of south China block from Gondwana. 3 – "Dongwu movement" Late Permian extension associated with Emeishan volcanism. 4. Indosinian orogeny, Triassic foreland basin development and accelerating subsidence. See text for discussion of tectonic history.

sive ridge forming units up to 50 m thick (Pei Donghong, unpublished data). The Luolou Formation consists of dark-gray to black, ammonoid bearing, thin-bedded and laminated lime mudstone with shale interbeds. Some intervals contain bedding parallel burrows and the unit contains debris-flow breccias adjacent to carbonate-platform margins. The Nanhong Formation occurs south of the Chongzuo-Pingguo platform and consists of ammonoid bearing sandstone, shale and siliciclastic mudstone.

During the Early Anisian much of the area of the southerly isolated carbonate platforms was terminated (drowned) during a deepening event and the platforms were subsequently overlain by siliciclastic turbidites of the Banna and Baifeng Formations (fig. 4). Just prior to carbonate platform drowning and shift to basin-clastics a thick pile of felsic pyroclastic volcanics and lava flows were deposited on top of the southern part of the Chongzuo-Pingguo platform (Guangxi Bureau, 1985). Although the volcanism effectively buried the platform, shallow-marine carbonate sedimentation resumed briefly following the cessation of volcanic activity. Deepening then resulted in a shift to pelagic carbonates and siliciclastics as the platform drowned in the Early Anisian. The northern part of the Pingguo-Chongzuo platform (Pingguo area) as well as the Heshan platform to the east also suffered drowning in the Early Anisian (fig. 3-4; Kessel and Gross, 2002). During the regional drowning of shallow-marine carbonate sedimentation in southern Guangxi, small areas of carbonate sedimentation accumulated to produce Anisian pinnacle platforms within the Pingguo area (fig. 4). The pinnacle platforms are represented by the Guohua Formation and are composed of peritidal dolomite and limestone containing *Tubiphytes* reefs. The pinnacle platforms accumulated 1700 m of shallow-marine carbonate in the Anisian prior to termination and burial with siliciclastic turbidites in the Ladinian (fig. 4, 5). The overall pattern of earlier termination, greater thickness of shallow-marine carbonate, step-back and pinnacle development in southern Guangxi in contrast to later termination in the Great Bank of Guizhou in the northern Nanpanjiang basin (fig. 3, 4, 5) is interpreted to be controlled by higher rates of tectonic subsidence in the southern basin (fig. 6).

Stratigraphy and depositional history of the Great Bank of Guizhou.

The Great Bank of Guizhou (GBG) is an isolated Triassic carbonate platform, extending approximately 70 km east-west and 20 km north-south in southern Guizhou Province (fig. 3, 8). The stark contrast in topography between the rugged, high-relief karst terrain of the carbonate platform and the lower stream-eroded siliciclastic turbidites in the basin spectacularly reveals the abrupt platform margins as one approaches the area on the ground (e.g.

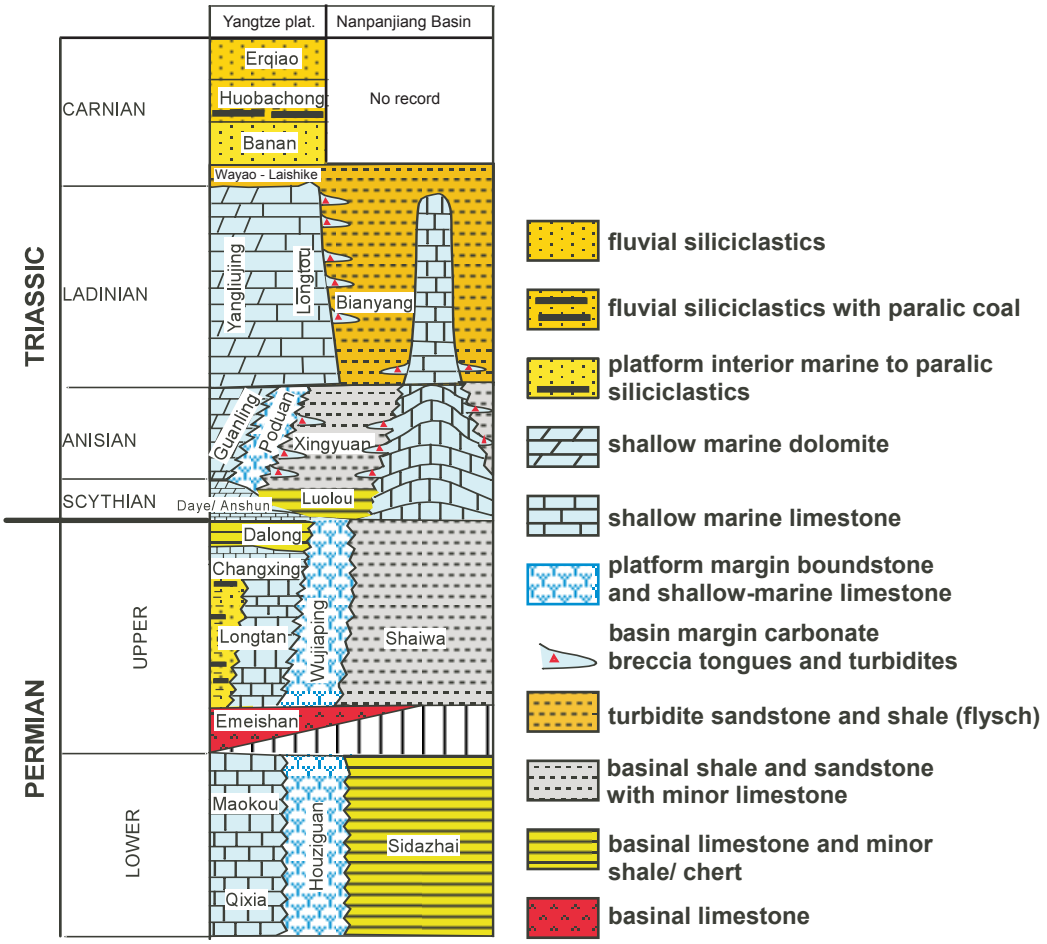

Figure 7: Schematic stratigraphic column illustrating the Permian and Triassic Formations of the Yangtze platform and GBG in southern Guizhou.

see stops 1-3) and outlines the GBG in satellite images (fig. 8).

Much of the GBG is nearly undeformed except for a NNW-trending asymmetric, faulted syncline that splits the platform perpendicular to its long dimension (Bianyang syncline; fig. 8, 9). The east limb of the syncline exposes a continuous cross section through the interior and margins of the platform and contains a complete record of the initiation of the GBG as an isolated platform in the Late Permian, progressive steepening of the platform from low-relief bank stage in the Early Triassic, aggrading reef-rimmed stage in the Anisian, high-relief escarpment development in the Ladinian, and finally drowning and burial by turbidites in the Carnian termination stage (fig. 10). The following provides a summary of the evolution of the GBG interpreted from mapping of the architecture and facies in the Bianyang syncline (Lehrmann, 1993).

Our field stops will provide an overview of the Bianyang syncline, the abrupt Ladinian margins of the GBG and the Carnian termination sequence in the axis of the syncline (stops 1-3; fig. 9). On the eastern limb of the syncline we will examine the Permian-Triassic boundary and the Lower Triassic platform interior succession at Dajiang and Rungbao sections (stops 4A, 4B; fig. 9), the Lower-Middle Triassic basin-margin facies on the northern margin of the GBG at Guandao section (stop 5-A, 6B; fig. 9) and the Middle Triassic *Tubiphytes* reef complex on the northern margin (stop 6A; fig. 9).

Late Permian to earliest Triassic: Initiation stage

The GBG was initiated in the latest Permian and earliest Triassic, during expansion of the Nanpanjiang basin, as a local area of shallow-marine carbonate accumulation (fig. 2, 3). Expansion of the basin drowned much of the shallow-marine carbonates in the eastern Yangtze platform north of the GBG beneath black, siliceous lutite of the Dalong Formation (fig. 2, 9). The siliceous lutite contains pelagic fossils such as radiolarians and ammonoids. The combination of the black color, pelagic fossils and bioturbation suggests a dysaerobic environment.

In the latest Permian, north of Luodian in the Bangeng-Bianyang area, shallow-marine skeletal grainstone-packstone and patch reefs of sponge boundstone formed the initial accumulation of the GBG (fig. 9, 10A). These shallow-marine strata extend across the base of the platform and across its adjacent basin margins. The strata extend horizontally into the basin with no indication of Permian faults or uplift, indicating that the GBG did not nucleate on a tectonic structure (fig. 9, 10A). The plat-

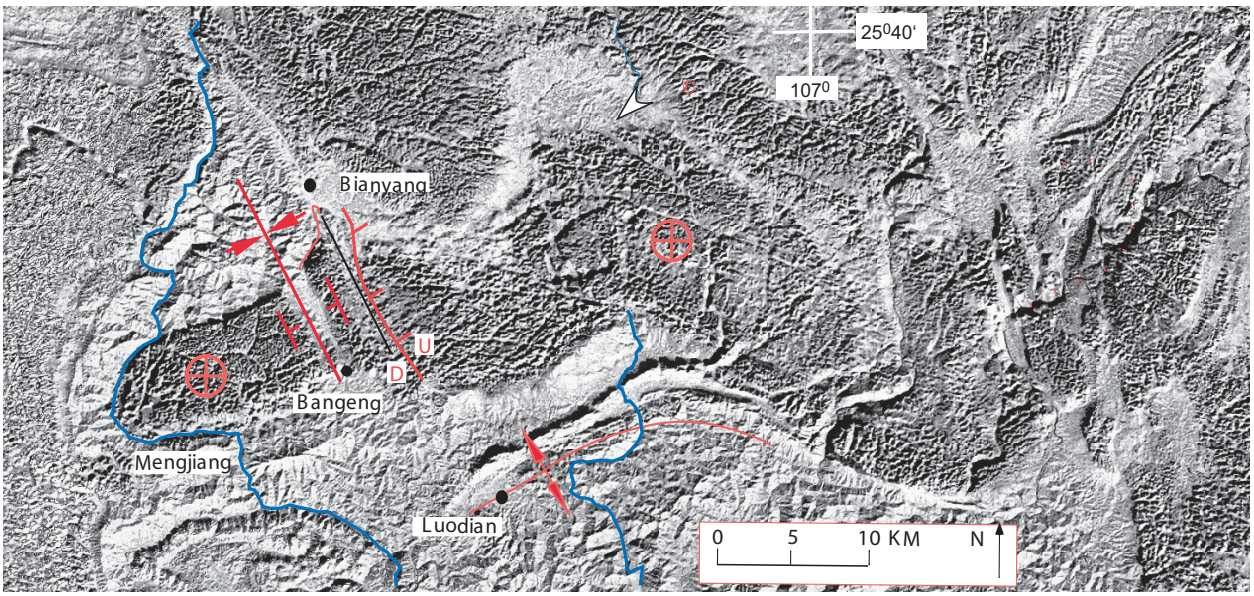

Figure 8: Landsat image of the Great Bank of Guizhou. The Bianyang syncline dissects the platform from Bianyang to Bangeng. Geological map of the east limb of the Bianyang syncline is shown in figure 9.

form nucleated on depositional topography near the margin of the former Yangtze platform (fig. 2, 3)

Upper Permian skeletal grainstone-packstone in the interior of the GBG (at the base of Dawen, Dajiang, Heping and Rungbao sections; fig. 10A, 11) contains diverse normal-marine fossils, which are extensively fragmented. The diverse fauna, fragmented fossils and grainstone texture indicate an open marine, shallow-subtidal environment occasionally winnowed by wave action. Sponge boundstones at the margins also contain diverse open-marine faunas (fig. 10A), but, in contrast, have muddy fabrics suggesting somewhat deeper, subtidal environments below normal wave-base. The sponge boundstone passes basinward into the siliceous lutite of the Dalong Formation (fig. 9, 10A).

During the earliest Triassic the GBG maintained a similar morphology despite the end-Permian mass extinction (fig. 10A). The end-Permian extinction is recorded across a conformable Permian-Triassic boundary at Dawen, Dajiang, Heping and Rungbao sections, which is marked by an abrupt shift in marine biota, but with no indication of a significant hiatus or an overall change in depositional environments (fig. 11). In the earliest Triassic, calcimicrobial framestone was deposited across the platform interior and the basin-margin shifted to the deposition of marine shale containing the bivalve *Claraia* at Guandao section (fig. 9, 10A, 13). PTB sections will be examined at Dajiang, Rungbao and Guandao sections: stops 4A, 4B, 5.

Early Triassic: Low-relief bank stage

After deposition of calcimicrobial framestone in the earliest Triassic, relative rise in sea-level caused the margins of the GBG to step back ~700 m as the GBG developed a low-relief bank profile with a shallow subtidal to peritidal interior, oolite-grainstone margins and basin-margin flanks composed of pelagic lime mudstone, debris-flow breccia and turbidite grainstone-packstone (fig. 9, 10B). Deepening and step back of the margins, at the beginning of the low-relief bank stage, are supported by the fact that the pelagic, debris-flow and turbidite facies overlie the former platform-margins of the initiation stage (fig. 10B). The basin-margin strata of the low-relief bank stage dip gently (~1.5^0) away from the platform, which is interpreted to have developed 50 to 100 m of relief based on differences in thickness of platform and basin-margin strata.

On the platform interior, the calcimicrobial framestone is overlain conformably by thin-bedded lime mudstone followed by dolo-oolite grainstone, oolitic cryptalgal-laminite and peritidal cyclic-limestone (fig. 9, 10B). The lime mudstone is light gray, thin bedded and contains a depauperate fauna of small bivalves and gastropods (fig. 11) suggesting restricted conditions in the interior at the beginning of the low-relief bank stage.

The lime mudstone is overlain by cross-bedded dolo-oolite grainstone (fig. 9, 10B). The shift to oolite deposition indicates that high-energy shoal environments spread across the platform interior. Overlying the dolo-oolite is oolitic, cryptalgal-laminite which consists of alternating cryptalgal laminae (horizontal stromatolite layers) and ooid packstone layers (fig. 10B). The oolitic cryptalgal-laminite contains fenestral pores, meniscus cements and leached-ooid fabrics indicating subaerial exposure in a supratidal environment.

During the later part of the low-relief bank stage, oolite shoals continued on the margins while a peritidal cyclic-limestone facies was deposited on the platform interior (fig. 10B). The peritidal cyclic-limestone is made up of meter-scale cycles with skeletal packstone, oolitic packstone or calcimicrobial framestone bases and caps of laminated "ribbon-rock" mudstone to packstone (fig. 12).

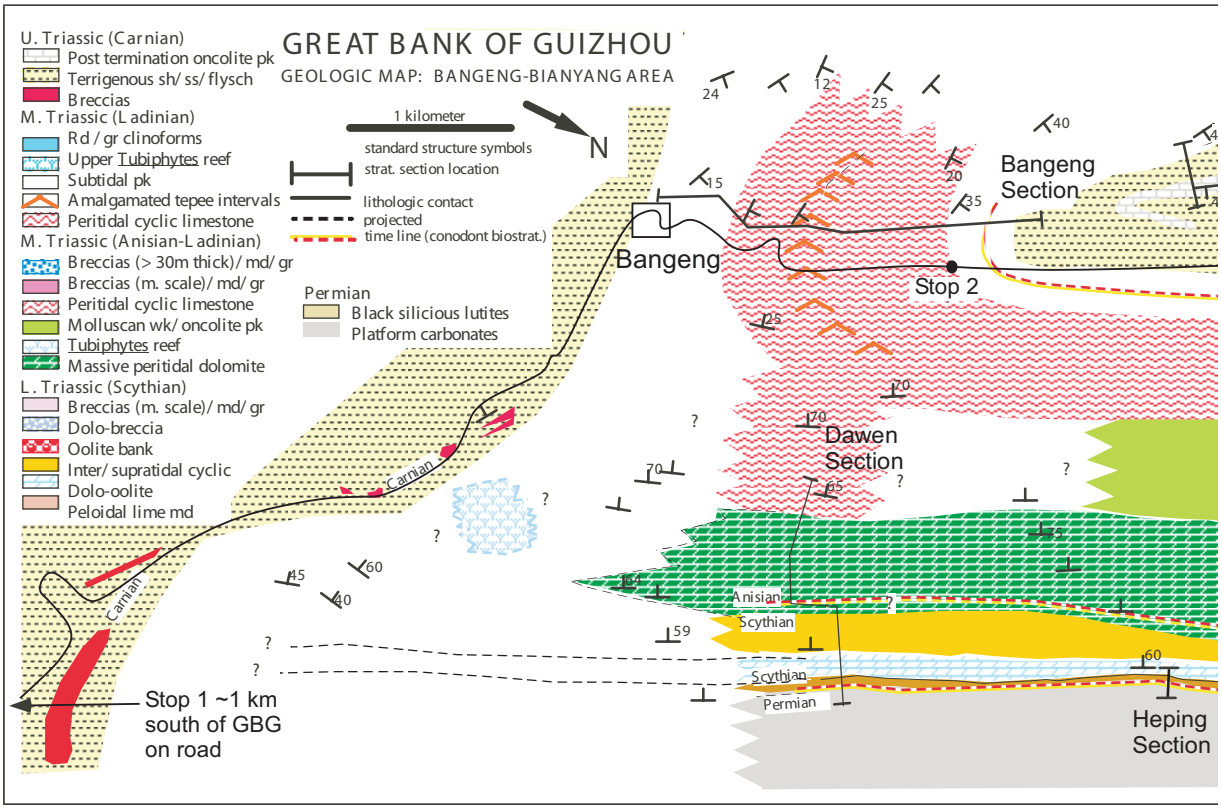

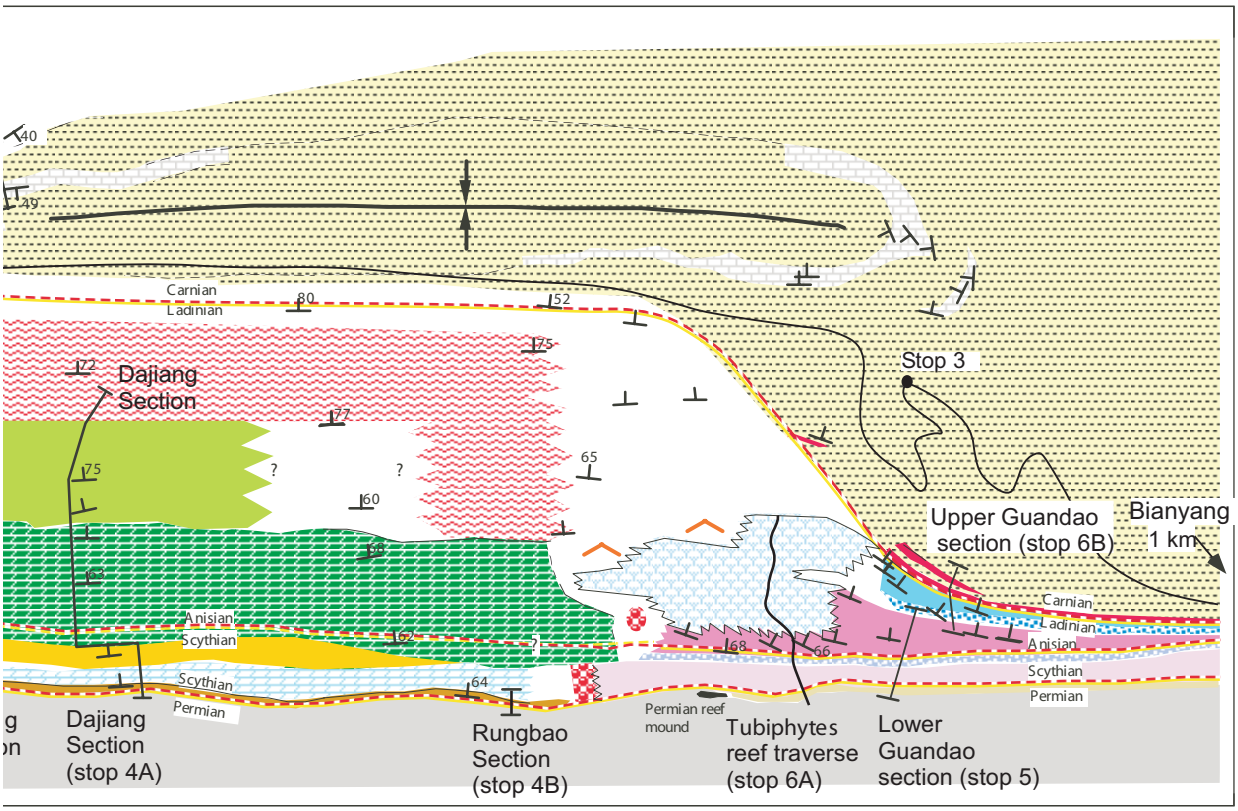

Figure 9: Geological map of the eastern limb of the Bianyang syncline (from Lehrmann, 1993). Location of map area is the eastern limb of the syncline shown in figure 8. Stops for the field excursion and stratigraphic sections discussed in the text are shown.

Dajiang section contains more than 60 such cycles. The peritidal cyclic-limestone is interpreted to have formed as shallowing-upward cycles in open-marine to restricted, subtidal and intertidal environments. We will have an opportunity to examine each of the Lower Triassic platform interior facies (thin bedded lime mudstone, dolo-oolite grainstone, oolitic cryptalgal-laminite and peritidal cyclic-limestone) as we hike through the Lower Triassic platform interior succession at Dajiang Section – stop 4A.

Middle Triassic Anisian-Early Ladinian: Aggrading reef-rimmed stage

During the Middle Triassic (Anisian-Early Ladinian) aggrading reef-rimmed stage, *Tubiphytes* boundstones developed at the platform margin and cyclic tidal-flats formed on the platform interior (fig. 9, 10C). Basin-margin deposition began with pelagic lime-mudstone, debris-flow breccia and turbidite grainstone-packstone and later shifted to mud-free talus breccia as the platform progressively steepened (fig. 9, 10C). At the beginning of the reef-rimmed stage the platform expanded in width as the platform margin prograded over the basin-margin strata of the low-relief bank stage (fig. 9). Later the platform aggraded and prograded slightly (fig. 9). The platform-interior, peritidal cyclic dolomite is composed of meter-scale, shallowing-upward cycles with burrowed molluscan-peloidal packstone and domal stomatolite bases and fenestral-laminite caps (fig. 10C). The unit is pervasively dolomitized and is locally coarsely crystalline, obliterating depositional fabrics.

The *Tubiphytes* boundstone forms extensive, unbedded deposits at the platform margin. The boundstone was found at all localities of the platform margin indicating that it forms a continuous rim, up to 1.5 km wide, around the GBG. The boundstone is composed of branching *Tubiphytes* frameworks with isopachous and botryoidal marine cements. The *Tubiphytes* frameworks are reinforced by micrite crusts, *Bacinella* and cement. In some areas marine cement makes up the majority of the volume of the boundstone. Locally the boundstone contains subsidiary frameworks of phaceloid scleractinian corals and sphinctozoan sponges. The *Tubiphytes* boundstone is interpreted to represent shallow-marine environments along a reef-rimmed margin. We will examine the *Tubiphytes* reef complex in a traverse through the northern platform margin (stop 6A; fig. 9).

Adjacent to the *Tubiphytes* reef complex, the basin-margin slope succession is exposed at Guandao section (fig. 9, 13-14). Basin-margin sedimentation consisted of pelagic shale and hemipelagic lime mudstone to wackestone with thin-shelled bivalves, allodapic carbonate turbidites and debris flows containing debris shed from the platform (polymict breccia). Lower Guandao section will be examined at stop 5; conodont biostratigraphy, magnetostratigraphy and radioisotope ages of volcanic ash layers provide a geochronology for the GBG. Allochthonous material shed from the platform also provides a "sampling" of sediment transported from the platform margin. At the Olenekian-Anisian boundary there is an abrupt shift from allodapic units dominated by oolite clasts to *Tubiphytes* boundstone clasts signaling the onset of *Tubiphytes* reef development in the uppermost Spathian and Early Anisian (fig. 10B, C, 17).

Preserved architecture allows evaluation of depositional slope and relief. During the early part of the aggrading reef-rimmed stage (Anisian), basin-margin strata had slopes of approximately 5^0 and were composed of pelagic lime-mudstone with interbeds of muddy, debris-flow breccia and carbonate turbidite grainstone-packstone at Guandao section. During the later part (Early Ladinian) the platform developed up to 400 m of relief, the basin-margin progressively steepened up to 30^0 and slope sedimentation shifted to mud-free breccias and lithoclastic grainstones interpreted as avalanche deposits (fig. 9, 10C).

Ladinian: High-relief escarpment stage

During the later part of the Middle Triassic (Ladinian) the basin margins starved and the GBG accumulated vertically forming an erosional escarpment-margin with up to 1700 m of relief (fig. 9, 10D). The escarpment interpretation implies that the GBG developed a tremendous amount of relief during the Ladinian and was subsequently overlain by a thick succession of siliciclastic turbidites (fig. 10E). We will view the escarpment margin at stops 1 and 3. The high-relief escarpment interpretation is supported by four lines of evidence: 1) the contact between the platform carbonates and the siliciclastic turbidites is extremely sharp (fig. 9, 15), 2) the platform strata contain no siliciclastic interbeds, 3) the siliciclastic turbidites flanking the margin lack carbonate beds or carbonate debris except for a few small wedges of breccia immediately adjacent to the escarpment (extending <200 m from margin; fig. 9) and 4) the siliciclastic turbidites in the basin are younger than the platform carbonates as determined by conodont biostratigraphy (Lehrmann 1993). In other words the GBG grew to over 1700 m high and was bounded by an erosional escarpment. The siliciclastic turbidites in the basin were deposited after the platform was terminated, and thus onlap the escarpment (fig. 9, 10E).

Platform-margin strata exposed along the escarpment are skeletal-peloid packstone and grainstone with local boundstone (fig. 9). The facies is thick bedded with beds extending from the platform interior to the edge of the escarpment. The facies contains a mixture of peloids, bivalves, gastropods, dasycladacean algae and miliolid forams most likely from restricted, platform interior environments and fragmented *Tubiphytes*, *Bacinella*, corals and echinoderms most likely representing open-marine environments along the platform margin. A few scleractinian bioherms are interbedded with the packstones and grainstones. This facies is interpreted to have been deposited as a mosaic of wave-winnowed shoals, local patch reefs and low-energy restricted areas between shoals and patch reefs. The facies could also represent such a mosaic of environments deposited in a back-reef setting, if reefs formerly occurred along the margin, but were sub-

sequently been stripped away by erosion.

The possibility that a reef rim existed along the escarpment, and was later removed by erosion, is suggested by diverse boundstone lithologies found in breccias at the base of the escarpment at the top of Guandao section (fig. 9). These breccias will be examined at the top of Guandao section (optional stop 6B). Boundstone clasts within the breccias have a biota with a greater diversity than the patch reefs interbedded in the platform margin. The boundstone clasts contain scleractinian corals, Tubiphytes, sphinctozoan sponges, bryozoans, Ladinella porata, solenoporacean algae and inozoan sponges.

At the beginning of the high-relief escarpment stage, the platform developed an atoll-like profile with an interior lagoon composed of molluscan-oncolite packstone-wackestone that is bounded outboard by peritidal cyclic-limestone (fig. 9, 10D). The unit is composed of extensively burrowed skeletal-peloidal wackestone with bivalves, gastropods and dasycladacean algae, punctuated by oncolite packstone beds. The unit also contains rare domal stromatolites. This facies is interpreted to have been deposited in a restricted subtidal lagoon with water depths ranging from shallow-subtidal to occasionally intertidal.

Later, a flat-topped profile was restored as tidal flats spread across the former lagoon, depositing peritidal cyclic-limestone across the platform interior (fig. 10D). On the southern interior of the platform, the unit contains a thick interval disrupted by tepee structures (fig. 10D). The tepees disrupt an interval 300 m thick restricted to the southern bank-top, suggesting that they formed along a crest of islands.

Near the end of the high-relief escarpment stage, deepening resulted in a shift to subtidal conditions across the platform interior. This deepening is represented by a shift from peritidal cyclic limestone to skeletal-peloidal packstone (fig. 10D). The skeletal-peloidal packstone is an extensively burrowed facies with bivalves, gastropods and calcareous algae. The unit lacks any evidence of peritidal facies such as fenestral laminites. The biota indicates restricted, quiet, subtidal environments.

Late Triassic Carnian: Termination (drowning)

At the beginning of the Late Triassic (Carnian) the GBG was terminated as water depths increased over the platform top and the platform was buried by a thick pile of siliciclastic turbidites and marine shales (fig. 7, 10D). The platform was terminated by drowning as indicated by an upward shift from shallow-subtidal carbonates to deep-marine, nodular-bedded carbonates with deep-water conodont biofacies (fig. 16). We will view the termination horizon from the distance at stop 2.

Record of end-Permian extinction and Early-Middle Triassic recovery

The GBG contains one of the most continuous and expanded known records of the end-Permian mass extinction and the subsequent Early and Middle Triassic recovery interval. In particular, the exposure of a two-dimensional cross section from platform-interior to platform-margin and basin-margin environments provides the opportunity to separate the effects of local environment from those of regional to global biotic recovery (fig. 8, 9). Although extracting macrofossils from the platform limestones for genus- and species-level identification is hindered by the small size of the fossils and their preservation in clean limestones, analyses of thin sections and polished slabs provide the opportunity to track broad changes in faunal composition and abundance that complement more detailed taxonomic studies in areas where environmental and stratigraphic controls are not as well developed. Decreases in fossil abundance and size are readily apparent in the field across the Permian-Triassic boundary in both platform and basin settings, as is the shift from a fauna dominated by crinoids, sponges and brachiopods to one dominated by mollusks. Faunal recovery occurs on the GBG through the Spathian and Middle Triassic, consistent with the timing of diversity and size increase observed elsewhere in the marine record (e.g., Schubert and Bottjer, 1995; Payne et al., 2004; Payne, in press).

End-Permian mass extinction

The end-Permian extinction horizon is distinct and well exposed in the platform interior sections at Dawen, Heping, Rungbao and Dajiang (fig. 9, 10). We will have the opportunity to examine the extinction horizon in detail at the Dajiang section (stop 4A) and another opportunity at Rungbao (stop 4B). Upper Permian (Changxingian) strata at Dajiang consist of fossiliferous packstones and grainstones containing a diverse fauna of sphinctozoan and inozoan sponges, crinoids, echinoids, brachiopods, bivalves, gastropods, diverse foraminifera (including fusulinids), *Tubiphytes* and dasycladacean algae (fig. 11). Many of these fossil grains are visible to the naked eye on weathered surfaces or with the aid of a hand lens. In particular, it is easy to find large and abundant crinoid ossicles and inozoan sponges.

The extinction horizon consists of a sharp but irregular surface upon which the calcimicrobial framestone developed. The surface is stylolitized in many locations, but analysis in thin section demonstrates that the boundary between diverse Upper Permian packstones and the calcimicrobial framestone is conformable where it is not stylolitized and lacks evidence of subaerial diagenesis. The calcimicrobial framestone contains a low-diversity fauna of ostracods, gastropods and bivalves that occur within the micrite matrix filling many of the voids in the microbialite (fig. 11). Small gastropods (< 1 cm) can often be identified in the field within hand samples of the microbialite. Immediately overlying the 15 meters of calcimicrobial framestone at Dajiang are several packstone beds containing abundant small (<1 mm) gastropods and bivalves with subordinate articulate brachiopods and rare echinoid spines (fig. 11). Many of these grains form the nuclei of small oncoids. Above this fossiliferous inter-

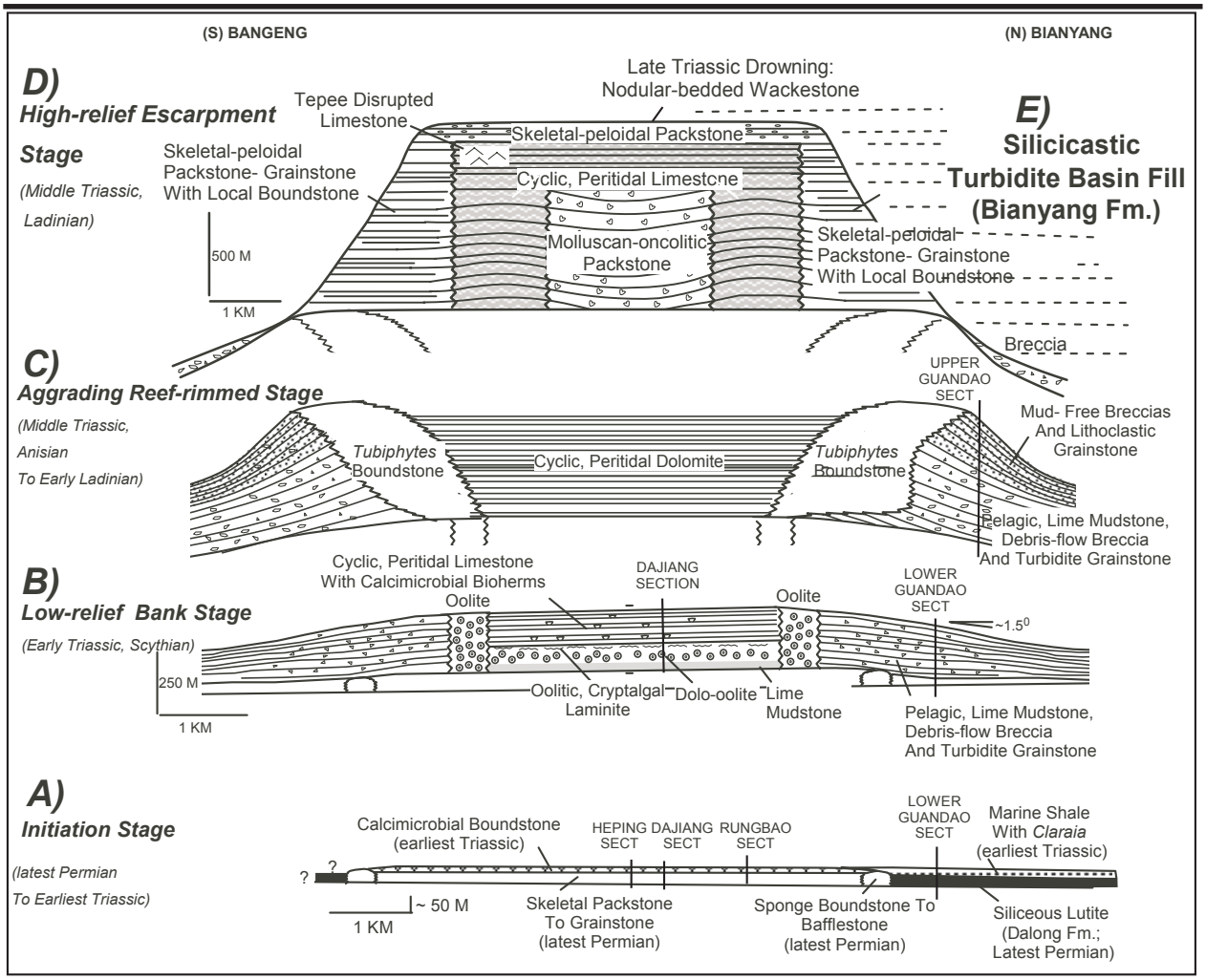

Figure 10: Restored cross-sections of the GBG illustrating Late Permian through Late Triassic evolution. Sections are from the Bianyang syncline and correspond to field trip localities (see figure 9). A) Upper Permian to basal Triassic: Initiation stage, B) Lower Triassic: Low-relief bank stage, C) Middle Triassic Anisian-Early Ladinian: Aggrading reef-rimmed stage, D) Ladinian: High-relief escarpment stage, E) Late Triassic Carnian: Termination (drowning)

val, fossil abundance decreases and remains low (<< 1%) through several tens of meters of lime mudstone (fig. 11).

The most salient features to note at the Dajiang section are: 1) the thickness (>40 m) and diversity of Upper Permian packstone and grainstone, 2) the dominance of the Late Permian fauna by taxa with low metabolic rates and heavy calcification (e.g., sponges, brachiopods, crinoids) and 3) the small size of Early Triassic fossils and the dominance of mollusks.

Early-Middle Triassic recovery:

The abundance, diversity and size of fossil grains on the GBG did not change significantly from the Griesbachian through the Smithian. The low abundance and low diversity of fossil grains in all environments, from the platform interior through the platform margin and into the basin margin, suggest that the pattern reflects more than merely local environmental controls on fossil abundance and diversity. The first evidence of biotic recovery locally is an increase in the abundance and diversity of fossils in Spathian basin-margin strata (fig. 13). We will have an opportunity to observe the increase in fossil abundance from the Smithian through the Anisian at the Guandao section during stop 5. Fossil abundance increased gradually through the Spathian, primarily due to an increase in the abundance of crinoid grains. This increase does not appear to result solely from increasingly effective transport of grains from the platform margin at this time because older Lower Triassic turbidites contain micritic grains of similar sizes but do not contain abundant crinoid ossicles. Anisian packstones and grainstones on the basin margin contain similarly abundant, but larger, crinoid ossicles as well as abundant *Tubiphytes* grains, gastropods, brachiopods, bivalves and rare ammonoids (fig. 13, 14). The first occurrence of *Tubiphytes* grains in the uppermost five meters of the Spathian indicates that the platform-margin reef complex was initiated by this time (fig.10C, 13). Growth of the reef complex from the latest Early Triassic and earliest Middle Triassic makes it significantly older than preserved Anisian reefs in the Dolomites and suggests that it was among the first platform-margin reefs to form after the end-Permian mass extinction. Large, framework-building metazoans are absent from the Anisian reef complex, however, which was constructed primarily by Tubiphytes, a problematic micritic tube that appears, at least locally, to reflect micritic cementation around a siphonous alga. Scleractinian cor-

als are first found in breccias on the basin margin in the Ladinian, but they are only large and abundant in the last breccia units prior to platform drowning. Thus, the basin margin turbidite and breccia record suggests that increase in diversity and abundance of large, reef-building organisms occurred gradually, beginning in the Anisian and continuing through the Carnian. Although the abundance and taxonomic composition of fossil grains did not change dramatically between the Early and Middle Triassic in the platform interior, the much larger size of Middle Triassic gastropods (up to 15 cm) and echinoids (spines up to 5 cm) provide clear evidence of biotic recovery. We will have an opportunity to investigate the reef in situ and elements of the reef preserved with basin margin breccia tongues during stop 6 and stop 6B.

Analysis of carbon isotopes demonstrates a pronounced negative excursion at the Permian-Triassic boundary section at Dajiang (fig. 11, 19) and continued instability of the carbon cycle throughout the Early Triassic (fig. 18). Stabilization of the carbon cycle occurred in the Middle Triassic coincident with biotic recovery (Payne et al., 2004; fig. 18). The carbon isotope data and their interpretation are further discussed in the guide descriptions of stops 4A and 5.

Acknowledgements

This research is based upon work supported by the National Science Foundation (under grant numbers EAR 9004783 and EAR-9805731 to P.E. and EAR-9804835 to D.J.L. and) and by the Petroleum Research Fund of the American Chemical Society (under grants ACS-PRF 34810-AC8 and ACS-PRF 37193-AC8 to P.E. and ACS-PRF 33122-B8 and ACS-PRF 40948-B2 to D.J.L.) The Guizhou Bureau of Geology and Mineral Resources and the Geological Survey of Guangxi provided additional support for field work**.** This is a contribution to IGCP project 467.

References

Allen P. A., Homewood, P, Williams, G. D., 1986, Foreland basins, an introduction., in Allen P. A., Homewood, P (eds.) Foreland basins: Special Publication of the International Association of Sedimentologists, vol.8, pp.3-12.

Bond, G. C., and Kominz, M. A., 1984, Construction of tectonic subsidence curves for the Early Paleozoic miogeosyncline, southern Canadian Rocky Mountains: implications for subsidence mechanisms, age of breakup and crustal thinning: Geological Society of America Bulletin, v. 95, p. 155-173.

Bowring, S.A., Erwin, D.H., Jin, Y.G., Martin, M.W., Davidek, K., and Wang, W., 1998, U/Pb zircon geochronology and tempo of the end-Permian mass extinction: Science, v. 280, p. 1039-1045.

Carter, A., Roques, D., Bristow, C., Kinny, P., 2001, Understanding Mesozoic accretion in southeast Asia: significance of Triassic thermotectonism (Indosinian orogeny) in Vietnam: Geology, v. 29, p. 211-214.Chaikin, Daniel H., 2004, Sedimentology and Provenance of the Bianyang Formation, Guizhou Province, South China: M.S. Thesis, University of Kansas, Lawrence, Kansas

Chen, J., Foland, K. A., Xing, F., Xu, X., and Zhou, T., 1991, Magmatism along the southeast margin of the Yangtze Block: Precambrian collision of the Yangtze and Cathasia blocks of China: Geology, v. 19, p. 815-818.

Chung S.L., and Jahn, B. M., 1995, Plume – lithosphere interaction in generation of Emeishan flood basalts at the Permian – Triassic boundary: Geology, v. 23, p. 889-892.

Dai Yongdin, Li Juying, Jiang Xieguang, Zhao Shengcai, Hou Kui, Huang Hualing, Xiao Qiyu, 1978, petrography of carbonate rocks of the Maokou Formation and their reservoir properties in the Sichuan Basin: Scientia Geologica Sinica, v. 3, p. 203-218.

Enkin, R.J., Zhenyu Yang, Yan Chen, and Courtillot, V., 1992, Paleomagnetic Constratints on the Geodynamic History of the Major Blocks of China From the Permian to the Present: Jour. Geophysical Res., v.97, no. B10, p. 13,953-13,989.

Enos Paul., Wei, Jiayon., and Lehrmann, D. J., 1998, Death in Guizhou—Late Triassic drowning of the Yangtze carbonate platform: Sedimentary Geology, v. 118, p. 55-76.

Enos, Paul, 1995, Permian of China, *in*, Scholle, P. A., Peryt, T. M., and Ulmer-Scholle, D. S. (eds.), The Permian of northern Pangea: Springer-Verlag, Berlin, v. 2, p. 225-256.

Enos, Paul, Wei Jiayong, and Yan Yangji, 1997, Facies distribution and retreat of Middle Triassic platform margin, Guizhou Province, south China: Sedimentology, v. 44, n. 3, p. 563-584.

Fan, C., and Zhang, Y., 1994, The structure and tectonics of western Yunnan: Journal of Southeast Asian Earth Sciences, v. 9, p. 355-361.

Findlay R. H., and Trinh P. T., 1997, The structural setting of the Song Ma region, Vietnam and the Indochina-South China plate boundary problem: Gondwana Research, v. 1, p. 11-33.

Findlay, R. H., 1999, Review of the Indochina-South China plate boundary problem; structure of the Song Ma-Song Da Zone, in, Metcalfe, I.,; Ren, J.,; Charvet, J., and Hada, S.: Gondwana dispersion and Asian accretion; IGCP 321 final results volume, p. 341-361.

Gilder, S. A., Coe, R. S., Wu Haorue, Kuang Guodun, Zhao Xixi and Wu Qi, 1995, Triassic paleomagnetic data from south China and their bearing on the tectonic evolution of the western circum-Pacific region: Earth and Planetary Science Letters, v. 131, p. 269-287.

Guangxi Bureau of Geology and Mineral Resources, 1985, Regional Geology of Guangxi: Geological Memoires, Ser. 1, no. 3, 785 p., [in Chinese, English summary; Geologic map 1:1,000,000].

Guizhou Bureau of Geology and Mineral Resources, 1987, Regional Geology of Guizhou Province: Geological

Memoires, Ser. 1, no. 6, 700 p., [in Chinese, English summary; Geologic map 1:500,000].

Gupta, S., 1989, Mesozoic overthrust tectonics in South China; discussion: Geology, v. 16, p. 418

He, Z., 1986, Formation environment of turbidity current deposits in the Middle Triassic of Guizhou and Guangxi: Oil and Gas geology, v. 7, n. 3, p. 207-217.

Hou F., and Huang, J., 1984, Research into the Permian and Triassic volcaniclastic turbidites of the Nanpan River Sag: Acta Sedimentologica Sinica, v. 3, p. 256-264.

Hsu, K. J., Li, J., Chen, H., Wang, Q., Sun, S., and Sengör, A. M.C., 1990, Tectonics of South China: Key to understanding West pacific geology: Tectonophysics, v. 183, p. 9-39.

Hsü, K. J., Sun Shu, Li Jiliang, Chen Haihong, Pen Haipo, and Sengör, A. M. C., 1988, Mesozoic overthrust tectonics in south China: Geology, v. 16, p. 418-421.

Huang Jiqing, Chen Bingwei, 1987, The evolution of the Tethys in China and adjacent regions: Geological Publishing House, Beijing, 109 p.

Huang, T. K., 1978, An outline of the tectonic characteristics of China: Ecologae Geol. Helv., v. 71, p. 611-635.

Hutchinson, C. S., 1989, The Palaeo-Tethyan realm and Indosianian orogenic system of Southeast Asia: in Sengör, A. M. C., (ed.) Tectonic evolution of the Tethyan region: Kluwer Academic Publishers, p . 585-643.

Ingersoll, R. V., Dickinson, W. R., Graham, S. A., 2002, Remnant-ocean submarine fans; largest sedimentary systems on Earth: Extreme depositional environments; mega end members in geologic time: Special Paper - Geological Society of America, vol.370, pp.191-208.- Kessel, B. J., Gross, J. D., and Lehrmann, D. J., 2002, Facies and microfossil study of the mechanisms and timing of termination of the Heshan carbonate platform, Nanpanjiang Basin, South China, Geological Society of America, Abstracts with programs, v. 34, n. 6, p. 15.

Klimetz, M.P., 1983, An outline of the Mesozoic plate evolution of eastern China: Tectonics, v. 2, p. 139-166.

Koenig, Jon, Dillett, Pete, Lehrmann, Dan, and Enos, Paul, 2001, Structural and paleogeographic elements of the Nanpanjiang basin, Guizhou, Guangxi, and Yunnan provinces, south China. A compilation from satellite images, regional geologic maps and ground observations: : American Association of Petroleum Geologists, Official Program, v. 10, p. A107.

Lacassin R., Leloup, P. H., Trinh, P. T., and Tapponier, P., 1998, Unconformity of red sandstones in North Vietnam: field evidence for Indosinian orogeny in northern Indochina?: Terra Nova, v. 10, p. 106-111.

Lehrmann, D. J., 1993, The Great Bank of Guizhou: Birth Evolution and Death of an Isolated Triassic Platform, Guizhou Province, South China: Ph.D. dissertation, University of Kansas, 457 p.

Lehrmann, D.J., 1999, Early Triassic calcimicrobial mounds and biostromes of the Nanpanjiang basin, south China: Geology, v. 27, n. 4, p. 359-362.

Lehrmann, D.J., Payne, J.L., Felix, S.V., Dillett, P.M., Wang, H., Yu, Y.Y., and Wei, J.Y., 2003, Permian-Triassic boundary sections from shallow-marine carbonate platforms of the Nanpanjiang basin, south China: Implications for oceanic conditions associated with the end-Permian extinction and its aftermath: Palaios, v. 18, p. 138-152.

Lehrmann, D.J., Wei, J., and Enos, P., 1998, Controls on facies architecture of a large Triassic carbonate platform: The Great Bank of Guizhou, Nanpanjiang basin, South China: Journal of Sedimentary Research, v. 68, p. 311-326.

Lepvrier, C., Maluski, H., Van Vuong, N., Roques, D., Axente, V., and Rangin, C., 1997, Indosinian NW-trending shear zones within the Truong Son belt (Vietnam) 40Ar-39Ar Triassic ages and Cretaceous to Cenozoic overprints: Tectonophysics, v. 283, p. 105-127.

Li Z. X., 1998, Tectonic history of the major East Asian lithospheric blocks since the mid-Proterozoic; a synthesis in mantle dynamics and plate interactions in East Asia: Geodynamics Ser?, v. 27, p. 221-243.

Lin J., Fuller, M. and Zhang, W., 1985, Preliminary Phanerozoic polar wander paths from the North and South China blocks: Nature, v. 313, p. 444-449.

Liu Baojun and Xu Xiaosong, eds., 1994, Atlas of lithofacies and paleogeography of south China: Science Press, Beijing, 192 p.

Luo Zhili, Jin Yinzhong, and Zhao Xikui, 1990, Emei taphrogenesis of the upper Yangtze platform in south China: Geological Magazine, v. 5, p. 393-405.

Martin, M.W., Lehrmann, D.J., Bowring, S.A., Enos, Paul, Ramezani, J., Wei Jiayong, and Zhang Jiyan, 2001, Timing of Lower Triassic carbonate bank buildup and biotic recovery following the end-Permian extinction across the Nanpanjiang basin, South China: Geological Society of America, Abstracts with Programs, v. 33, p. A-201. Mattauer M., Matte, P., Malavielle, J., Tapponier, P., Maluski, H., Xu, Z., Lu, Y., and Tang, Y., 1985, Tectonics of the Qinling belt: build up and evolution of eastern Asia: Nature, v. 317, p. 496-500.

Meng, Q., and Zhang G., 1999, Timing of collision of the North and south China blocks: controversy and reconciliation: Geology v. 27, p. 123-126.

Metcalfe, I., 1996, Pre-cretaceous evolution of SE Asian terrranes, in Hall, R., and Blundell, D., (eds.), Tectonic evolution of Southeast Asia, Geological Society Special Publication, n. 106, p. 91-122.

Metcalfe, I., 2002, Permian tectonic framework and palaeogeography of SE Asia: Journal of Asian Earth Sciences, vol.20, no.6, pp.551-566.

Mundil, R., Ludwig, K. R., Metcalfe, I., and Renne, P. R., 2004, Age and timing of the end Permian mass extinction: U/Pb geochronology on closed system zircons: Science: v. 305, p. 1760-1763.

NewKirk, T. T., Lehrmann, D., and Hudak, G., 2002, Tephrastratigraphy and analysis of tectonic setting of Triassic intermediate volcanic strata: Nanpanjiang ba-

sin, South China**,** Geological Society of America, Abstracts with programs, v. 34, n. 6, p. 512.

Payne, J. L., Lehrmann, D. J., Wei, Jiayong, Orchard, M. P., Schrag, D. P., Knoll, A. H., 2004, Large Perturbations of the Carbon Cycle During Recovery from the End-Permian Extinction, Science, v. 23, p. 506-509.

Qing, J., Wu Y., Yan, Y., and Zhu, Z., 1991, Hercinian – Indosinian geotectonic evolution of Dian – Qian – Gui basin, southwestern China – north marginal basin of the eastern end of east Tethys: International symposium on Gondwana dispersion and Asian accretion , IGCP Project 321, p. 206-211.

Reid, R. P. and Macintyre, I. G., 1988, Foraminiferal-algal nodules from the eastern Caribbean; growth history and implications on the value of nodules as paleoenvironmental indicators: Palaios, v. 3, p.424-435

Ren, J., Jiang, C., Zhang, Z., and Qin, D., 1987, Geotectonic evolution of China: Science Press, Beijing, 203 p.

Rodgers, J., 1989, Comment on "Mesozoic overthrust tectonics in south China: Geology, v. 17, p.671-672.

Rowley, D. B., Ziegler, A. M., and Gyou, N., 1989, Comment on "Mesozoic overthrust tectonics in south China: Geology, v. 17, p.384-386.

Schubert, J.K., and Bottjer, D.J, 1995, Aftermath of the Permian-Triassic mass extinction event: paleoecology of Lower Triassic carbonates in the western USA: Palaeogeography, Palaeoclimatology, Palaeoecology, v. 116, p. 1 - 39.

Sengör, A. M. C., 1987, Tectonics of the Tethysides- Orogenic collage development in a collisional setting: Annual Review of Earth and Planetary Sciences, v. 15, p. 213-244.

Song, X. Y., Zhou, M. F., Cao, Z.M., and Robinson, P. T., 2004, Late Permian rifting of the south China craton caused by the Emeishan mantle plume?; Journal of the Geological Society of London, v. 161, p. 773-781.

Sun Shu, Li Jilang, Chen Haihong, Peng Haipo, Hsu, K. J., Shelton, J. W., 1989, Mesozoic and Cenozoic sedimentary history of South China: American Association of Petroleum Geologists Bulletin, v. 73, no. 10, p. 1247-1269.

Sun W., and Li, S., 1998, Pb isotopes of granitoids suggest Devonian accretion of the Yangtze (South China) craton to North China craton: comment and reply: Geology, v. 29, p. 859-861.

Tan X.., Kodama, K. P., Wang, P., and Fang, D., 2000, Paleomagnetism of Early Triassic limestones from the Huanan Block, south China: no evidence for separation between the Huanan and Yangtze blocks during the Early Mesozoic: Geophysical Journal International, vl.142, n.1, p.241-256.

Tapponier, P. Lacassin, R., Leloup, P. H., Scharer, U., Zhong D., Wu, H., Liu, X., Ji, S., Zhang L., and Zhou J., 1990, the Ailao Shan/ Red River metamorphic belt: Tertiary left-lateral shear between Indochina and South China: Nature, v. 343, p. 431-437.

Thompson G. M., Ali, J. R., Song, X., and Jolley, D. W., 2001, Emeishan basalts, SW China: reappraisal of the formations type area stratigraphy and a discussion of its significance as a large igneous province: Journal of the Geological Society of London, v. 158, p. 593-599.

Van-der-Voo, R., 1993, Paleomagnetism of the Atlantic, Tethys and Iapetus oceans: Cambridge University Press, Cambridge, 411 p.

Wang, H., (ed.), 1985, Atlas of the Paleogeography of China: Cartographic publishing house, Beijing, 281p.

Wang, Y., 1988, The outline of regional geological characteristics of Yunnan: Yunnan geology, v, 2.

Xia B., Fang, Z., Lu, H., Zhu, B., and Zhou, W., 1993, The Middle Triassic back-arc flysch in nanpanjiang area, southwest China: Journal of Nanjing University, v. 5, n. 3, p. 320-329.

Xie Z., Zhou, K., Xu, Z., and Dong, Z., 1984, On the petroleum prospects of marine sediments in south China, in Zhai, G, and Foster, R. J., (eds.), Beijing Petroleum Geology Symposium, Beijing, 16 p.

Xu Qiang, Liu Baojun, and Xu Xiaosong, 1996, Formation and development of the Early Palaeozoic carbonate platform in southern China: Sedimentary Facies and Palaeogeography, v. 16, no. 4, p. 1-5.

Xu Xiaosong, Xu Qiang, Pan Guitang, and Liu Qiaohong, 1996, Palaeogeography of the South China continent and its correlation with Pangea: Sedimentary Facies and Palaeogeography, v. 16, no. 2, p. 1-23. (in Chinese, English summary).Yang Shouren, Liu Jiang, and Zhang Mingfa, 1995, Conodonts of the Falang Formation of southwestern Guizhou and their age: Journal of Stratigraphy, v. 19, p. 161-170, [in Chinese, English summary].

Yang Z. Y., Cheng, Y. Q., and Wang, H. Z., 1986, The geology of China, Cleredon Press, Oxford.Yin GongZheng, Zhou XiuGao, Cao ZeTian, Yu YouYi, and Luo YongMing, 2000, A preliminary study of the Early Late Triassic marine reptiles from Guanling, Guizhou, China, Geology-Geochemistry, v. 28, n. 3, p. 1-23.

Yunnan Bureau of Geology and Mineral Resources, 1984, Regional Geology of Yunnan Province: Geological Memoires, Ser. 1, no. 6, 700 p., [in Chinese, English summary; Geologic map 1:500,000].

Zhang H., Gao, S., Zhang, B., Luo, T., and Yin W., 1997, Pb isotopes of granitoids suggest Devonian accretion of the Yangtze (South China) craton to North China craton: Geology, v. 25, p. 1015-1018.

Zhang Zhimeng, Liou, J.G., and Coleman, R.G., 1984, An outline of the plate tectonics of China: Geol. Soc. America Bull., v. 95, p. 295-312.

Zhang, Zuqi, 1984, The Permian system in South China: Newsletters on Stratigraphy, v. 13, p. 156-174.

Field Excursion 2: Permian-Triassic boundary and a Lower-Middle Triassic boundary sequence on the Great Bank of Guizhou, Nanpanjiang basin, southern Guizhou Province

Daniel J. Lehrmann[1], Jonathan L. Payne[2], Paul Enos[3], Paul Montgomery[4], Jiayong Wei[5], Youyi Yu [5], Jiafei Xiao[5], and Michael J. Orchard[6].

[1]University of Wisconsin, Oshkosh, WI, U.S.A., lehrmann@uwosh.edu;

[2]Harvard University, Cambridge, MA, U.S.A;

[3]University of Kansas, Lawrence, KS, U.S.A.;

[4]ChevronTexaco, Perth, West Australia

[5]Guizhou Bureau of Geology, Guiyang, Guizhou, P.R.C.;

[6]Geological Survey of Canada, Vancouver, B.C., Canada;

Introduction

The stratigraphic framework and Permian-Triassic depositional history of the Great Bank of Guizhou are presented in a preceding paper in this volume titled: Permian and Triassic depositional history of the Yangtze platform and Great Bank of Guizhou in the Nanpanjiang basin of Guizhou and Guangxi, south China. To avoid duplication, all figures referenced in this guide are found in the preceding paper (see pages 147-166, this volume). The following stop descriptions provide additional detailed information on the Permian-Triassic stratigraphy and record of the end-Permian extinction and biotic recovery in the Great Bank of Guizhou (GBG). The GBG is dissected by a NNW trending syncline (Bianyang syncline; fig. 8). The steeply dipping strata on the eastern limb of the syncline provide a two dimensional cross section through the platform permitting reconstruction of the depositional history and providing access to our field stops (fig. 9, 10).

Stops of the Excursion:

Stop-1 Overview Nanpanjiang basin and southern margin of Great Bank of Guizhou (southeast of Bangeng)

During the field excursion we will stay in the town of Luodian 10 km south of the Great Bank of Guizhou (fig. 8). Luodian is situated on an ENE trending anticline; Devonian, Carboniferous and Permian marine strata are exposed along its axis. As we drive northward we will cross Paleozoic strata on the anticline and then enter Triassic basinal strata. Most of the drive will be through Upper Triassic (Carnian) siliciclastic turbidites of the Bianyang Formation (fig. 5, 7). In satellite images the siliciclastic turbidites are distinguished from the platform by the sharp contrast in rounded stream-eroded topography of the siliciclastics versus the tower karst developed in the carbonate of the GBG (fig. 8).

The Bianyang Formation, exposed along much of the road between Luodian and Bangeng, is a typical flysch deposit (Chaikin, 2004). It has the sedimentologic attributes of great thickness (1000-3000 m), alternation of thin, matrix-rich clastic beds with hemipelagic background deposits, and abundant sole marks on the clastic beds. The spectrum of sedimentary structures (flute casts, groove casts, prod marks, load casts, climbing ripples, mud diapirs, dish structures, piping structures and flame structures) are diagnostic of turbidity-current deposition. The abundance and exquisite detail of the fluid-escape structures may reflect unusually rapid deposition, consistent with Lehrmann's corollary of extremely rapid filling of the Nanpanjiang basin surrounding the Great Bank of Guizhou in the Early Carnian, rather than Ladinian as generally assumed (Lehrmann, 1993; Lehrmann et al., 1998).

The lower part of the Bianyang Formation (300-400 m) is characteristically dominated by sandstone with many thick, amalgamated beds, well exposed along the field trip route. The upper part, thicker than 1100 m, is dominated by mudstone. The sandstones are consistently very fine sand. They are matrix rich, with the average matrix content between 9% and 18%, depending on how much of the abundant calcite is calcitized matrix. The average QFL ratio is 74/10.5/16. Lithic components are claystone, siltstone, metasiltstone and metaquartzite; igneous rock fragments are rare.

Paleocurrents within the Bianyang Formation in southern Guizhou are generally directed from east to west (Hou and Huang, 1984; Sun et al., 1989; Chaikin, 2004), with apparent local interaction with the carbonate platforms (Chaikin, 2004). Measurement of 57 paleocurrent vectors from the Luodian section gave a dominant mode of 317°, a southerly secondary mode (185°) and a mode of 265° from ripple marks. The mean of 79 lineations, mostly groove casts, is 325°, consistent with the vector mode. An obvious eastern source terrain would be the Jiangnan massif, which was largely exposed during Ladinian and Carnian times (fig. 5; Liu and Xu, 1994, p.158). It possibly merged with the Yunkai massif to the south to form the entire eastern border of the Nanpanjiang basin. Much

of the rock currently exposed in the Jiangnan massif consists of low-grade, siliciclastic metasedimentary rocks. Volcanoclastics, glacial-marine deposits and granitic intrusions are also well represented (Guizhou Bureau, 1987). The fine-grained quartz, siltstone clasts and feldspar could derive from such a source area. This vast terrain could have readily provided the voluminous deposits of the Bianyang Formation without necessitating extensive or rapid uplift. In order to deliver the sediment to the basin rapidly enough to fill it, however, whether during the entire Ladinian or only a part of the Carnian seems to require storing large quantities of fine-grained, unconsolidated sediment in large, mature drainage basins to be rapidly flushed out with rejuvenation. The upper part of the Bianyang Formation, well over half the total volume, consists of mudrock and siltstone, with virtually no sandstone. Thus, the source area ceased to deliver sand, but must then have supplied mud at a prodigious rate.

As we approach the GBG a large plateau of tower karst will be visible to the north. At stop 1, approximately 1 km south of the GBG (fig. 9) we will overview the siliciclastic turbidites of the Bianyang Formation and the southern margin of the GBG. The carbonate strata visible from the distance are primarily Ladinian in age. The abrupt Ladinian margins of the GBG are interpreted to have formed as an aggradational and erosional escarpment that developed approximately 1700 m of syndepositional relief above the adjacent basin margin and then was onlapped by the siliciclastic turbidites of the Bianyang Formation (fig. 9, 10D). Although the abrupt escarpment of the GBG is visible on the southern margin, the stratigraphic relationships are best demonstrated along the northern margin south of Bianyang (seen at stop 3, fig. 8, 9). As the road approaches the base of the escarpment, east of the town of Bangeng, tongues and isolated pods of carbonate breccia are visible enclosed within the Upper Triassic siliciclastic strata of the Bianyang Formation (fig. 9). These breccias occur at the base of the Ladinian escarpment and are equivalent to the Carnian breccias interbedded with the Bianyang Formation exposed at the top of Guandao section at stop 6B (see below). The breccias contain a diverse reef fauna of *Tubiphytes*, scleractinian corals, sphinctozoan and inozoan sponges and solenoporacean algae and are interpreted to have been eroded from Ladinian patch reefs or a fringing reef developed along the high-relief escarpment (fig. 10D). When we reach the town of Bangeng the road turns north and enters Ladinian platform-interior strata along the axis of the Bianyang syncline (fig. 8, 9).

Stop-2 Overview of Bianyang syncline and termination sequence of the GBG. Uppermost carbonates (Ladinian) followed by drowning and shale deposition (Carnian). Roadside stop 1.5 km north of Bangeng (fig. 9)

As we drive from the town of Bangeng northward to stop 2, we traverse Ladinian carbonate strata from platform-margin facies near Bangeng to peritidal, cyclic, platform-interior facies. The road crosses a zone of amalgamated tepee structures south of stop 2 (fig. 9). At Bangeng section, just west of the road, the tepee structures disrupt an interval of platform carbonates 300 m thick and provide abundant evidence of prolonged subaerial exposure (fig. 9). The tepee interval is interpreted to represent a zone of emergent islands restricted to the southern banktop (fig. 10D). Above the peritidal carbonate at Bangeng section is an interval of subtidal molluscan packstone 200 m thick followed by deepening-upward carbonate facies and a shift to marine shale (fig. 9). The marine shale in the axis of the syncline marks the termination of carbonate deposition on the GBG (fig. 9).

During the termination, the last carbonates to be deposited on top of the platform were oolitic-skeletal grainstone to packstone beds that grade upward to nodular-bedded, skeletal-oncolitic lime wackestone (fig. 16). Deepening is supported by a shift to diverse open-marine biota over the bank top and the nodular-bedded facies at the very top of the section. Included are Neogondolellid conodonts, representing deep-marine biofacies (fig. 15). Deepening conditions are inferred to have ended restricted shallow-subtidal conditions, beginning with wave-agitated conditions resulting in ooid grainstones which later pass upward to quieter, deeper, open-marine conditions represented by the nodular-bedded, skeletal-oncolitic wackestones (fig. 16). Oncoids within the nodular-bedded wackestone facies are encrusted by a consortium of cyanobacteria, serpulid worms and bryozoans. They probably formed as algal nodules in relatively deep-water environments similar to algal nodules found in deep environments adjacent to modern Carribean platforms (Reid and Mcintyre, 1988). Similar algal nodules have also been reported from 135 foot water depths in Florida (Enos and Perkins, 1977).

Stop-3 Overview of the northern high-relief escarpment of the GBG. Roadside south of Bianyang (fig. 9, 15)

From stop 2 we continue to drive northward through Carnian shale in the axis of the Bianyang syncline. Eventually the road emerges on the northern margin of the GBG and winds its way northward and upward through siliciclastic turbidites of the Bianyang Formation (fig. 9). Stop 3, on a tall mountain in the Bianyang Formation, provides an ideal vantage point to look southeast and examine the Ladinian high-relief escarpment from a distance. At stop 3 we are approximately on structural strike (NNW-SSE) with the Ladinian carbonate of the GBG escarpment which dip 70^0 to the SW. The most conspicuous features are the extremely thick and well-bedded Ladinian carbonates of the platform and the extremely sharp contact between the carbonates and basinal clastics in the foreground. From this vantage point the first impression is that the contact is a fault. However, a fault interpretation is ruled out because mapping demonstrates that there is no offset of underlying or overlying strata (fig. 9, 15). The sharp contact between the carbonates and clastics is

interpreted to have formed as a high-relief aggradational and erosional escarpment with 1700 m of syndepositional relief developed as the platform aggraded in the Ladinian (fig. 10D). After the platform was drowned during the Early Carnian (see stop 2) the siliciclastic turbidites onlapped the escarpment and buried the platform. The escarpment interpretation is supported by conodont biostratigraphy which demonstrates that the siliciclastic turbidites at the top of Guandao section (fig. 9) are Carnian and entirely younger than the uppermost platform carbonates (which are Ladinian). Further support comes from the lack of intertonguing of the carbonates and siliciclastics except for small tongues of breccia at the base of the escarpment at the top of Guandao section (fig. 9).

Stop-4a Permian-Triassic boundary and Lower Triassic platform-interior facies at Dajiang

Permian-Triassic boundary at Dajiang section (including a description from Heping section 1 km south of Dajiang)

Lithofacies and stratigraphy- Continuous Permian-Triassic boundary (PTB) successions are exposed in several sections in the interior of the GBG on the east limb of the Bianyang syncline (fig. 9). Stop 4A will examine the boundary at Dajiang section. Optional stop 4B will examine the PTB at Rungbao section (fig. 9, 10). From base to top the overall facies succession of the PTB in the GBG platform interior consists of: (1) cherty skeletal lime packstone with diverse normal-marine fossils in the uppermost Permian, overlain by a sharp contact with (2) calcimicrobial framestone in the basal Griesbachian with interbeds of (3) molluscan lime grainstone, followed by a thin interval of (4) microgastropod packstone and finally (5) platy, thin-bedded lime mudstone (fig. 11).

Upper Permian strata at Dajiang section are the Wujiaping Formation and consist of thick, massive-bedded skeletal lime packstone with chert nodules. Fossils in the upper Wujiaping Formation include crinoids, brachiopods, bryozoans, sphinctozoan sponges, rugose corals, dasycladacean algae, fusulinids, other foraminifera and *Tubiphytes* (fig. 11). The upper meter of the Wujiaping Formation at Dajiang and Heping sections is composed of non-fusulinacean foraminifers and fragmented shell material. *Palaeofusulina* and the Changxingian foraminifers *Colaniella* and *Nodosaria* occur near the top of the Wujiaping Formation at Heping section. Skeletal packstone of the Wujiaping Formation is interpreted to represent a shallow-subtidal, open-marine platform environment with relatively low to moderately high current energy. The diverse normal-marine biota and presence of green algae indicate shallow photic-zone conditions and open-marine circulation. Mud-poor intervals with infiltrated lime mud indicate winnowing by wave action. Homogenous, mud-rich packstone intervals may have been thoroughly bioturbated.

The Wujiaping Formation is overlain by an 8 to16 m thick interval of calcimicrobial framestone that has a distinctive wavy, vaguely stromatolitic or thrombolitic appearance in outcrop (fig. 11). The calcimicrobial framestone is composed of irregular to dendritic black globular fossils similar to *Renalcis* that surround an interconnected network of irregular primary cavities filled with lime mud and skeletal debris. The calcimicrobial framestone lacks recognizable Permian macrofossils and overlies the Wujiaping Formation across a sharp, planar contact, or an undulating seam stylolite contact (fig. 11). The contact and underlying strata contain no evidence of erosion or subaerial diagenesis. At Heping section the calcimicrobial framestone contains several interbeds of molluscan lime grainstone (fig. 11); the Dajiang section lacks the interbeds. The calcimicrobial framestone is overlain by a skeletal packstone interval a few meters thick that is composed mostly of minute (< 2 mm) gastropods (microgastropod packstone, fig. 11). It also contains bivalves, inarticulate brachiopods, small articulate brachiopods and rare echinoid spines. This interval is overlain by 60 m of monotonous, thin-bedded lime mudstone of the Lower Triassic Daye Formation (Figs. 10B, 11).

The calcimicrobial framestone extends continuously across the interior of the GBG (fig. 10A). Near the northern margin of the GBG, it gradually thins and pinches out. Near the ‑pinchout, the calcimicrobial framestone overlies a thin interval of siliceous lutites of the Upper Permian Dalong Formation (fig. 10A). The Dalong Formation contains the Changxingian ammonoids *Rotodiscoceras, Pseudotirolites and Pleuronodoceras* as well as radiolarians (Guizhou Bureau of Geology and Mineral Resources, 1987).

Conodont Biostratigraphy- Closely spaced samples from the Heping section yielded abundant conodonts. The Upper Wujiaping Formation at Heping yielded only *Hindeodus typicallis* (fig. 11) and lacked *H. parvus*. Although diagnostic Late Permian conodonts were not recovered from this section, the presence of *Palaeofusulina* and *Colaniella* indicate a Late Permian, Changxinian age. Fragments of *Neogondolella changxingensis* were recovered from the upper Wujiaping Formation at Dajiang and Guandao sections (fig. 11). The lowermost sample from the calcimicrobial framestone at Heping section was collected 65 cm above the base of the unit and contains *Hindeodus parvus* (fig.11). *Hindeodus parvus* occurs upsection through the calcimicrobial framestone and into the lime mudstone of the Daye Formation (fig. 11). The first occurrence of *H. parvus* is widely used to define the base of the lowermost Triassic, Griesbachian stage (Paull and Paull, 1994; Orchard et al., 1994; Yin et al., 1996). Thus, the conformable biostratigraphic PTB is interpreted to occur within the basal 65 cm of the calcimicrobial framestone at Heping (fig. 11). *Isarcicella isarcica* occurs in the microgastropod packstone immediately overlying the calcimicrobial framestone. The consecutive appearances of *H. parvus* followed by *I. isarcica* thus place the microbialite in the *H. parvus* zone (fig. 11).

Depositional environments- Calcimicrobial framestone

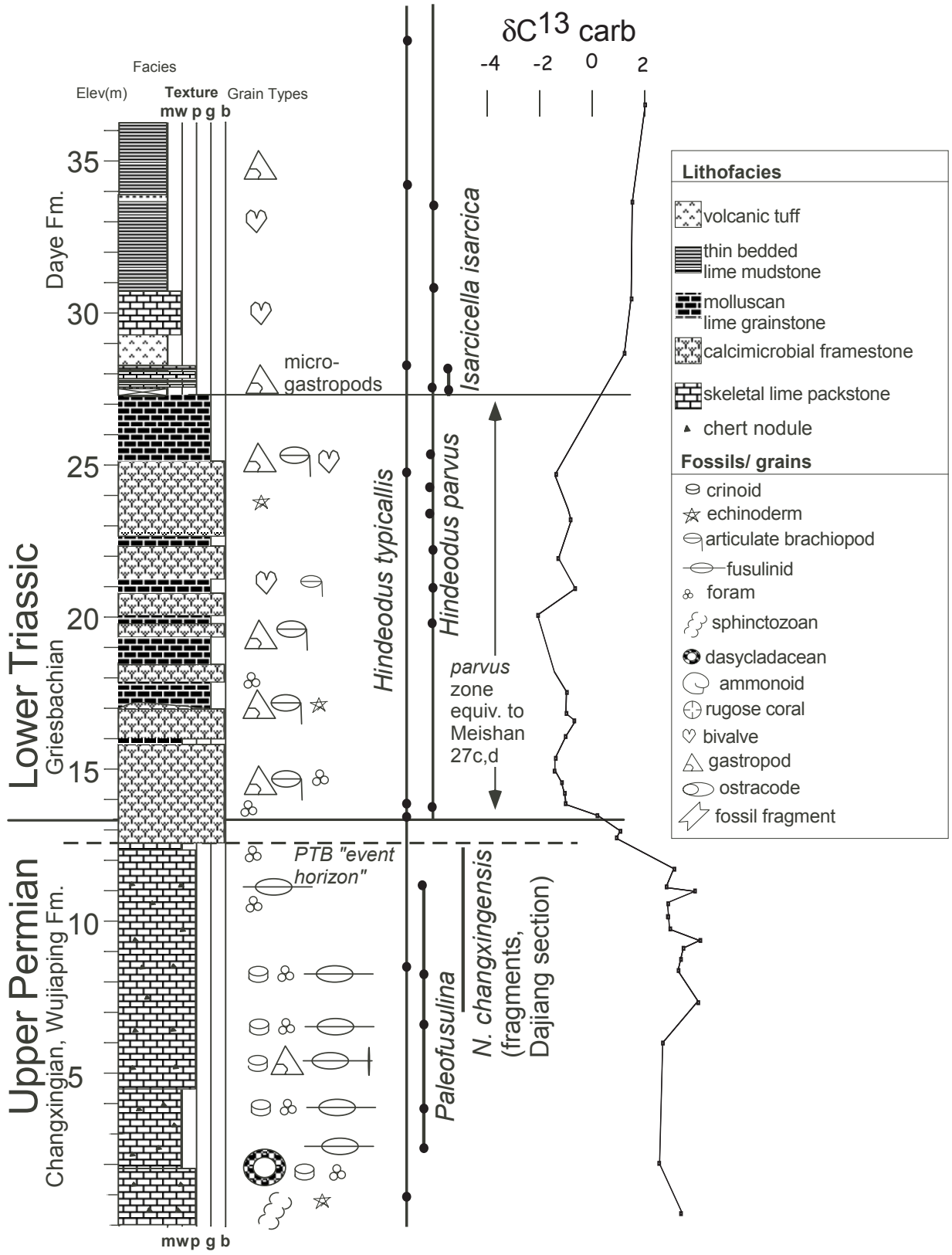

Figure 11: Permian-Triassic boundary section at Heping (1 km south of Dajiang) with biostratigraphic and carbon isotope data. The PTB event horizon is marked by the last occurrence of diverse Permian fossils at the top of skeletal packstone of the Wujiaping Formation. The biostratigraphic Permian-Triassic boundary is defined by the first appearance of *Hindeodus parvus* slightly higher, in the lower part of the calcimicrobial framestone. See figures 9 and 10 for location.

of the Lower Triassic Griesbachian is interpreted to represent shallow-subtidal, open-marine environments similar to the environment of deposition of the underlying Permian skeletal packstone. The framework is composed of equant to lunate, globular fossils with micrite walls that form irregular, tufted, and dendritic aggregates surrounding irregular internal cavities. These structures are interpreted as calcified, coccoid cyanobacteria similar or identical to *Renalcis* (Lehrmann, 1999). The environment of deposition is interpreted in the context of the interbedded skeletal grainstone and metazoan fossils contained within the framework. Cyanobacteria flourish in a great variety of environments, including saline lagoons (Playford and Cockbain, 1976), open-marine platforms (Gebelein, 1976) and even in anaerobic or acidic environments (Schopf, 1992). The calcimicrobial framestone lacks sedimentary, biotic, or diagenetic evidence for hypersalinity or tidal-flat conditions. The occurrence of interbedded molluscan grainstone with normal-marine fauna indicates wave agitation and free exchange of seawater across the area during the deposition of the calcimicrobial framestone. The occurrence of echinoderms and articulate brachiopods within the framestone further supports open-marine conditions.

Grainstone and packstone beds, composed mainly of fragmented bivalves, are intercalated with the calcimicrobial framestone at Heping (fig. 11). The presence of articulate brachiopods and echinoderms provides evidence for an environment with normal-marine salinity. The grainy texture and fragmented fossils indicate a shallow-marine environment subject to wave action and possibly storm events exchanging marine water across the platform interior. Shell fragments may be randomly oriented or aligned parallel to bedding. Rarely, the packstone contains infiltrated lime mud and peloids perched on shell fragments. The low-diversity biota is interpreted to reflect the drop in biodiversity in the immediate aftermath of the end-Permian extinction rather than restricted marine circulation. Grainstone beds within the calcimicrobial framestone are broadly lenticular as they are discontinuous between sections. Grainstone interbeds are abundant in Dawen and Heping sections but pinch out laterally and are absent in the Dajiang section (fig. 10). The lenticular geometry of the grainstone beds and fact that the interlayers of calcimicrobial framestone contain similar metazoan fossils (bivalves, echinoderms, brachiopods, etc.) indicates that these two facies were deposited in adjacent coeval, shallow-subtidal environments.

Overlying the microbialite is microgastropod packstone followed by thin-bedded lime mudstone of the Daye Formation (fig. 11). The microgastropod packstone is in places composed almost entirely of minute gastropods 1-2 mm in diameter. The muddy texture of this facies and the absence of open-marine biota, except for a few small, articulate brachiopods, suggest a change to a low-energy, lagoonal environment with restricted circulation. The thin-bedded lime mudstone of the Daye Formation overlies the microgastropod packstone and contains a few scattered bivalves and gastropods and contains extremely rare thin beds of oolite packstone. The low-diversity fauna suggests a shallow, restricted lagoonal environment. The homogenous structure of the lime mudstone suggests extensive bioturbation, but the paucity of discrete burrows, burrow mottling and bedding-plane traces is puzzling.

Carbon isotope and TOC data- Organic and carbonate carbon isotopes were measured across the PTB in Heping section approximately 1 km south of Dajiang (Krull et al., 2004). Negative excursions across the Permian-Triassic boundary in $\delta^{13}C_{org}$ and $\delta^{13}C_{carb}$ occur immediately above the PTB "event horizon", marked by the onset of the calcimicrobial framestone, and immediately below the first occurrence of *H. parvus* (fig. 11). The carbon isotope shifts are associated with a drop in average total organic carbon (TOC) and the depleted values in both $\delta^{13}C_{org}$ and $\delta^{13}C_{carb}$ together with low TOC content persist throughout the Griesbachian *H. parvus* zone. These data document a negative shift of $\delta^{13}C_{org}$, $\delta^{13}C_{carb}$, and TOC correlative with the base of the Griesbachian *H. parvus* zone and the onset of growth of calcimicrobial framestone following the extinction. Correlation of the $\delta^{13}C$ excursion with the GSSP at Meishan shows that calcimicrobial framestones and *H. parvus* zone (8 to 16 m thick) have exceptionally high sediment accumulation rates relative to the correlative zone at Meishan, which is only 18 cm thick (beds 25-27c).

Lower Olenekian (Smithian) peritidal cyclic limestone of the platform interior

General lithofacies and depositional environments- Lower Triassic strata in the interior of the GBG are approximately 400 meters thick. They begin with calcimicrobial framestone biostromes 8-16 m thick in the Lower Griesbachian, 50 m of thin-bedded lime mudstone in the Griesbachian and Dienerian, overlain by 100 m of oolite dolo-grainstone and oolitic microbial laminites in the Dienerian, 180 m of peritidal cyclic limestone in the Lower Olenekian (Smithian) and finally massive peritidal dolomite in the Upper Olenekian (Spathian; fig. 9, 10B). The Olenekian-Anisian boundary in the platform interior occurs within the massive peritidal dolomite. The age of the peritidal cyclic limestone is constrained by the occurrence of the conodont *Lonchodina nevadensis* and by correlation of carbon isotope profiles to the biostratigraphically constrained Guandao section at the basin margin (Payne et al, 2004; fig. 18).

The entire Lower Triassic platform-interior succession of the GBG contains fabrics consistent with shallow subtidal to peritidal conditions and lacks evidence of major deepening events. Furthermore, the underlying Upper Permian strata and overlying Middle Triassic strata represent open-marine shallow-subtidal and restricted-marine, tidal flat environments, respectively (Lehrmann et al., 1998). Reef mounds of calcimicrobial framestone occur in the platform-interior, peritidal cyclic limestone, but are absent from the platform margin, suggesting that these features formed only in relatively low-energy environments of the platform interior. Thus, the facies succession and strati-

graphic architecture of the platform constrain the Olenekian cyclic limestone facies to a relatively low energy, restricted- to normal-marine, shallow subtidal and peritidal environment.

Lithofacies and depositional cycles- The Olenekian peritidal cyclic limestone extends across the interior of the GBG (fig. 9, 10B). It is 145 m thick and contains 66 shallowing-upward parasequences in the Dajiang section (fig. 12). Individual parasequences range from 0.2-7.4 m in thickness. The parasequences are composed of five shallow-subtidal to supratidal facies: skeletal packstone, oolitic packstone and grainstone, calcimicrobial biostromes and reef mounds, flaser-bedded and horizontally burrowed ribbon rock, and microbial laminite. A typical parasequence has a skeletal packstone or oolite base followed by calcimicrobial mounds, and capped by flaser-bedded ribbon rock (fig. 12). Variations include parasequences with calcimicrobial facies at the base, those lacking calcimicrobial mounds, or those capped by a microbial laminite rather than ribbon rock.

Skeletal packstones are typically massive or contain horizontally-oriented bivalve fragments with perched infiltrated sediment. Skeletal grains include thin-shelled bivalves, gastropods, ostracodes, foraminifers, minor echinoderm fragments and sparse lingulid brachiopods and worm tubes. The skeletal packstone is interpreted to represent open to restricted, shallow-subtidal environments with relatively low current energy. Most of the skeletal grains probably represent restricted marine circulation; the presence of echinoderms, however, suggests occasional open-marine circulation. Abundance of mud indicates low-energy conditions. The massive fabric suggests bioturbation.

Oolitic packstone and grainstone beds, at the base or in the middle of parasequences, are thin to medium bedded. No lamination or cross-bedding was observed. Grainstone is rare; much of the oolite is mud-poor packstone with infiltrated internal sediment. Peloids, bivalve fragments and imbricated flat-pebble conglomerates are locally abundant. The oolitic packstone and grainstone represent subtidal shoals. Grainstone fabrics and imbricated interclasts indicate a current-swept shoal environment. Infiltrated mud fabrics suggest shoal stabilization and shift to lower energy conditions in the upper parts oolitic beds.

Biostromes and bioherms composed of calcimicrobial framestone occur in the middle and base of parasequences immediately below parasequence cap facies. Bioherms include small domal mounds as well as inverted conical mounds up to 1.5 m tall. Individual bioherms range from 10 cm to 1.5 m thick and have diameters of one to two times their height. Bioherms within individual beds are generally of similar size and have a lateral spacing of one to several meters. Where they form syndepositional relief, skeletal packstone interfingers with the lower mound and flaser-bedded ribbon rock onlaps and overlaps the upper mound. The calcimicrobial framestone fabrics are identical to those described from the basal Griesbachian of Dajiang section.

Flaser-bedded ribbon rock most commonly caps the shallowing-upward cycles. It consists of laminated interlayers of lime mudstone and flaser-bedded grainstone. The ribbon appearance results from flaser bedding produced by the interlayering of grainstone lenses with continuous lime mudstone drapes. Grainstone lenses contain ripple cross laminae and isolated starved ripple forms. Scoured surfaces are commonly overlain by imbricated intraclasts. Opposed current indicators suggest reversing currents. Rare interlayers of lime mudstone and grainstone contain tidal bundling (spring/neap packages) with progressive upward thinning of grainstone-mudstone couplets. In some parasequence caps, near the top of Dajiang section, the ribbon rock contains water-escape structures - fissures that disrupt lamination into small antiformal structures. The ribbon rock represents muddy tidal flats dominated by intertidal conditions. Reversing-current indicators, scours, grainstone lenses and starved ripples formed during flood and ebb tides. Lime mud drapes were deposited from suspension during submergence and slack tide. Minor burrowing occurred during submergence of the tidal flat. Autoclastic brecciation and v-shaped cracks associated with water-escape structures suggest these features formed by desiccation during subaerial exposure of the tidal flat. The dominance of hydrodynamic structures indicates low intensity of bioturbation. Microbial laminite occurs in parasequence caps within the upper parts of Dajiang section (fig. 12). A few of the layers contain evidence for significant subaerial exposure such as prism cracks, autoclastic breccia with reddened clasts and calcareous soil concretions. This facies represents rare supratidal conditions and prolonged exposure of the tidal flats.

The Lower Triassic platform-interior sequence of the Great Bank of Guizhou is notable for its extremely low biodiversity and predominance of unusual microbialite precipitates and ribbon rock facies dominated by physical sedimentary structures. The low biodiversity corresponds to a period of pronounced instability of the carbon cycle, suggesting that environmental perturbations may have prevented rediversification of life during the Early Triassic (Payne et al., 2004; fig. 18). Notably, two of the large negative carbon excursions coincide with the onset of major packages of microbialite deposition in the platform interior (fig. 18). These observations suggest that microbialite genesis may be linked with environmental disturbances also reflected in the carbon isotope record.

Milankovitch cyclicity- Parasequence thickness and facies stacking patterns in the peritidal cyclic limestone display three orders of cyclicity, suggesting hierarchical stratigraphic packaging (fig. 12). Yang and Lehrmann (2003) performed spectral analysis on the strata in Dawen and Dajiang sections (fig. 9) using the gamma analysis technique. Spectral analysis of the time series displayed multiple statistically significant spectral peaks, suggesting a quasi-periodic nature of the record. Prominent short-eccentricity, short-obliquity, and long-precessional index peaks, and minor long-eccentricity, long-obliquity, short-precessional index, and constructional-tone peaks were

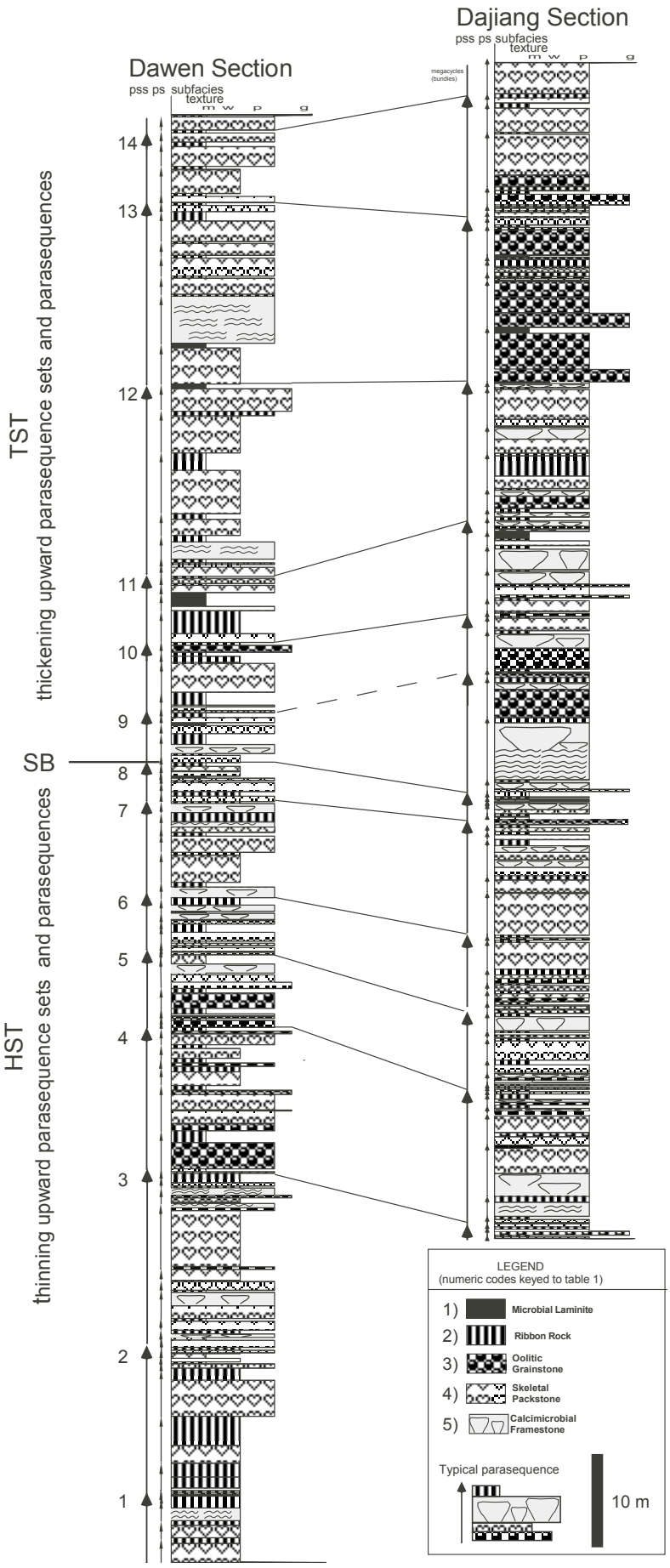

Figure 12: Lower Triassic peritidal cyclic limestone in Dawen and Dajiang sections. The locations of the sections are keyed to figures 9 and 10. Numbered arrows to the left of sections indicate 4th order parasequence sets. Unnumbered arrows immediately left of the columns denote 5th order parasequences. Systems tracts and 3rd order sequence boundary are indicated to the left of Dawen section. TST = transgressive systems tract, HST = highstand systems tract, SB = sequence boundary. The typical or most common parasequence type ("ideal cycle") is indicated on the lower right.

calibrated on the gamma-corrected spectra. Thus, Milankovitch climatic forcing probably greatly influenced sedimentation. On the basis of the calibration, the subtidal facies has sedimentation rates of 24.6 to 30.7 cm/ky and the intertidal-supratidal facies has rates of 2.7 to 6.0 cm/ky. The estimated duration of deposition of the interval in the two sections is 1139 to 1423 ky, corresponding to a stratigraphic completeness of 60 to 75%. The high level of stratigraphic completeness was attributed to low amplitude sea level oscillation in a greenhouse climate of the Early Triassic.

Stop- 4b Optional stop at Permian-Triassic boundary at Rungbao section

The Permian-Triassic boundary succession at Rungbao section is essentially identical to that described for Dajiang section (see description in stop 4A and fig. 11). The section is, however, easily accessible from the road and contains well-developed microbial fabrics and undulatory bedding superficially resembling stomatolites, cherty Upper Permian carbonates and a volcanic ash layer within the uppermost Permian carbonate. Geochemistry and petrography demonstrate that the claystone is indeed volcanic ash and has a rhyolitic composition (Newkirk et al., 2002).

Stop-5 Lower-Middle Triassic (Olenekian-Anisian) boundary section in basin-margin facies at Guandao section

Guandao section occurs on the east limb of the Bianyang syncline at the basin margin immediately north of the GBG (fig. 8, 9). Several aspects make this one of the most important sections in the Nanpanjiang basin for chronostratigraphy. The section: (1) is approximately 750 m thick and has continuous exposure of Upper Permian through Upper Triassic (Carnian) strata, (2) is composed primarily of deep-marine, pelagic, carbonate strata that contain abundant conodonts, (3) apparently records continuous sedimentation without significant unconformities, (4) preserves primary magnetic signature and several volcanic horizons, (5) occurs adjacent to a carbonate platform with preserved paleobathymetry allowing physical correlation between shallow-marine platform strata with deep-marine strata at the basin margin and (6) is easily accessible from the nearby town of Bianyang (figs. 9, 10, 15). Furthermore, although Guandao section has the disadvantage of lacking abundant ammonoid faunas, the section should provide useful constraints on the global geologic time scale as it contains a long, continuous record of Triassic sedimentation in contrast to the numerous short marine sections that have commonly been used in composite for reconstructing Triassic chronostratigraphy.

Lithofacies and record of Triassic biotic recovery

Guandao section was measured in two overlapping segments: lower Guandao, which spans the Upper Permian through the Middle Triassic Anisian (Pelsonian) (fig. 9, 13) and upper Guandao section, which spans the Lower Triassic, Upper Olenekian (Spathian) through the Upper Triassic Carnian (fig. 9, 15). The sections are offset and correlated along an interval with volcanic ash horizons that straddles the Lower-Middle Triassic (Olenekian-Anisian) boundary (fig. 17).

Lower Guandao Section— The base of lower Guandao section was measured in cherty skeletal packstone of the Upper Permian Wujiaping Formation. The Wujiaping Formation represents sedimentation prior to the initiation of the GBG as an isolated platform and was deposited near the southern margin of the Upper Permian Yangtze platform (fig. 2, 3, 9). It contains a diverse assemblage of shallow-marine benthic fossils including articulate brachiopods, mollusks, echinoderms, bryozoans and foraminifers.

Overlying the Wujiaping Formation is the Upper Permian Dalong Formation that represents the initial "drowning" of a large area of the Yangtze platform north of the area of the GBG (fig. 2, 13). The Dalong Formation adjacent to the GBG is 10-15 m thick and is composed of deeply weathered, dark brown to black, nodular-bedded siliceous lutite (chert), cherty nodular-bedded lime mudstone and shale. One of the "shaly" interbeds near the top of the Dalong Formation at Guandao section may be a volcanic ash.

The Dalong Formation contains radiolarians and the ammonoids *Rotodiscoceras*, *Pseudotirolites* and *Pleurondoceras*. The combination of dark color and pelagic fauna with minor bioturbation and presence of small articulate brachiopods suggests a dysaerobic environment. The Dalong Formation reaches a maximum thickness of 78 m in southern Guizhou (Guizhou Bureau, 1987). Further work is needed to determine the depositional environments of the Dalong Formation and the conditions that led to the termination and step back of a vast area of the Yangtze platform in southern Guizhou (fig. 2). Two observations suggest that the "drowning" cannot be explained simply as the result of eustatic sea level rise: 1) the Yangtze platform was terminated in the eastern sector only (fig. 2), and 2) paleobathymetry adjacent to the Upper Permian reef mound on the north margin of the GBG (fig. 9; Lehrmann, 1993) suggests water depths of approximately 30 meters for Dalong Formation deposition.

The Permian-Triassic boundary occurs between the Dalong Formation and the overlying shale containing the bivalve *Claraia* (fig. 13). The shale is 18 m thick, deeply weathered and has a brown-tan color and is laminated. Overlying the Griesbachian shale, the Induan succession is dominated by hemipelagic lime mudstone, allodapic lime packstone and grainstone, submarine debris-flow breccia beds and shale interbeds (fig. 13). These facies correlate biostratigraphically with the Luolou Formation that has been mapped regionally in the Nanpanjiang basin of southern Guizhou and Guangxi (fig. 3, 7).

The Induan lime mudstone is thin-bedded, dark gray to black and commonly laminated, rarely it is burrowed. At the base of debris-flow breccia beds lime mudstone is

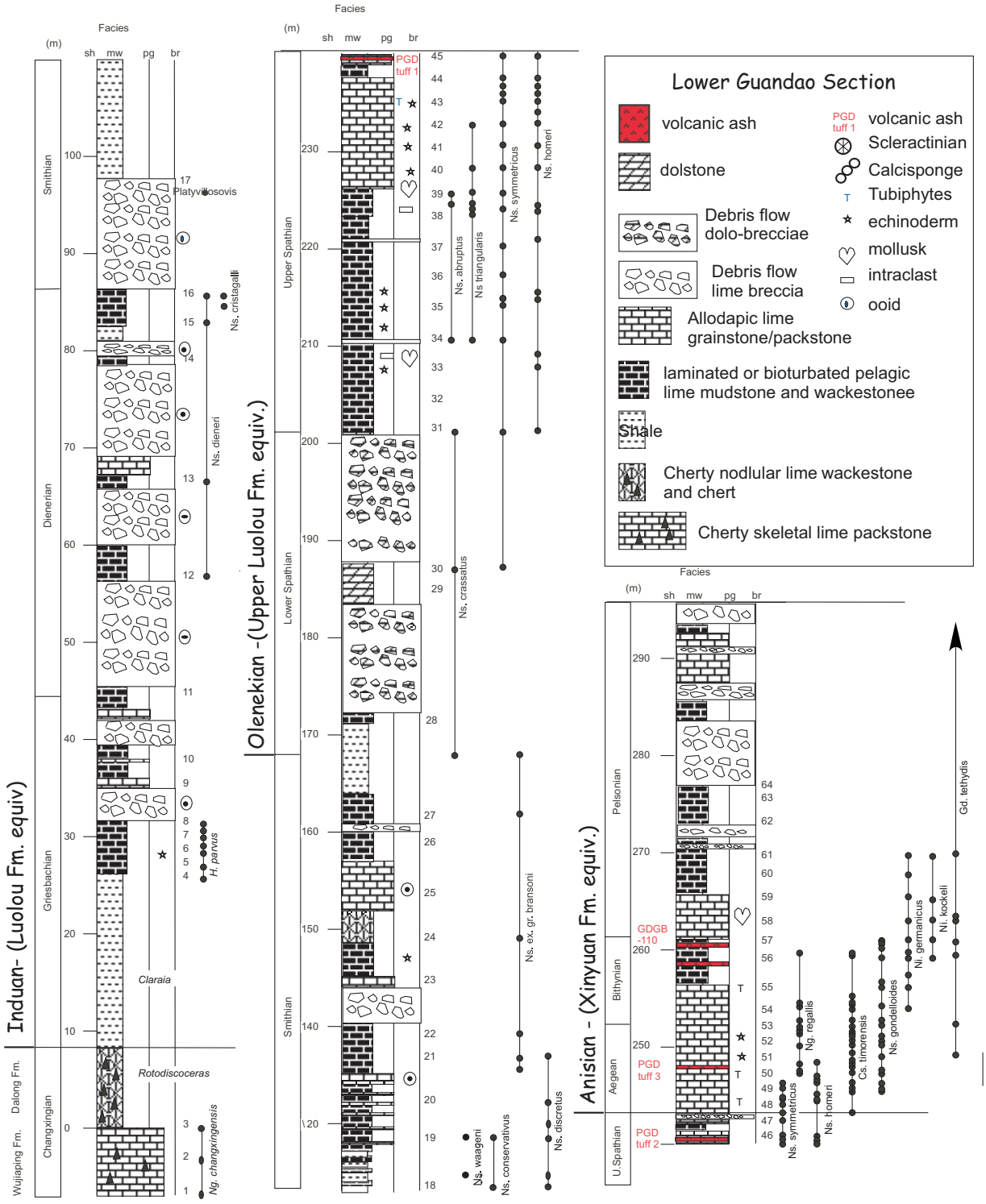

Figure 13: Upper Permian through Middle Triassic (Anisian) strata at lower Guandao section. Facies are from the basin-margin slope succession on the northern margin of the GBG. See figures 9 and 10 for location. Dominant carbonate grain types (ooids, intraclasts, and various skeletal grains) are indicated immediately right of the lithofacies column. Conodont biostratigraphy and volcanic-ash horizons are also indicated. U-Pb dates of volcanic ash layers are shown in fig. 17.

commonly contorted by soft-sediment deformation into wavy or overturned folds. Allodapic packstone and grainstone beds are dominantly composed of oolite, peloids and intraclasts of lime mud or oolite packstone. Debris-flow breccias are matrix-rich and contain a mix of oolite clasts derived from the platform margin and lime-mudstone clasts derived from the slope. The Induan succession at Guandao section is notable for extremely low skeletal content and dominance of non-skeletal grains (ooids, intraclasts, peloids; fig. 13). Thin-section point counts indicate skeletal abundance near zero (J. Payne, unpublished data). Allodapic packstones and breccia clasts contain a few bivalve fragments.

Facies types and depositional environments are similar in the Olenekian strata: pelagic lime mudstone, allodapic packstone and grainstone, debris-flow breccia beds and shale. The Olenekian strata at Guandao section are biostratigraphically correlated with the upper Luolou Formation in southern Guizhou (fig. 3, 13). Near the base of Olenekian succession are two dolomitized breccia intervals, each greater than 10 m thick, that form a prominent ridge in the landscape (fig. 9, 13). The strata overlying the dolomitized breccia beds contain more conspicuous fossils (bivalves, crinoids and *Tubiphytes,* indicating the beginning of biotic recovery near the end of the Olenekian (Upper Spathian; fig. 13). Thin-section point counts indicate that abundance and diversity of skeletal grains increased only in the Upper Olenekian (5% skeletal abundance in the Upper Spathian) after remaining low throughout the preceding Lower Triassic (J. Payne, unpublished data). Thin sections reveal the presence of bivalves, crinoids, cephalopods, foraminifera, brachiopods, ostracods and *Tubiphytes* fragments. Volcanic-ash horizons occur in the upper Olenekian and Anisian (fig. 13). Notably the pelagic lime mudstone and packstone beds near the Olenekian and Anisian boundary at Guandao section contain chert nodules. In southern Guizhou, chert nodules are commonly found in Upper Permian carbonates but are almost entirely absent from Triassic strata. The occurrence of chert nodules at this level may reflect either increased abundance of biogenic silica from radiolarians or siliceous sponges or mobilization of silica from the volcanic ashes.

Upper Guandao section- Upper Guandao section was measured in the valley and up the hillside approximately 200 meters north (basinward) of lower Guandao section**.** The base of the section is in Upper Olenekian (Spathian) strata containing volcanic-ash horizons (fig. 14). The volcanic units thicken and apparently amalgamate basinward away from the platform (fig. 17). The section continues up through the Anisian and Ladinian. It represents the basin-margin slope succession deposited north of the massive, aggrading *Tubiphytes* reef (fig. 9, 10). Biostratigraphically the Anisian succession correlates with the Xinyuan Formation of southern Guizhou (fig. 4, 7). The siliciclastic turbidites of the Bianyang Formation at the top of upper Guandao section (fig. 9, 10) are Carnian in age whereas in other areas of Guizhou this unit is considered largely Ladinian (fig. 5).

The lithofacies consist of pelagic lime mudstone, allodapic skeletal and intraclastic lime packstone or grainstone and debris-flow breccia beds with clasts derived from the platform-margin *Tubiphytes* reef. Skeletal abundance and diversity is greater in the Anisian-Ladinian succession than in the uppermost Olenekian. Thin-section point counts record 8 to 9% skeletal grains averaged over all lithologies (J. Payne, unpublished data). Whereas the increase in skeletal abundance from near zero to approximately 5% in the upper Olenekian reflects an increase in the abundance of animal skeletal grains, the additional increase in the Anisian and Ladinian records the additional input of *Tubiphytes* grains at this time. Thin-bedded lime mudstone and wackestone contains thin-shelled pelagic bivalves, radiolarians, echinoderms and rarely ammonoids. Skeletal packstone and grainstone and clasts within breccias contain *Tubiphytes* fragments, crinoids, echinoids, foraminifers, calcareous algae, mollusks, brachiopods, ostracodes, calcisponge fragments and a few sclearactinian corals. Notably, the skeletal abundance and diversity remains relatively constant throughout the Anisian and Ladinian succession (J. Payne, unpublished data).

Conodont biostratigraphy – the Olenekian-Anisian boundary

A total of 603 samples, each 3-5 kg., were collected from lower and upper Guandao sections. Sample spacing ranged from about 2 meters to 20 cm, with more closely spaced samples near important boundaries such as the Olenekian-Anisian boundary. Most of the samples contained abundant conodonts, many with hundreds or thousands of elements. From the entire stratigraphic succession we have identified 56 conodont species, enabling a substage zonation of the Upper Permian through Carnian (ranges of important species are shown in fig. 13, 14).

The Olenekian-Anisian boundary is especially well constrained by conodont biostratigraphy, providing a high-resolution record of this critical interval of biotic recovery (fig. 14). The Olenekian-Anisian boundary is placed at the first occurrence of *Chiosella timorensis. Cs. timorensis* has been recognized as a key index fossil for definition of the boundary as it has a narrow stratigraphic range and global distribution (Orchard, 1995; Orchard and Tozer, 1997). Further, the International Commission on Stratigraphy has reported agreement that the first occurrence of *Cs. timorensis* will define the O-A boundary in the global stratotype to be designated at the Desli Caira section in Dolobrogea, Romania (Ogg, 2004). At Desli Caira the first occurrence of *Cs. timorensis* closely corresponds with the occurrence of biostratigraphically important ammonoids *Japonites*, *Paradanubites* and *Paracrochordiceras* (Gradinaru, 2001).

Additional constraints on placement of the Olenekian-Anisian boundary at Guandao section include: the last occurrences of *Neospathodus abruptus* and *Ns. triangularis* (Orchard, 1995) well below the boundary, the occurrence of *Ns. symmetricus* and *Ns. homeri* below and

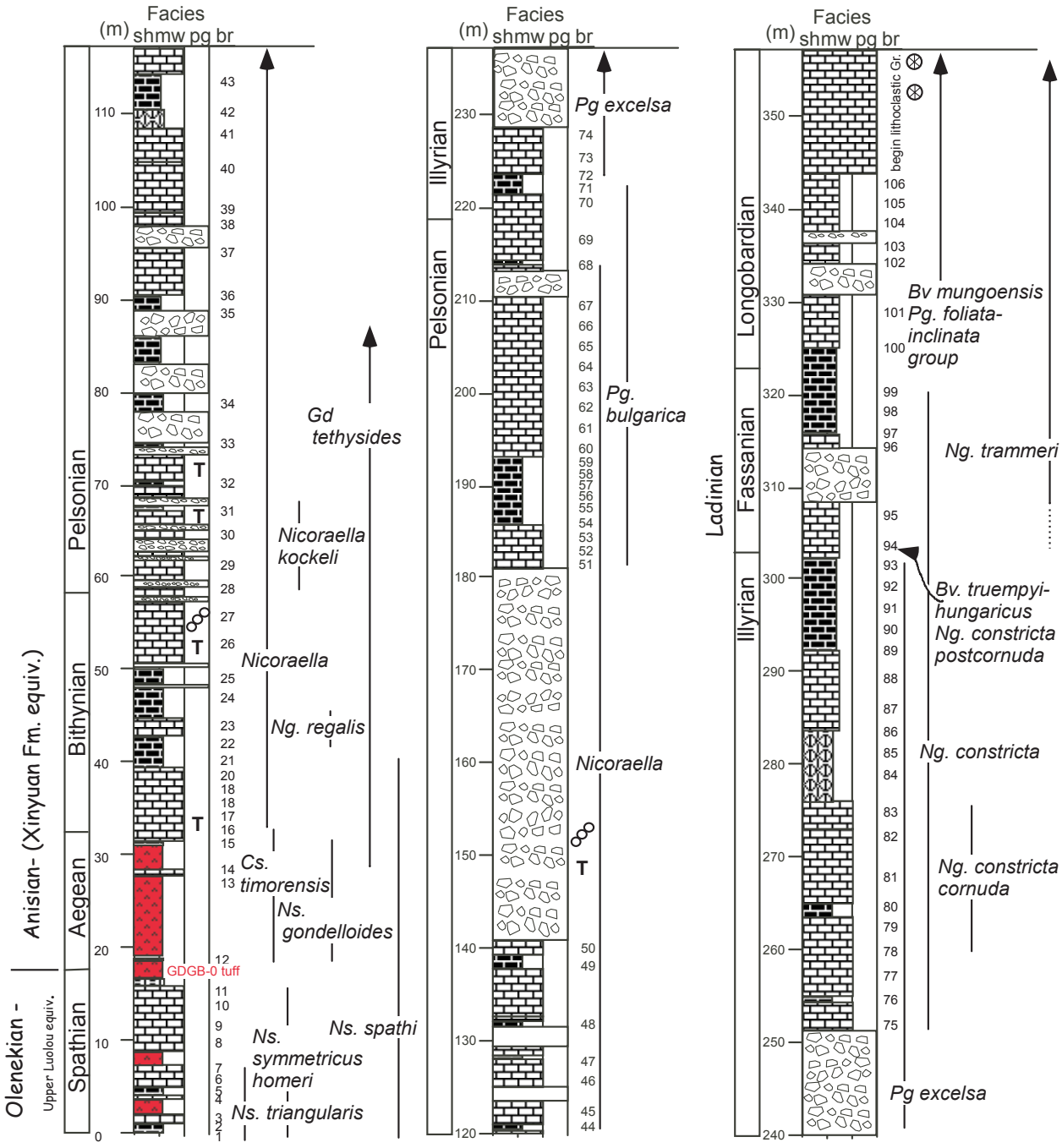

Figure 14: Lower Triassic (Spathian) through Middle Triassic (Ladinian) strata at upper Guandao section. Facies are from the basin-margin slope succession on the northern margin of the GBG. See figures 9 and 10 for location. Lithology and grain type symbols are the same as those shown in figures 13. Conodont biostratigraphy and volcanic ash horizons are indicated. U-Pb dates of volcanic ash layers are shown in fig. 17.

extending slightly above the boundary and the first occurrence of *Gladiogondolella tethydis, Nicoraella germanicus* and *Ni. kockeli* above the boundary (fig. 14).

Volcanic ash layers- preliminary U-Pb dates

Several volcanic ash horizons straddle the boundary (fig. 17). Preliminary age dates are as follows. We emphasize that these age dates are preliminary and should not be cited as certain boundary ages until the data are sufficiently refined. The lowest dated horizon occurs 4.5 m above the O-A boundary in the lower *Cs. timorensis* biozone and is age dated to be 247.8 MA. The highest dated horizon occurs in the uppermost *Cs. timorensis* biozone and is age dated at 246.5 MA. These preliminary data indicate an age of > 247.8 MA (probably around 248MA) for the O-A boundary. Given that age dates for the end-Permian extinction horizon from independent labs appear to be converging near 252 MA (see Bowring et al., 1998; Mundil et al., 2004), the duration of the Early Triassic Epoch and the interval of delayed recovery was approximately 4 million years.

Magnetostratigraphy

Magnetostratigraphic data collected (total of 322 paleomagnetic samples from lower and upper Guandao sections) defined a series of ten normal and ten reversed magnetozones in lower Guandao section that characterize a geomagnetic polarity record for the Lower Triassic and basal Anisian. Detailed demagnetization experiments have resulted in the isolation of a Lower Triassic paleomagnetic directional data. Magnetostratigraphic data from Guandao were subjected to the reversal test and passed at a grade 'B' level (Paul Montgomery, personal communication). Comparison with predicted Lower Triassic paleomagnetic directions for the Guandao area show good agreement (Enkin et al 1992; Van der Voo, 1993). Based on this evidence a primary paleomagnetic signal is interpreted.

Magnetic reversal stratigraphy from Guandao section correlates with the reversal zonation of the O-A boundary in western Tethyan sections (Muttoni et al., 2000). In both areas normal polarity occurs in the Lower Spathian followed by a predominantly reversed zone with a few thin reversals in the upper half of the Spathian and straddling the Olenekian-Anisian boundary (fig. 14). This is followed by a zone of normal polarity in the Bithynian to Lower Pelsonian (fig. 14).

Carbon-isotope record

Samples were collected for carbon-isotopic analyses from the lower Guandao and upper Guandao sections with an average spacing of approximately one meter where exposure permitted. The results provide a detailed and relatively continuous record of large fluctuations in the global carbon cycle that continued through the Early Triassic and into the Middle Triassic before stabilization occurred rapidly in the Anisian (fig. 18). Unfortunately, heavily weathered shales across the P-Tr boundary at the Guandao section reduce the quality of the record near the extinction event itself. This part of the record is well recorded in the platform-interior sections (fig. 18). The Smithian-Carnian record from the lower Guandao and upper Guandao sections, on the other hand, is excellent. In particular, two large cycles are apparent with positive peaks near the Smithian-Spathian boundary and within the base of the Anisian. The Anisian peak is followed by a trend to lighter values and subsequent stabilization at values around 1.5‰. From the Anisian through the Carnian values do not vary by more than approximately 1‰.

Evidence is strong that the pattern of carbon-isotopic fluctuations through the Early Triassic reflects global changes in the carbon cycle. The magnitude and timing of the

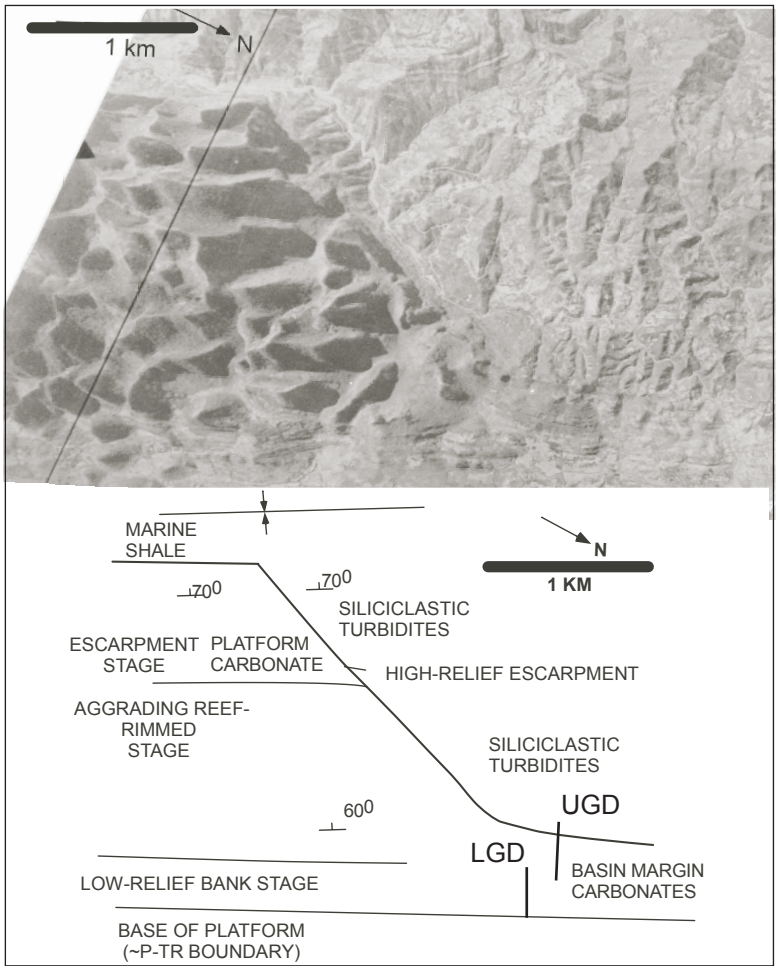

Figure 15: Air photo and sketch map of platform margin relationships on the northern margin in the Bianyang syncline (northern margin in figure 9). The air photo illustrates the sharp contact between carbonate strata of the high-relief Ladinian escarpment and onlapping Carnian siliciclastic turbidites. LGD = Lower Guandao section. UGD = Upper Guandao section. See text for details.

Permian-Triassic boundary excursion is well known from localities around the globe (e.g., Magaritz et al., 1988; Baud et al., 1989). The Smithian-Spathian and Early Anisian positive peaks have been observed at other localities around the Tethys (e.g., Atudorei, 1999; Baud et al., 1996), and the large positive excursion near the Dienerian-Smithian boundary is found in the Dolomites and elsewhere (Horacek, et al., 2001; J. Payne, unpublished data; S. Richoz, pers. comm.). Only the second negative excursion in the platform interior, near the Griesbachian-Dienerian boundary, has yet to be observed within other marine carbonate sections.

The instability of the carbon cycle during the Early Triassic is remarkable both for its magnitude and for its contrast with Middle Triassic stability. The cause of Early Triassic carbon-cycle instability is poorly understood. Suggestions of a role for methane hydrate destabilization at the end of the Permian (e.g., Krull et al., 2004; Krull and Retallack 2000) could account for the negative excursion at the PTB, but cannot explain continuing carbon-cycle instability because the time scale involved in repeated excursions is too short to allow replenishment of the clathrate reservoir. A more conventional explanation of the repeated excursions, reflecting changing ratios of carbon burial as organic matter versus carbonate rocks, is challenged by the magnitude of the excursions. Generating such large and rapid excursions requires an extraordinarily high fraction of organic carbon burial (>0.5 vs. carbonate burial) given any reasonable isotopic fractionation between organic and inorganic carbon. If the excursions do represent changes in the fraction of organic burial, it will be essential to determine the conditions (such as episodes of shallow-shelf anoxia) that were capable of producing such elevated levels of organic carbon burial, as well as the reasons why such conditions did not persist beyond the Early Triassic.

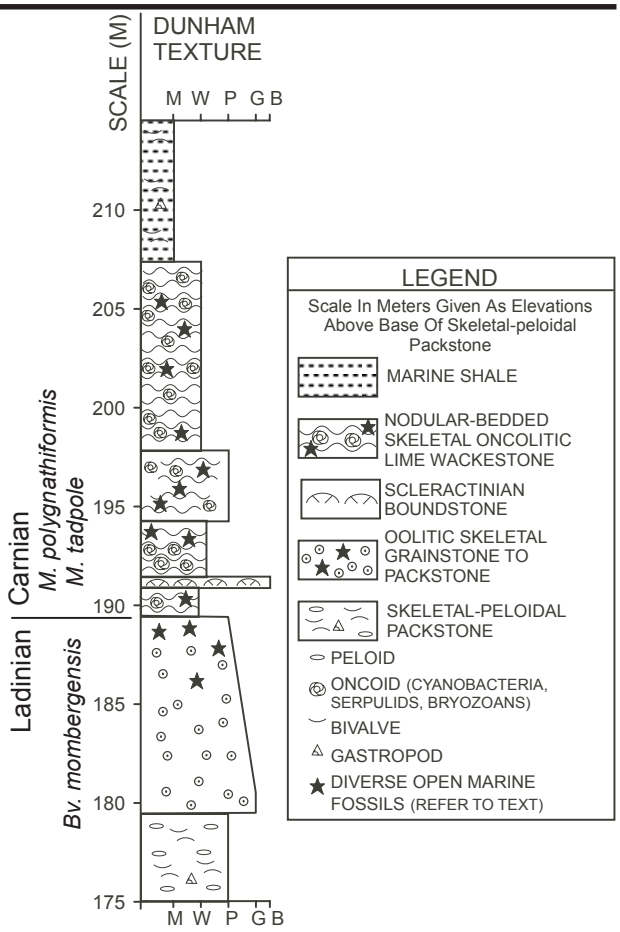

Figure 16: Stratigraphic section of the Ladinian- Carnian platform termination succession at the top of Bangeng section, in the axis of the Bianyang syncline. See figure 9 for location. See text and stop 2 of the field guide for further details.

Stop-6a Anisian-Ladinian platform-margin *Tubiphytes* reef traverse. Rigorous traverse on trail through karst terrain south of Guandao (fig. 9)

Extensive Anisian and Ladinian reef complexes are preserved in the Nanpanjiang basin of Guizhou, Guangxi and Yunnan of southern China. Reefs occur on the edge of the extensive Yangtze platform that fringed the basin and along the margins of isolated platforms within the basin (Poduan and Guohua Formations, fig. 4; see also Enos et al., 1997; Lehrmann et al., 1998; Lehrmann et al., 2003). These reef complexes add greatly to the geographic distribution of known Anisian reefs (see review in Flügel, 2002). Furthermore, they are among the oldest Triassic reefs in the world and, unlike many of their counterparts in western Tethys, they are preserved *in situ* as limestone. The Great Bank of Guizhou (GBG) contains the best-exposed reef complex among the isolated platforms because a faulted syncline provides a two-dimensional cross-section of the platform, including the reef margin (fig. 9). Exposure of a cross-section from the platform interior to the basin margin allows the physical stratigraphic correlation from the massive reef complex into the basin-margin clinoforms. Occurrence patterns of reef-derived grains within the basin-margin strata provide biostratigraphic constraints on the timing of reef formation.

Lehrmann et al. (1998) recognized a Middle Triassic platform-margin reef complex rimming the GBG that is exposed in cross-section on the northern margin near the town of Bianyang. The reef complex south of Bianyang extends approximately 1 km from the platform margin toward the platform interior and is approximately 800 m thick (fig. 9). Physical tracing of basin-margin strata into the platform margin indicates that the preserved reef complex is primarily Anisian (Early Middle Triassic) in age (Lehrmann et al., 1998). Rare grains of a problematic microfossil commonly identified as *Tubiphytes* first occur within basin-margin strata in the uppermost Spathian (fig. 18), several meters below the first occurrence of the conodont *Cs. timorensis*, the datum likely to define the Early-Middle Triassic boundary in the GSSP section (Ogg, 2004). *Tubiphytes* is characteristic of the reef-boundstone facies on the GBG and is commonly found in Middle Triassic reefs worldwide (Flügel, 2002).

Tubiphytes is a problematic fossil (cf. Senowbari-Daryan

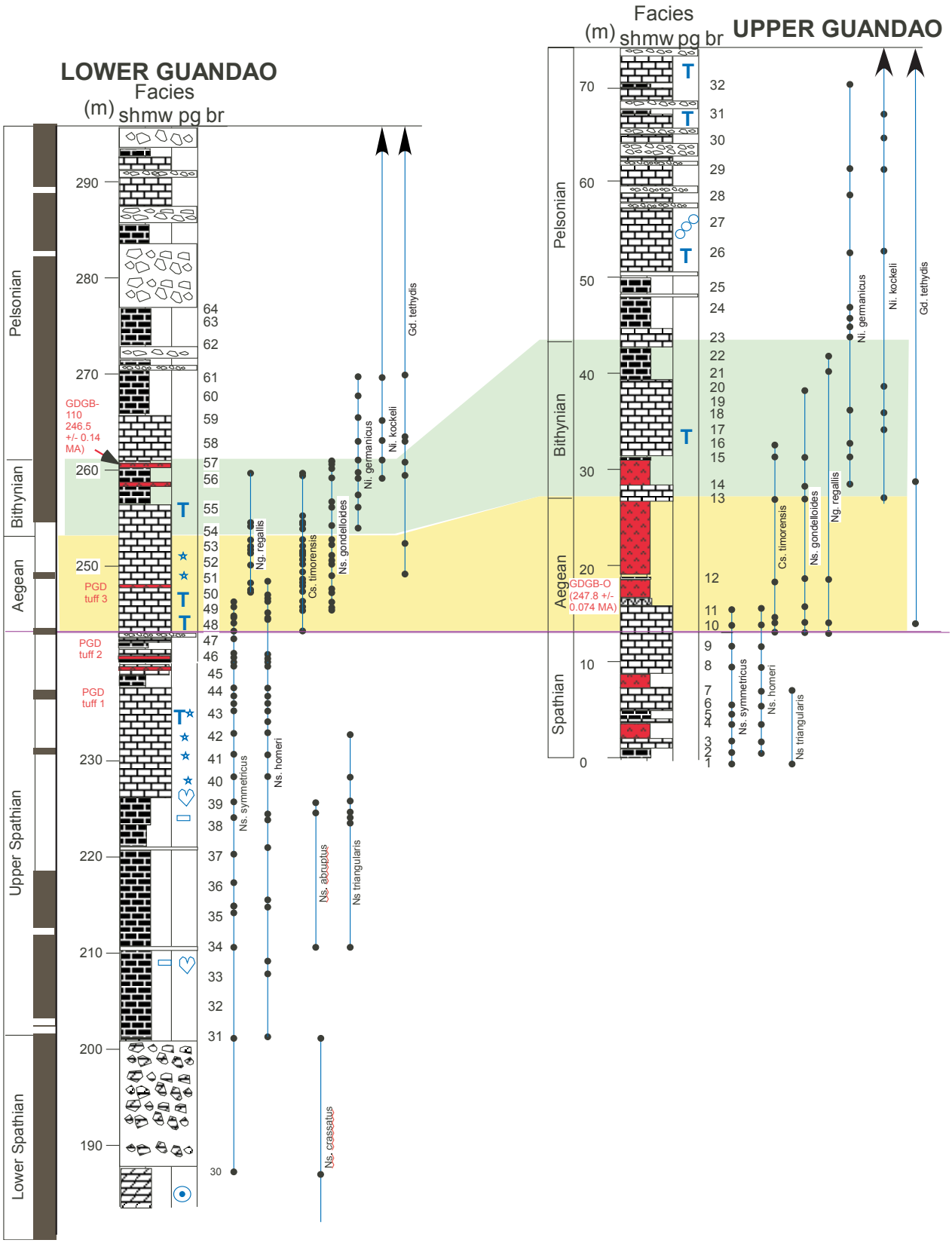

Figure 17: Olenekian-Anisian boundary section in basin margin facies in Lower Guandao and Upper Guandao sections (see figures 9 and 10 for locations). Lithology and grain type symbols are the same as those shown in figures 13 and 14. Magnetic reversal stratigraphy (black is normal polarity) is shown at left of Lower Guandao section. Conodont biostratigraphy and preliminary U-Pb age dates of volcanic ash layers are shown for both sections. We emphasize that the U-Pb age dates are still preliminary and should not be cited as certain boundary ages until the data is sufficiently refined. Further discussion of the biostratigraphy, geochronology, and magnetostratigraphy is provided in the stop descriptions of the field guide in this volume.

and Flügel, 1993) composed of micritic tubes that appears, at least locally, to reflect micritic cementation around a siphonous alga (J. Payne, unpublished data; Lehrmann, 1993). *Tubiphytes* grains are common in basin-margin strata from the Anisian into the Carnian (figs. 13, 14). The abundance of *Tubiphytes* grains increases across the Early-Middle Triassic boundary, suggesting a rapid increase in the extent and/or rate of carbonate production on the reef complex at this time. Geological mapping and correlation to the basin margin indicates that the top of the preserved reef complex is Late Anisian or Early Ladinian in age and that the Ladinian and Carnian platform was rimmed by a high-relief escarpment (Lehrmann et al., 1998). The presence of abundant *Tubiphytes* grains and blocks of *Tubiphytes* boundstone in Anisian through basal Carnian strata on the basin-margin provide evidence for the persistence of a reef or patch reefs also on the high-relief escarpment margin into the Ladinian. Apparently the Ladinian reefs along the high-relief escarpment were largely stripped away by erosion and their remnants are largely preserved in clasts in breccias found at the foot of the escarpment (fig. 9; see description for stop 6B).

Much of the volume of the reef complex is composed of discontinuous units of *Tubiphytes* boundstone, *Tubiphytes* grainstone and breccia cemented by large volumes of isopachous marine cement. Although sampling reveals the spectrum of lithologies and alternation of boundstone and grainstone can be detected in outcrop, the reef facies is generally massive, without distinct bedding.

A variety of free-living organisms are also found within the reef complex. The reef-dwelling fauna includes crinoids, gastropods, bivalves, ostracodes and brachiopods. Among the reef dwellers, crinoid grains are the most abundant, with subordinate bivalves and gastropods. Benthic foraminifers and dasyclad algae are also present in low abundance. Fossils of free-living organisms generally occur within grainstones and are rare within *Tubiphytes* boundstone, suggesting that much of the reef-dwelling fauna lived near, but not within, the *Tubiphytes* framework.

Several generations of marine cements contribute significantly to the reef framework, often contributing the majority of the total rock volume. Cements include: 1) peloidal microcrystalline cement; 2) brownish fibrous cement; 3) botryoidal cement; and 4) isopachous fibrous marine cement. What little void space remained within the reef after marine cementation was occluded by equant sparry calcite after burial.

We interpret the history of cementation of the *Tubiphytes* reef complex as follows. The earliest generation of carbonate precipitation occurred around a soft-bodied siphonous alga to form the *Tubiphtyes* framework. This generation of cement must have formed during the life of the alga, for the substrate for nucleation likely consisted of mucopolysaccharides excreted by the living alga. The second generation of cement consisted of clotted micrite surrounding the *Tubiphytes* framework. It seems likely that this micrite, like the micrite forming the tube of *Tubiphytes*, reflects biotically mediated carbonate precipitation in open contact with seawater. The subsequent generation of brownish fibrous marine cement shows no evidence for dissolution prior to precipitation and is found surrounding *Tubiphytes* in grains transported to the basin margin in turbidity currents. These two pieces of evidence indicate that even the brownish fibrous cement was precipitated in open contact with seawater prior to any significant burial. Given the generally high depositional rates, approximately 200 m/Ma in the reef complex, open contact with seawater must have lasted on the order of 10^4 years. Evidence for dissolution prior to the precipitation of isopachous fibrous cements suggests possible exposure or burial of the reef boundstone prior to this episode of cementation. On the other hand, the deposition of micrite between layers of isopachous cement in some cavities suggests that, at least in some cases, the isopachous cement was also precipitated in contact with shallow-marine water. Botryoidal cements appear to postdate isopachous cements in several samples, but are generally interpreted as shallow-marine cements. Finally, the remaining voids were completely occluded by sparry calcite after burial.

Despite the extent of the reef complex and the fact that the reef aggraded to produce at least 400 m of relief above the adjacent basin floor (fig. 9, 11C), there is little evidence that the framework elements – primarily *Tubiphytes* and marine cements – attained any significant local relief above the seafloor. In the field, local relief of less than one meter was observed where hemispherical *Tubiphytes* boundstones are in contact with grainstones. Karst topography and locally thick vegetation, however, preclude the determination of detailed stratigraphic relationships within the reef complex over distances greater than a few tens of meters.

Stop-6b Optional stop examine the Anisian through Carnian basin-margin succession at upper Guandao section (fig. 9, 14)

Upper Guandao section- Upper Guandao section was measured in the valley and up the hillside approximately 200 meters north (basinward) of lower Guandao section**.** The base of the section was measured in Upper Olenekian (Spathian) strata containing volcanic-ash horizons. The section continues up through the Anisian and Ladinian and represents the basin-margin slope succession deposited north of the massive, aggrading *Tubiphytes* reef complex (fig. 9, 10). The siliciclastic turbidites of the Bianyang Formation at the top of upper Guandao section (fig. 9, 10) are Carnian in age.

Lithostratigraphically the Anisian-Ladinian strata in upper Guandao section can be subdivided into 3 major units (fig. 14). 1) The Aegean-Lower Pelsonian succession consists of thin-bedded, pelagic lime mudstone and wackestone, containing thin-shelled bivalve debris; allodapic skeletal packstone and grainstone, composed primarily of fragmental *Tubiphytes* debris and crinoid

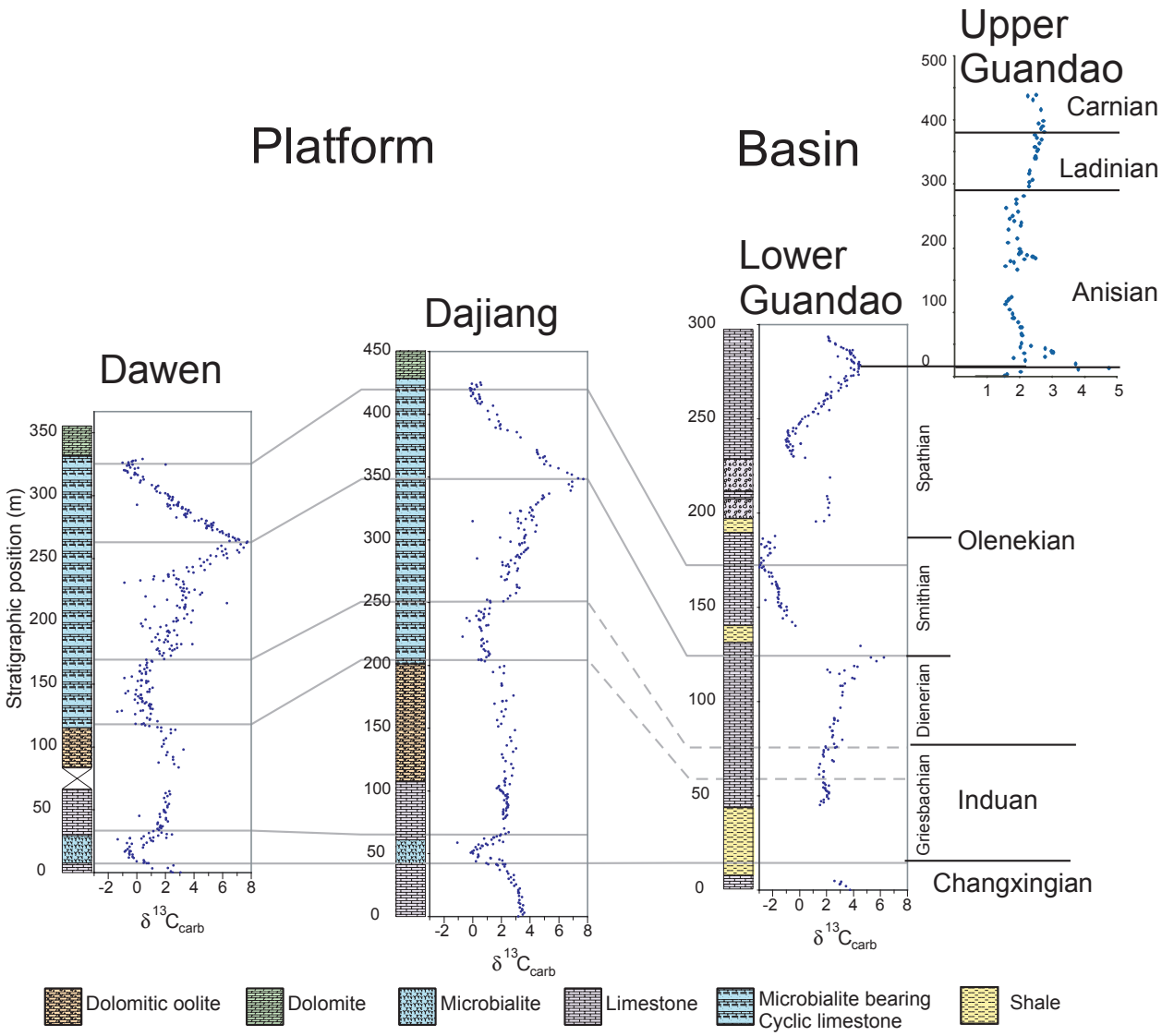

Figure 18: Carbonate isotope data from Upper Permian through Upper Triassic (Carnian) of the GBG (from Payne et al., 2004). Dawen and Dajiang sections are from the platform interior and lower and upper Guandao sections are from the basin margin (see figures 9 and 10 for section locations). Age correlations are based on conodont biostratigraphy from Guandao section and correlation of carbon isotope excursions.

ossicles; and thin, polymict debris-flow breccia beds (each no more than a few meters thick). 2) The Upper Pelsonian-Illyrian succession also contains pelagic lime mudstone, allodapic skeletal packstone and grainstone and polymict, debris-flow breccia, but in this interval breccia tongues range from about 10 m to more than 50 m thick. Soft-sediment deformation of the beds underlying the breccia tongues is spectacularly exposed near the path. 3) The Ladinian through the Carnian succession is composed of lithoclastic grainstone breccias and skeletal grainstone composed of *Tubiphytes* boundstone clasts, fragmented *Tubiphytes* debris, crinoid ossicles and other subordinate skeletal grains (fig. 14). The three units are mapped in figure 9. The upward change records progressive steepening of the basin-margin slope (from 5^0 in the Early Anisian to $>30^0$ with ~400 m of relief in the Early Ladinian) as the platform-margin reef complex aggraded. Steepening slopes yielded thicker debris-flow breccia units and more abundant slumping of pelagic lime mudstones in the Upper Pelsonian and Illyrian. Eventually slope deposition shifted to lithoclastic grainstone in the Ladinian as the slope reached the angle of repose and transport shifted from subaqueous debris flow to subaqueous debris fall and grain flow (fig. 10).

Grains in the allodapic packstone and grainstone beds of upper Guandao section are dominantly derived from the platform-margin reef complex and are dominated by *Tubiphytes* fragments. Skeletal grains are dominated by crinoids, with subordinate bivalves, gastropods, echinoids and brachiopods. Clasts in the breccias include lime mudstone, or packestone and grainstone derived from the slope and *Tubiphytes* boundstone derived from the platform-margin reef. No platform-interior lithologies are found in the breccia clasts, indicating that allodapic sediment was derived primarily from the margin and that no major subaerial erosion events occurred to transport material eroded from the platform interior. The lack of definitive exposure fabrics in debris-flow breccia clasts suggests deliv-

ery primarily by high-stand shedding. Skeletal abundance and diversity is greater in the Anisian-Ladinian succession than in the uppermost Olenekian. Thin-section point counts record 8 to 9% skeletal grains averaged over all lithologies (J. Payne, unpublished data). Skeletal packstone and grainstone beds and breccia clasts contain *Tubiphytes* fragments, crinoids, echinoids, foraminifers, calcareous algae, mollusks, brachiopods, ostracodes, calcisponge fragments and a few scleractinian corals. Skeletal abundance and diversity remains relatively constant throughout the Anisian-Ladinian succession (J. Payne, unpublished data).

Breccia clasts derived from the platform margin provide an indirect sampling of the platform-margin reef complex through the Middle Triassic. The broad evolution of the platform-margin biota is apparent in the changing biotic content of the breccia tongues. The thick Anisian breccia tongues contain only clasts of *Tubiphytes* boundstone along with slope lithologies. The large extent of the Anisian reef, despite the lack of framework elements other than cements and *Tubiphytes*, suggests controls beyond the recovery and evolution of framework-building metazoans in the re-establishment of platform-margin reefs in the Middle Triassic. A better understanding of the origin of *Tubiphytes* and of the biological and geochemical controls on early marine cementation of the Middle Triassic platform margin should provide new insights into the recovery of reefs during the Middle Triassic.

In contrast, the Carnian breccia tongues (interbedded with siliciclastic turbidites at the top of upper Guandao section, fig. 9) contain reef blocks with a much greater biotic diversity than the *Tubiphytes* reef complex. This reef material, which was derived from patch reefs or narrow fringing reefs along the high-relief Ladinian escarpment (fig. 9, 10C), contains solitary and colonial scleractinian corals, with colonies reaching 50 cm or more in diameter. They also contain large calcareous solenoporacean red algae and inozoan and sphinctozoan calcareous sponges that are well preserved and easy to identify on weathered surfaces. These blocks of Ladinian reef material demonstrate significant local increase in metazoan diversity on the GBG.

Acknowledgements

This research is based upon work supported by the National Science Foundation (under grant numbers EAR 9004783 and EAR-9805731 to P.E. and EAR-9804835 to D.J.L. and) and by the Petroleum Research Fund of the American Chemical Society (under grants ACS-PRF 34810-AC8 and ACS-PRF 37193-AC8 to P.E. and ACS-PRF 33122-B8 and ACS-PRF 40948-B2 to D.J.L.) The Guizhou Bureau of Geology and Mineral Resources and the Geological Survey of Guangxi provided additional support for field work**.** This is a contribution to IGCP project 467.

References

Atudorei, N.-V., 1999, Constraints on the Upper Permian to Upper Triassic marine carbon isotope curve. Case studies from the Tethys [PhD thesis]: Lausanne, University of Lausanne.

Baud, A., Atudorei, V., and Sharp, Z., 1996, Late Permian and early Triassic evolution of the Northern Indian margin: Carbon isotope and sequence stratigraphy: Geodinamica Acta, v. 9, p. 57-77.

Baud, A., Magaritz, M., and Holser, W.T., 1989, Permian-Triassic of the Tethys - Carbon Isotope Studies: Geologische Rundschau, v. 78, p. 649-677.Chaikin, Daniel H., 2004, Sedimentology and Provenance of the Bianyang Formation, Guizhou Province, South China: M.S. Thesis, University of Kansas, Lawrence, Kansas

Enkin, R.J., Zhenyu Yang, Yan Chen, and V.Courtillot, 1992, Paleomagnetic constratints on the geodynamic history of the major blocks of China from the Permian to the Present: Journal of Geophysical Research, v.97, no. B10, p. 13,953-13,989.Enos, Paul, and Perkins, R. D., 1977, Quaternary sedimentation in south Florida: Memoir – Geological Society of America, v. 147, 198p.

Enos, Paul, Wei Jiayong, and Yan Yangji, 1997, Facies distribution and retreat of Middle Triassic platform margin, Guizhou Province, south China: Sedimentology, v. 44, n. 3, p. 563-584.

Flügel, E., 2002, Triassic reef patterns, *in* Kiessling, W., Flügel, E., and Golonka, J., eds., Phanerozoic Reef Patterns: SEPM Special Publication, Tulsa, OK, Society for Sedimentary Geology, p. 391-464.

Gebelein, C.D., 1976, Open marine subtidal and intertidal stromatolites (Florida, the Bahamas and Bermuda), *in* Walter, M.R., ed., Stromatolites: Elsevier, New York, p. 381–388.

Gradinaru, E., Orchard, M., Nicora, A., Mirauta, E., Atudorei, V., 2001, Conodont succession across the Olenekian-Anisian boundary at Desli Caira, Romania: STS/IGCP 467 Field Meeting, Abstract Volume, Vesprem, Hungary, p. 11-13.

Guizhou Bureau of Geology and Mineral Resources, 1987, Regional Geology of Guizhou Province: Geological Memoires, Ser. 1, no. 6, 700 p., [in Chinese, English summary; Geologic map 1:500,000].Horacek, M., Bradner, R., and Abart, R., 2000, A positive (super 13) C excursion recorded by Lower Triassic marine carbonates from the western central Dolomites, N.-Italy, a special situation in the western Tethys?: International Geological Congress, Abstracts = Congres Geologique International, Resumes, vol.31, unpaginated.

Hou Fanghao, and Huang Jixiang, 1984, Research into the Permian and Triassic volcanoclastic turbidites of the Nanpan River sag: Scientia Geologica Sinica, v. 3, p. 256-264.

Krull, E.S., Lehrmann, D.J., Druke, D., Kessel, B., Yu, Youyi, and Li, Rongxi., 2004, Stable carbon isotope stratigraphy across the Permian-Triassic boundary in shallow marine carbonate platforms, Nanpanjiang Basin, south China: Palaeogeography Palaeoclimatology Palaeoecology, v. 204, p. 297-315.

Krull, E.S., and Retallack, G.J., 2000, delta C-13 depth

profiles from paleosols across the Permian-Triassic boundary: Evidence for methane release: Geological Society of America Bulletin, v. 112, p. 1459-1472.-Lehrmann, D. J., 1993, The Great Bank of Guizhou: Birth, evolution, and death of an isolated Triassic platform, Guizhou Province, South China: Ph.D. dissertation, University of Kansas, 457 p.

Lehrmann, D.J., 1999, Early Triassic calcimicrobial mounds and biostromes of the Nanpanjiang basin, south China: Geology, v. 27, n. 4, p. 359-362.

Lehrmann, D.J., Payne, J.L., Felix, S.V., Dillett, P.M., Wang, H., Yu, Y.Y., and Wei, Jiayong, 2003, Permian-Triassic boundary sections from shallow-marine carbonate platforms of the Nanpanjiang basin, south China: Implications for oceanic conditions associated with the end-Permian extinction and its aftermath: Palaios, v. 18, p. 138-152.

Lehrmann, D.J., Wei, Jiayong, and Enos, Paul, 1998, Controls on facies architecture of a large Triassic carbonate platform: The Great Bank of Guizhou, Nanpanjiang basin, South China: Journal of Sedimentary Research, v. 68, p. 311-326.

Magaritz, M., Bar, R., Baud, A., and Holser, W.T., 1988, The carbon-isotope shift at the Permian Triassic boundary in the southern Alps is gradual: Nature, v. 331, p. 337-339.

Muttoni, G, Gaetani, M. Budurov, K., Zagorchev, I., Trifonova, E., Ivanova, D., Petrunova, L., Lowrie, W., 2000. Middle Triassic palaeomagnetic data from northern Bulgaria: constraints on Tethyan magnetostratigraphy and palaeogeography: Palaeogeography Palaeoclimatology Palaeoecology, 160**,** 223-237.

NewKirk, T. T., Lehrmann, D.J., and Hudak, G., 2002, Tephrastratigraphy and analysis of tectonic setting of Triassic intermediate volcanic strata: Nanpanjiang basin, South China**,** Geological Society of America, Abstracts with programs, v. 34, n. 6, p. 512.

Ogg, J., 2004, Overview of global boundary stratotype sections and points (GSSP's), International Commission on Stratigraphy.

Orchard, M. J., 1995, Taxonomy and correlation of Lower Triassic (Spathian) segminate conodonts from Oman and revision of some species of Neospathodus: Journal of Paleontology, v. 69, p. 110-122.

Orchard, M. J., and Tozer, E. T., 1997, Triassic conodont biochronology, its calibration with the ammonoid standard, and a biostratigraphic summary for the western Canada sedimentary basin: Bulletin of Canadian Petroleum Geology, v. 45, p. 675-692.

Orchard, M.J., Nassichuk, W.W., and Rui, Lin, 1994, Conodonts from the Lower *Griesbachian Otoceras Latilobatum* bed of Selong, Tibet and the position of the Permian-Triassic boundary*, in* Embry, A.F., Beauchamp, B., and Glass, D.J., eds., Pangea: Global Environment and Resources: Canadian Society of Petroleum Geologists, Memoir 17, p. 823-843.

Paull, R.K. and Paull, R.A., 1994, *Hindeodus parvus*; proposed index fossil for the Permian-Triassic boundary: Lethia, v. 27, no.3, pp. 271-272.

Payne, J. L., Lehrmann, D. J., Wei, Jiayong, Orchard, M. P., Schrag, D. P., Knoll, A. H., 2004, Large perturbations of the carbon cycle during recovery from the End-Permian extinction, Science, v. 23, p. 506-509.

Playford, P.E., and Cockbain, A.E., 1976, Modern algal stromatolites at Hamelin Pool, a hypersaline barred basin in Shark Bay, Western Australia, *in* Walter, M.R. ed., Stromatolites: Elsevier, New York, p. 389–411.-Reid, R. P. and Macintyre, I. G., 1988, Foraminiferal-algal nodules from the eastern Caribbean; growth history and implications on the value of nodules as paleoenvironmental indicators: Palaios, v. 3, p.424-435.Senowbari-Daryan, B., and Flügel, E., 1993, *Tubiphytes* Maslov, an enigmatic fossil: classification, fossil record and significance through time, Part I: discussion of Late Paleozoic material, *in* Barattolo, F., De Castro, P., and Parente, M., eds., Studies on Benthic Algae: Bolletino della Societa Paleontologica Italiana: Modena, p. 353-382.

Schopf, W.J., 1992, The oldest fossils and what they mean*, in,* Schopf, W.J., ed., Major events in the history of life: Symposium proceedings, IGPP Center for the study of the evolution and origin of life, UCLA, Jones and Bartlett Publishers, Boston, p. 29-63.

Van-der-Voo, R., 1993, Paleomagnetism of the Atlantic, Tethys and Iapetus oceans: Cambridge University Press, Cambridge, 411 p.

Yang, Wan and Lehrmann, D. L., 2003, Testing Milankovitch climatic signals in Lower Triassic (Olenekian) peritidal carbonate successions, Nanpanjiang basin, South China: Palaeogeography, Palaeoclimatology, Palaeoecology: v. 201, n. 3-4, p. 283-306.

Yin, H., Sweet, W.C., Glenister, B.F., Kotlyar, G., Kozur, H., Newell, N.D., Sheng, J., Yang, Z., and Zakharov, Y.D., 1996, Recommendation of the Meishan section as Global Stratotype Section and Point for basal boundary of Triassic System: Newsletters on Stratigraphy, v. 34, p. 81-108.

Subcommission on Triassic Stratigraphy

STS Chairman

Dr. Mike Orchard, Geological Survey of Canada, 101-605 Robson Street, Vancouver, British Columbia, Canada.

Vice Chairman

Dr. Marco Balini Professore associato, Paleontology Dipartimento di Scienze della Terra "Ardito Desio" Universita' degli Studi di Milano Via Mangiagalli 34, 20133 Milano, Italy

Vice Chairman

Dr. Ying Hongfu, Office of the President, China University of Geosciences, Yujiashan, Wuhan, Hubei, 430074, People's Republic of China

STS Secretary General

Dr Chris McRoberts Department of Geology State University of New York at Cortland P.O. Box 2000 Cortland, New York 13045 USA

ALBERTIANA is published twice a year by the Subcommission on Triassic Stratigraphy. Individuals can obtain ALBERTIANA for the sum of US $ 20,- or EURO 20,- per year. Readers are kindly requested to pay their annual contribution timely.
European readers can send a Eurocheque made payable in Euro to Dr. Zwier Smeenk, Laboratory of Palaeobotany and Palynology, Utrecht University, Budapestlaan 4, 3584 CD Utrecht, The Netherlands. Everyone else is kindly requested to send cash in a closed non-transparent envelope to the above Utrecht adress. Because of the high provision costs of other cheques/currencies, other methods of payment cannot be accepted. Institutions can receive ALBERTIANA on an exchange basis.

All correspondence regarding the distribution of ALBERTIANA should be sent to Dr. Z. Smeenk.